Pure

Bangor University

MASTERS BY RESEARCH

Quantifying Similarity of Correlations between Seabird and Cetacean Distributions and Environment in the Northeast Atlantic

Greensmith, Rose

Award date:
2021

Awarding institution:
Bangor University

Link to publication

General rights
Copyright and moral rights for the publications made accessible in the public portal are retained by the authors and/or other copyright owners and it is a condition of accessing publications that users recognise and abide by the legal requirements associated with these rights.

- Users may download and print one copy of any publication from the public portal for the purpose of private study or research.
- You may not further distribute the material or use it for any profit-making activity or commercial gain
- You may freely distribute the URL identifying the publication in the public portal ?

Take down policy
If you believe that this document breaches copyright please contact us providing details, and we will remove access to the work immediately and investigate your claim.

Download date: 28. Apr. 2024

Quantifying Similarity of Correlations between Seabird and Cetacean Distributions and Environment in the Northeast Atlantic

Rosemary Greensmith

Supervised by Dr James Waggitt

Abstract

Understanding the role of mechanistic processes in species distributions is a key aspect of understanding the species spatial ecology, particularly interspecific interactions between species with overlapping resource requirements. However, comprehensive understanding is often hindered by spatial and temporal coverage of abundance data and lack of established statistical methodology to derive this from abundance data. This study aims to address these challenges by quantifying similarity among distributions of seabird and cetacean species. Intra-guild or taxa separation could indicate potential habitat partitioning, and equally, similarity between sympatric species could indicate potential coexistence. This study used zero-inflated generalised linear models to model a large-collation of seabird and cetacean abundance data across the northeast Atlantic, so that relationships within their likely ranges can be identified. Clustering and principal component analysis of the conditional model regression coefficients were used to quantitatively identify similarity between seabird and cetacean distributions and their environment within each species likely range. There was dissimilarity within guilds, and similarity between some sympatric species from different guilds. Furthermore, the scale of the relationship between abundance and their environment was distinct between taxa, as non-delphinid cetaceans had much stronger correlations than delphinids and seabirds. Explainers of dissimilarity can be simplified into species' spatial, behavioural and prey differences. These outcomes align with coexistence and competition theories, indicate that products of mechanistic processes are observable on a large scale, and that interspecific interactions are potentially involved. Future research includes identifying if interspecific interactions are the responsible mechanisms driving this similarity structure, then how to appropriately integrate this in species distribution modelling processes to improve ecological realism.

Contents

List of Figures 3
List of Tables 4
Table of abbreviations 6

1. Introduction 7

2. Methods 11

2.1. Model validation and Selection 16
2.2. Quantifying Similarity 17

3. Results 21

4. Discussion 28

4.1 Critical appraisal of the methods 32
4.2 Conclusion 33

5. References 34

6. Appendices 48

Appendix 1: Methodology 48
Appendix 2: Results 52
Appendix 3: Discussion 94

List of Figures

Figure 2.1 Map of study area 12
Figure 3.1 Biplot of principle components 1 and 2, of coefficients from the conditional models. Colour coded by the cluster to which the *k* means cluster algorithm assigned each species. Eigen vectors (direction of the variable plane through the matrix) of the variables are represented by the direction of the black arrows (each labelled with variable name in black) and the Eigen values (loading, or weighting of the variable) of the variables are represented by the length of the black arrows (each labelled with variable name in black). The scores of species are represented by positioning of the points (labelled with species abbreviation). Blue rectangles highlight rorquals, green rectangles highlight deep-diving odontocetes. 21
Figure 3.2 Unrooted dendrogram of hierarchical clustering. Unrooted dendrogram quantitatively derived from agglomerative hierarchical clustering of species ZIGLM conditional coefficients. Black arrow denotes increasing dissimilarity between species from right to left (length of arrow is arbitrary). Green shading highlights non-delphinid cetaceans, orange shading highlights delphinids and blue shading highlights seabirds. 22

Figure 3.3 Biplot of principle components 1 and 2, of coefficients from the conditional models from the subset analysis of k means cluster 3. Eigen vectors (direction of the variable plane through the matrix) of the variables are represented by the direction of the black arrows (each labelled with variable name in black) and the Eigen values (loading, or weighting of the variable) of the variables are represented by the length of the blue arrows (each labelled with variable name in blue). The scores of species are represented by the grey points (labelled with species abbreviation). The scores of species are represented by positioning of the points (labelled with species abbreviation). Shaded rectangles highlight species groups, orange: auks, green: small-sized delphinids, yellow: gulls, purple: procellariiformes. 23
Figure 3.4 Dendrograms of hierarchical clustering of species ZIGLM conditional coefficients. Figure A is clustering of all species and figure B is the subset clustering. Shaded rectangles highlight species groups; in figure A, blue : rorquals and green: deep-diving odontocete, in figure B, orange: auks, green: small-sized delphinids, yellow: gulls, purple: procellariiformes. 24

List of Tables

Table 1.1 Table of species abbreviations and environmental parameter codes. 6
Table 2.1 Table of study species. Taxa (from Order to Species) and common name. 11
Table 2.2 Details of environmental parameters and parameter codes. The sources of these data are described by Waggitt *et al*. (2020). 13
Table 2.3 Details of chosen models. The species column details the common name of each species. The logistic parameter column lists the environmental parameter codes used in the logistic models and a colon between two parameters denotes interaction term between the two parameters. The environmental parameters corresponding to the codes are detailed in table 2.2. The offset column, 'Km': kilometres travelled per observation, 'Hr': survey time (in hours) per observation. Distribution column, 'NB 1': negative binomial distribution where the variance increases linearly with the predicted mean, 'NB 2': negative binomial distribution where the variance increases quadratically with the predicted mean, 'P': poisson distribution. 14
Table 2.4 Guilds/ taxa groups to investigate. 18
Table 2.5 Table of distance matrix equation terms. Term description and non-standardised parameter the term represents (ZiGLM parameter code). 19
Table 2.6 Table of inputs for Pearson product-moment correlation coefficient used in latent similarity structure cross validation. Distance metrics detail how the structure identified in the analysis type is represented as an input in the Pearson product-moment correlation coefficient to cross-validate the latent similarity structure. 20
Table 3.1 Summary of conditional model slope estimates. Bold text highlights where species are above the 75th percentile. '<25th' identifies that the species absolute value is lower than the 25th percentile of all species absolute values for the corresponding predictor. '>75th' means that the species absolute value is greater than the 75th percentile of all species absolute values for the corresponding predictor, 'IQR' denotes the interquartile range. When the value contains '+', the abundance of that species increases linearly with an increase in the value of the corresponding predictor. When the value contains '-', the

abundance of that species decreases linearly with an increase in the value of the corresponding predictor. Dark grey shading highlights the parameter with the steepest slope estimate compared to the other parameters for the species, light grey shading highlights the parameter with the shallowest slope estimate for the species. 26
Table 3.2 Pearson product-moment correlation coefficient matrix of cophenetic distances derived from the agglomerative hierarchical clustering analysis (HClust. cophenetic dist.), Euclidean distances between the observation (species) scores from principle dimensions 1 and 2 from principle component analysis (Euclid dist. between pc1 and pc2 scores) and the Euclidean distances between the conditional coefficients of the zero-inflated generalised mixed models for each species (Euclid dist. between ZIGLM coefficients (conditional) for each species) and the Euclidean distances between coordinates derived from classical multi-dimensional scaling (Euclid dist. between coordinates from classical MDS). 27

Table of abbreviations

Table 1.1 Table of species abbreviations and environmental parameter codes.

Type	Abbr.	Definition
Species	ATPF	Atlantic Puffin
	BLKW	Black-legged Kittiwake
	BTND	Bottlenose Dolphin
	CMGM	Common Guillemot
	COMD	Common Dolphin
	EPSH	European Shag
	EPSP	European Storm Petrel
	FINW	Fin Whale
	HRBP	Harbour Porpoise
	HRGL	Herring Gull
	KILW	Orca
	LBGL	Lesser Black-backed Gull
	MINW	Minke Whale
	MXSH	Manx Shearwater
	NTFU	Northern Fulmar
	NTGA	Northern Gannet
	PILW	Pilot Whale
	RAZB	Razorbill
	RISD	Risso's Dolphin
	SPRW	Sperm Whale
	STRD	Striped Dolphin
	WHBD	White-beaked Dolphin
	WHSD	White-sided Dolphin
Environmental Parameter	BAT	Depth (m)
	CHS	Total Chlorophyll (mg) in surface layer (satellite imagery)
	CHT	Total Chlorophyll (mg) depth summed between 0 and 150m from surface (modelled)
	CON	Distance to 300m isobath (m)
	FEA	Depth gradient (m), calculated using terrain ruggedness index
	LND	Distance to Land (m)
	SPM	Mean surface current speed (ms-1), including tidal influence
	TPF	Thermal stratification gradient, where higher values indicate greater frontal activity
	TPM	Mean potential temperature (Celsius) between 0 and 150m from surface (modelled)
	TPR	Range of potential temperature (Celsius) between 0 and 150m from surface (modelled)
	TPS	Potential temperature (Celsius) in surface layer (satellite imagery)

1.Introduction

Seabirds and cetaceans have an ecologically important role in top-down mediation of species assemblages (Heithaus *et al.*, 2008; Townsend *et al.*, 2008; Baum & Worm, 2009; Certain *et al.*, 2011; Mann & Karniski, 2017), therefore, population size and dynamics of predators in the highest trophic levels are often considered to be indicators of ecosystem health (Moore & Kuletz, 2019). As seabirds and cetaceans are highly mobile, they can fill functional roles in multiple ecosystems, for example transporting and cycling nutrients. Seabird and cetacean populations are susceptible to a wide variety of pressures, such as overfishing on prey resources (DeMaster *et al.*, 2001; Bearzi *et al.*, 2006; Herr *et al.*, 2009; Grémillet *et al.*, 2016), noise disturbance (Bailey *et al.*, 2010, 2014; Baltzer *et al.*, 2020), bycatch mortality from fisheries (Reeves *et al.*, 2013) and climate change impacts (C. D. Macleod *et al.*, 2005; Burthe *et al.*, 2014).

To mitigate these issues, a comprehensive understanding of seabird and cetacean spatial ecology is necessary (Grémillet & Boulinier, 2009). One of the fundamental aspects in ecological theory is species interactions, such as habitat partitioning or coexistence (Kneitel & Chase, 2004). Understanding these processes on a large scale could be particularly relevant for seabirds and cetaceans due to their highly mobile nature (Ritchie, 2002), however, there is a lack of understanding of how these processes operate on a large scale, potentially in part due to a lack of adequate large-scale data.

Environmental conditions are widely used as proxies for prevalence of suitable prey resources in seabird and cetacean distribution or habitat models, which is widely considered to be one of the main drivers of marine top predator distribution (Cox *et al.*, 2018; Waggitt *et al.*, 2020). The key components of a prey type being suitable include abundance or prey patch density (Friedlaender *et al.*, 2020), nutritional quality (Wanless *et al.*, 2005; Paredes *et al.*, 2012; Spitz *et al.*, 2012, 2018), size (Burke & Montevecchi, 2009), and accessibility, such as position in the water column (Anderwald *et al.*, 2012; Embling *et al.*, 2012; Lambert *et al.*, 2014; Baptist *et al.*, 2019), which can vary by season, to month and even at a diurnal scale (van der Kooij *et al.*, 2008; Romero-Romero *et al.*, 2019) related to their behaviours, ontogeny and quality and accessibility of their prey (Røjbek *et al.*, 2014). The distribution of

the top predators can change throughout the year often related to seasonal variation in availability of suitable prey resources within the predators range (Nichol, 1990; Couperus, 1997; K. Macleod *et al.*, 2004; Visser *et al.*, 2011; Sveegaard *et al.*, 2012; Esteban *et al.*, 2014; Berrow *et al.*, 2015). The physical and biological oceanographic characteristics or environmental conditions of a habitat can influence how suitable the prey is as a resource for the top predators, as certain conditions can influence the nutritional value (Røjbek *et al.*, 2014), behaviour (Embling *et al.*, 2013), distribution (Pacariz *et al.*, 2016), and abundance of the prey (Maravelias *et al.*, 2000), which can influence the distribution of the top predators (Hastie *et al.*, 2004; Teloni *et al.*, 2008; Paredes *et al.*, 2014; Shoji *et al.*, 2015). Environmental parameters commonly used have been found to correlate with seabird and cetacean distribution and abundance, for example, sea surface temperature (MacLeod *et al.*, 2007; Nøttestad *et al.*, 2015; Víkingsson *et al.*, 2015; Rogan *et al.*, 2017; Wakefield *et al.*, 2017; Mannocci *et al.*, 2020), water depth (K. Macleod *et al.*, 2003, 2009; Wall *et al.*, 2006; Ingram *et al.*, 2007; Teloni *et al.*, 2008; Pirotta *et al.*, 2011; Nøttestad *et al.*, 2015; Laran, Pettex, Authier *et al.*, 2017), seabed gradient (Cañadas *et al.*, 2002; Weir *et al.*, 2007; Canning *et al.*, 2008; Skov & Thomsen, 2008; Booth *et al.*, 2013; Jones *et al.*, 2014; Wakefield *et al.*, 2017), chlorophyll concentration as a proxy for primary productivity (MacLeod *et al.*, 2007; de Stephanis *et al.*, 2008; Cotté *et al.*, 2010; Gilles *et al.*, 2011; Wong & Whitehead, 2014; Griffiths, 2015) and fronts (Doniol-Valcroze *et al.*, 2007; Scales *et al.*, 2014).

Seabird and cetacean distributions relative to oceanographic parameters over a large spatiotemporal scale is also an amplification or reflection of their varying modern morphologies and life strategy, driven by convergent evolution (analogous and homologous) and radial expansion, between and within the seabirds and cetaceans (Woodward *et al.*, 2006; Sato *et al.*, 2007; Mccurry *et al.*, 2017), since the divergence of their lineages around 310 million years ago (Hedges *et al.*, 1996). In the current stage of the seabird and cetacean evolutionary history, simplified as aquatic (shared ancestor) to terrestrial (diverged from shared ancestor), then back to aquatic dependency (independent lineages) (Carroll, 2001), there is overlap in resource use and varying degrees of plasticity of resource use between modern seabirds and cetaceans (Camphuysen *et al.*, 2006). Therefore, there are convergent evolutionary traits, for example, related to energy-efficient locomotion underwater,

breathe-holding, coping with low oxygen, carbon dioxide build-up and changes in pressure between cetaceans and seabirds that forage below the sea surface (Davis & Guderley, 1990; Kooyman & Ponganis, 1998; Sato *et al.*, 2007; Mirceta *et al.*, 2013). There is great dietary overlap between the seabirds and cetaceans in this study, within and across taxonomic and foraging guilds (Pierce *et al.*, 2004; Santos *et al.*, 2004; Jansen *et al.*, 2010; Fayet *et al.*, 2021), even seabirds and cetaceans with no obvious convergent evolutionary traits, for example surface feeding seabirds such as gulls that feed on the same forage fish as cetaceans such as minke whales and are commonly observed in multi-species feeding aggregations (Anderwald *et al.*, 2011).

The foraging behaviour and strategy of the seabirds and cetaceans can lead to interspecific differences and similarities in their distribution, through influencing what prey types are accessible to them, and allowing them to occupy a niche (Woodward *et al.*, 2006; Garthe *et al.*, 2014; Lambert *et al.*, 2014; Petalas *et al.*, 2021). Furthermore, the energetic demands related to morphology (i.e., influences of body size on thermoregulatory constraints) and life history/strategy (all of which can vary by gender and ontogeny), can influence what prey types, densities, abundances and behaviours are required to maintain healthy body condition by consumption rate and quality of prey (Spitz *et al.*, 2012; Kahane-Rapport *et al.*, 2020). In turn, this can have a confounding effect on the fluctuations of distribution and abundance of the top predators within their ranges, if they are to match these resources spatially and temporally (Anderwald *et al.*, 2012; Nøttestad *et al.*, 2015).

Other studies have used overlap (often distance-based calculations) of species distribution model (SDM) predictions (using individual species occurrence data) as a metric of potential for species interactions (Godsoe, 2014). An alternative is to compare species environmental niches to infer interspecific interactions (related to how this influences species distribution) (Broennimann *et al.*, 2012). It has been considered that the niche of a species can be described by the environmental conditions where a species is present (Godsoe, 2014), and species occurrence and environmental data is suitable for describing a species' environmental niche (Broennimann *et al.*, 2012). Whilst species niche differences defined by biological data relating success and resource use are commonly used in species comparisons, (Broennimann *et al.*, 2012) suggest that comparing species based on how

species distribution relates to environmental conditions is more relevant to answering questions about changes in species distribution and consider this method of defining environmental niche to align with Grinellian niche theory.

Based on the logic of (Broennimann *et al.*, 2012) and (Godsoe, 2014), identifying how similar or dissimilar relationships with environmental parameters are between species, could potentially provide insight into influences of interspecific dynamics on species distribution within a community (Broennimann *et al.*, 2012). Exploring the structure of similarity or dissimilarity of relationships between seabird and cetacean distribution and environmental parameters could provide context to anecdotal observations, investigate validity of assumptions of similarities between guilds and closely related taxa. It could also be useful to understand how similar data-poor species are to other species, especially where multiple species' distribution data are sometimes amalgamated (Baines *et al.*, 2017; Lambert, Pettex *et al.*, 2017; Wong *et al.*, 2018; Leonard & Øien, 2020).

Based on Wilson's theory (Wilson, 1999) that species within intrinsic guilds would not co-occur, it could be expected that species in the same intrinsic guild should be most abundant in dissimilar environmental conditions. The theory of Phylogenetic Niche Conservatism (Pyron *et al.*, 2015) would expect there to be partitioning (dissimilarity) between seabirds and cetaceans in the similarity structure. For count data of closely related species to be amalgamated in species abundance models with an assemble first, predict later approach, these species should be similar in the similarity structure. The aim of this study is to quantify the similarity structure of correlations between large-scale seabird and cetacean distributions and their environment, and the objective is to identify if there are patterns of similarity or dissimilarity between species that share guilds and/or are closely related taxa, as this could indicate potential habitat partitioning or coexistence.

2.Methods

Sightings data of 23 species were used in this study, 11 species representing three seabird orders, with two families each, and 12 species representing two cetacean orders, with one family in one order, and three families in the other order (table 2.1). These species were chosen to maximise use of available abundance data, which was collated from a variety of sources, described by (Waggitt *et al.*, 2020). The temporal extent of the data was between the years 1985 and 2015, and the temporal resolution was on a monthly scale and the spatial resolution of the data was 10 km ^{2}.

Table 2.1 Table of study species. Taxa (from Order to Species) and common name.

Order and Family	Genus and species	Common name
Charadriiformes		
Alcidae	*Fratercula arctica*	Atlantic Puffin
	Uria aalge	Common Guillemot
	Alca torda	Razorbill
Laridae	*Rissa tridactyla*	Black-legged Kittiwake
	Larus argentatus	Herring Gull
	Larus fuscus	Lesser Black-backed Gull
Pelecaniformes		
Phalacrocoracidae	*Phalacrocorax aristotelis*	European Shag
Sulidae	*Morus bassanus*	Northern Gannet
Procellariiformes		
Hydrobatidae	*Hydrobates pelagicus*	European Storm Petrel
Procellariidae	*Puffinus puffinus*	Manx Shearwater
	Fulmarus glacialis	Northern Fulmar
Mysticete		
Balaenopteridae	*Balaenoptera acutorostrata*	Minke Whale
	Balaenoptera physalus	Fin Whale
Odontocete		
Delphinidae	*Tursiops truncatus*	Bottlenose Dolphin
	Delphinus delphis	Common Dolphin
	Globicephala melas	Pilot Whale
	Stenella coeruleoalba	Striped Dolphin
	Lagenorhynchus albirostris	White-beaked Dolphin
	Lagenorhynchus acutus	White-sided Dolphin
	Orcinus orca	Orca
	Grampus griseus	Risso's Dolphin
Physeteridae	*Physeter macrocephalus*	Sperm Whale
Phocoenidae	*Phocoena phocoena*	Harbour Porpoise

The study area covers the northeast Atlantic (figure 2.1), which has a varied and complex biogeography, including shelf seas and oceanic waters, with a variety of topographic features such as islands, seamounts, ridges, canyons and shallow banks and complex coastlines (figure 2.1). The study area is influenced by multiple oceanographic processes, such as large-scale oceanic currents with varying properties, large tidal ranges on the continental shelf, producing features such as fronts, and regions of freshwater influence. The study area has high primary productivity, particularly in areas of upwelling of nutrient rich water, which peaks in spring, and again in autumn. The study area has a temperate climate, which is highly influenced by the north Atlantic oscillation of the jet stream and the Atlantic meridional overturning circulation.

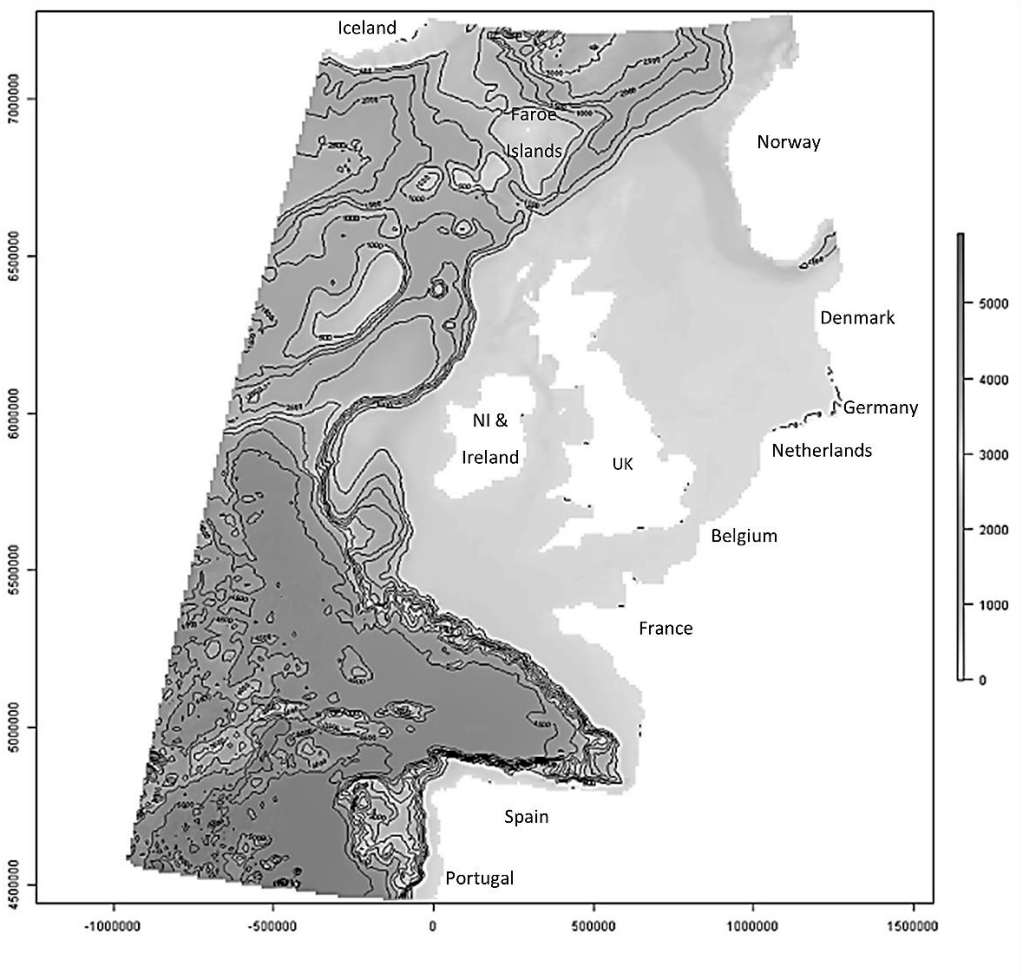

Figure 2.1 Map of study area

To model the effects of different environmental factors listed in Table 2.2 on the distribution of 12 cetacean and 11 seabird species (table 2.1), Zero-inflated generalised linear models were used, as frequency graphs showed that the data was zero-inflated. these models are also referred to as ZIGLM throughout this thesis. The package "glmmTMB" (Brooks *et al.*, 2017) was used for the zero-inflated generalised linear models. To compare model coefficients between all of the species, the parameters of the ZIGLM conditional model were chosen to be consistent, and the parameters for the logistic model were unique to each species, to improve model parsimony. Model covariates for the logistic component of the ZIGLMs (table 2.3) were selected from the pool of ecologically relevant environmental parameters (table 2.2) if they improved model fit. To reduce overparameterisation of the ZIGLM, a maximum of five variables were chosen for the conditional model. The variables for the conditional model (Table 2.2; highlighted grey) were chosen to represent sea temperature, primary productivity, fronts, and static landscape features, due to their ecological relevance to the species, and more comparable to other studies because these environmental . Maps of these environmental parameters are displayed in appendix 1.

Table 2.2 Details of environmental parameters and parameter codes. The sources of these data are described by (Waggitt *et al.*, 2020).

Parameter codes	**Explanation**
BAT	Depth (m)
CHS	Total Chlorophyll (mg) in surface layer (satellite imagery)
CHT	Total Chlorophyll (mg) depth summed between 0 and 150m from surface (modelled)
CON	Distance to 300m isobath (m)
FEA	Depth gradient (m), calculated using terrain ruggedness index
LND	Distance to Land (m)
SPM	Mean surface current speed (ms-1), including tidal influence
TPF	Thermal stratification gradient, where higher values indicate greater frontal activity
TPM	Mean potential temperature (Celsius) between 0 and 150m from surface (modelled)
TPR	Range of potential temperature (Celsius) between 0 and 150m from surface (modelled)
TPS	Potential temperature (Celsius) in surface layer (satellite imagery)

Table 2.3 Details of chosen models. The species column details the common name of each species. The logistic parameter column lists the environmental parameter codes used in the logistic models and a colon between two parameters denotes interaction term between the two parameters. The environmental parameters corresponding to the codes are detailed in table 2.2. The offset column, 'Km': kilometres travelled per observation, 'Hr': survey time (in hours) per observation. Distribution column, 'NB 1': negative binomial distribution where the variance increases linearly with the predicted mean, 'NB 2': negative binomial distribution where the variance increases quadratically with the predicted mean, 'P': poisson distribution.

Species	Logistic parameter	Offset	Distribution
Puffin	CHT, TPS, BAT, TPF	Km	NB 1
black-legged kittiwake	TPM, TPF	Km	NB 1
bottlenose dolphin	CHT:BAT, TPS	Km	P
common guillemot	TPM, SPM, CHS, TPF	Km	NB 1
Common Dolphin	TPM:CON, CHT, TPR	-	NB 1
European shag	SPM, TPF, CHS, TPR	-	P
European Storm petrel	TPM, TPF, TPR	-	NB2
Fin whale	CHT:BAT	Km	NB 1
harbour porpoise	TPM:BAT, CHT, SPM	Km	NB 1
herring gull	CHT, TPM, SPM	Km	P
Lesser Black Backed Gull	CHT, TPM, SPM	Km	NB 1
Manx Shearwater	CHT, SPM	Km	P
Minke Whale	TPF, SPM	Km	NB 1
Northern Fulmar	CHT, FEA	Hr	P
Northern Gannet	TPM, TPF	Km	NB 1
Orca	TPR:TPS, CON:BAT	-	P
Pilot Whale	CON:TPM, FEA	-	NB 1
Razorbill	LND, TPF, TPM, TPR	Km	NB 1
Risso's Dolphin	BAT:TPM, CON	-	P
Sperm Whale	BAT:FEA, CON	Km	NB 2
Striped Dolphin	BAT:TPM	Km	P
White-beaked Dolphin	BAT:TPM	-	P
White-sided Dolphin	SPM:TPM	-	NB 1

As pod size of cetaceans can vary greatly (from pods of 2, to superpods from 200 to 1,000), a qualitative decision was made that it is reasonable to consider the maximum count values (for cetacean abundance in the dataset used for this study), non-anomalous, as it is probable that the values were accurate and not a produce of error. For many species, extremely high-count values were identified from visual inspection of Cleveland Dotplots. Since these high values are extreme (although not necessarily anomalous), there was not

enough observations to model the abundance and distribution of superpods with high accuracy. Furthermore, these values could have a large and disproportionate, influential effect on the model, skewing the fit, and so the rest of the observations would not have a close fit with the model, and little predictive power. When there are extreme values within a dataset, an option is to apply a transformation to the response data, however, transformations affect the relationship between the response and explanatory variables, so should be used with caution (Zuur *et al.*, 2009). Consequently, the extreme observations were discarded, and no transformation used. Influential observations are usually identified by visually inspecting a Cook's distance plot, however, published R functions did not have the capability to use zero-inflated models. It was not within the scope of this project to write a custom function that would not be ignorant of the zero-inflated nature of the data. Consequently, Cook's distance was calculated using the fit of a generalised linear model (GLM) of the count data only, and interpreted with caution, as it did not represent the full dataset. To assess for collinearity among explanatory variables, pair plots were generated and analysed, and Variance Inflation Factor (VIF) analysis was also conducted.

Overdispersion arises when the mean is smaller than the variance (Zuur *et al.*, 2009), which is common in heteroskedastic data. When a model is overdispersed, an option is to include overdispersion parameters, however this uses parameter space. Too many parameters can lead to overfitting, which lowers the predictive power of a model. The distribution families tested were poisson distribution and two functions of negative binomial. Poisson distribution is often used for count data (Zuur *et al.*, 2009), as it doesn't predict negative values.

Negative binomial function 1 is where the variance increases linearly with the predicted mean (Hardin & Hilbe, 2007):

$$variance = \mu * (1 + \varphi)$$

Where μ (mu) is the predicted mean, and φ (phi) is the dispersion parameter:

$$\varphi = \exp(\eta)$$

Where η (eta) is the linear predictor from the dispersion model.

Negative binomial function 2 is where the variance increases quadratically with predicted mean

$$variance = \mu * (1 + \frac{\mu}{\varphi})$$

The link is the relationship between the expected value of the response variable and the systematic part (Zuur *et al.*, 2009), (put more simply, it is the type of relationship between the mean and the variance). As the link specifies the expected relationship, it affects the coefficient values. Within the nested models, the log link function was used in the conditional regression model, and the logit link was used in the logistic model; this remained consistent among all models for comparability. The R function glmmTMB has capabilities of using Matern, Gaussian and Exponential covariance structures, to model the correlation between decay and distance and autoregressive order-1 functionality. When there is likely a bias in the data from collection, an option is to include an offset parameter, if, however, the effort bias does not influence the response variable, then parameter space should be saved, so the model does not become overparameterised.

Because the logistic part of the model refines the range of the conditional model to only the areas where they are likely to be present, the estimates for the slope values are only based on the relationship between their abundance and the environment within their likely range rather than the whole study area and represents the conditions where they are most likely to be abundant allowing us to see the nuance of their relationships with environment and facilitating more detailed comparisons between species that occur sympatrically.

2.1. Model validation and Selection

The use of both *k*-fold cross validation and Random-Walk Metropolis Sampling provides information on how parsimonious the models are. The *k*-fold cross validation assesses the predictive power of the model, and the Random-Walk Metropolis Sampling assesses the reproducibility of the regression coefficients on new data. The models were validated using the *k*-fold cross validation technique, where *k* is equal to 5. To understand how well the coefficients of the last parameters represent the model, posterior distribution samples of the coefficients were simulated using a random walk Metropolis sampling algorithm, using MCMCpack::MCMCmetrop1R (Martin *et al.*, 2011), which is a frequently used Markov Chain Monte Carlo algorithm. Trace and density plots from the random walk Metropolis sampling are displayed in appendix 2. Mean squared error for the predicted values of training data as a function of the test dataset for each iteration of the k-fold cross validation are reported in

appendix 2, along with other fit statistics of the ZIGLM, and maps of ZIGLM predictions of species distributions.

Histograms and density plots of the model residuals were used to assess normality. Pearson residuals were plotted against fitted values to assess whether the model was heteroskedastic. Residuals were plotted against explanatory variables to assess for non-independence. Akaike Information Criterion (AIC) and Bayesian Information Criterion (BIC) were considered when selecting the best model for each species. The log-likelihood values were compared when selecting the best model for each species.

2.2. Quantifying Similarity

As guilds and taxa groups are used to describe ecological or morphological similarity, it could be relevant to identify if their similarities are reflected in relationships between their distribution and environment. The results of this study identified where species sharing guilds/ taxa groups (table 2.4) are in the similarity structure in relation to each other and other species. Guilds/taxa groups (table 2.4) will be highlighted in the results section figures that represent the similarity structure, to assist visualisation of patterns. The guilds/ taxa groups defined in table 2.4 that are highlighted in the results section have been subset from guilds/ taxa groups and species with amalgamated data as they are commonly used groups. Furthermore, the groups provide simplification to interpretation of similarities between guilds/ taxa groups and are at a similar level of shared trait uniqueness compared to other species in the study and include more than two species within groups. Additionally, crossover between guild and closely related taxa are represented in some of these groups, for example auks are deep pursuit diving seabirds, gulls are surface feeders, rorquals (balaenopterids) are lunge filter-feeding cetaceans and deep diving odontocetes also represent teuthophageous cetaceans. The harbour porpoise, orca, European shag, and gannet were not highlighted in guilds/ taxa groups but were included for context, as they have similarities with other species in guilds/ taxa groups such as shared diet (although only the piscivorous orca ecotype share diet with the other species) and occur sympatrically in large parts of their ranges, and the European shag forages at similar depths to the auks.

Moreover, this maximised use of available data of many species in the marine top predator community in the northeast Atlantic.

Table 2.4 Guilds/ taxa groups to investigate.

Guilds/ taxa groups	Species common names	References
Auks	Razorbill, common guillemot, Atlantic puffin	(Anderwald *et al.*, 2011; McClellan *et al.*, 2014; Le Rest *et al.*, 2016; Wong *et al.*, 2018)
Deep diving odontocetes	Sperm whale, pilot whale, Risso's dolphin	(Praca & Gannier, 2008; Spitz *et al.*, 2011; Giorli *et al.*, 2016)
Small-sized delphinids	Common dolphin, striped dolphin, white-sided dolphin, white-beaked dolphin, bottlenose dolphin	(Sigurjónsson *et al.*, 1991; Lambert, Laran *et al.*, 2017; Lambert, Pettex *et al.*, 2017)
Gulls	Lesser black-backed gull, herring gull, black-legged kittiwake	(Anderwald *et al.*, 2011; Wong *et al.*, 2018)
Procellariiformes	Manx shearwater, European storm petrel, northern fulmar	
Rorquals	Fin whale, minke whale	(Kot *et al.*, 2014; Baines *et al.*, 2017; Kahane-Rapport *et al.*, 2020)

2.2.1. Slope value scaling

Because $m = \frac{dy}{dx}$, the response variables (*y*) need to be scaled if they are to be compared with slope values of other models with different response variables. However, models struggle to converge when a response variable is scaled 0-1, resulting in Standard Errors of around 4-5 orders of magnitude larger than the slope value. Therefore, the response variable was not scaled. To allow slope values of models with different response variables to be comparable, the slope values were scaled using the following equation:

$$m_{sc} = \frac{m(x_2 - x_1) - Y_{min}}{Y_{max} - Y_{min}} \cdot (s_{max} - s_{min}) + s_{min}$$

Where:

m_{sc} = scaled slope value
Y = response variable (vector)
x_1 = sample value of x
x_2 = sample value of x , where $x_2 > x_1$
S_{max} = maximum value to scale slope values to (0.8) (arbitrary positive value)
S_{min} = minimum value to scale slope values to (-0.8) (negative value with equal proximity to 0 as S_{max})

This equation was derived from $y = (\sum m_i\, x_i) + c$, the Straight-Line Equation.

Percentage change in population with a 20% increase in the value of the predictor was calculated using the following equation, where x_1 = 0.1 and x_2 = 0.3:

$$\frac{m(x_2 - x_1)}{y_{max}} \cdot 100$$

2.2.2. Dissimilarity

A distance matrix was calculated, using stats::dist (R Core Team, 2018), as a proxy for dissimilarity. The Euclidean distance measure was used.

$$S_{au}\sqrt{{S_{tu}}^{-2} + {S_{cu}}^{-2} + {S_{tfu}}^{-2} + {S_{du}}^{-2} + {S_{dgu}}^{-2}}$$

Table 2.5 Table of distance matrix equation terms. Term description and non-standardised parameter the term represents (ZiGLM parameter code).

Equation Term	Term Description	ZiGLM parameter code
S_{au}	Standardised Abundance Units	-
S_{tu}	Standardised Temperature Units	TPM
S_{cu}	Standardised Chlorophyll Units	CHT
S_{tfu}	Standardised Thermal Front Units	TPF
S_{du}	Standardised Depth Units	BAT
S_{dgu}	Standardised Depth Gradient Units	FEA

2.2.3. Clustering

Using stats::kmeans (R Core Team, 2018). To select the *k* value, an elbow method was used. The apex of the curve was six, which was therefore selected to represent *k.* Agglomerative hierarchical clustering was also used, an unsupervised machine learning technique was used to group the species by similarity in how their abundance varies with variation in environmental parameters. Agglomerative clustering starts off with all observations in individual clusters, (whereas divisive clustering starts with all observations in one cluster). Clusters most proximate to one another are merged with each time-step. The point where the clusters are joined is the node, the height of which shows the extent to which the leaves are similar. Various linkage criteria for agglomerative hierarchical clustering exist, which is the function used to compute pairwise distances. The function used determines the way in

which the clusters are considered distant. There are four main linkage criterions for agglomerative clustering; single, average, complete and ward's link and a distance matrix (Euclidean or Manhattan are commonly used metrics) as a measure of dissimilarity between observations. The clustering algorithm used Ward's 1963 linkage criterion (Murtagh & Legendre, 2014), which minimizes the total within-cluster variance. Clusters with minimum between-cluster distance are agglomerated. Using stats::hclust (R Core Team, 2018). Code used, including project package "MScResPACK" available at: https://github.com/RGreensmith/MScResPACK The use of these methods allowed 2,645 comparisons (number of species squared, multiplied by the number of parameters) to be evaluated and quantitatively simplified into latent similarity structures.

2.2.4 Cross-validation of similarity structure

To cross-validate the similarity structure, Pearson product-moment correlation coefficients were calculated between distance metrics representing structure of the different analyses (listed in table 2.6), to identify how well the latent structure identified by the analyses was mirrored throughout the different analyses.

Table 2.6 Table of inputs for Pearson product-moment correlation coefficient used in latent similarity structure cross validation. Distance metrics detail how the structure identified in the analysis type is represented as an input in the Pearson product-moment correlation coefficient to cross-validate the latent similarity structure.

Analysis type	Distance metrics
Hierarchical clustering	Cophenetic distances derived from the agglomerative hierarchical clustering analysis
Principle Component Analysis	Euclidean distances between the observation scores from principal components 1 and 2 from principal component analysis
ZIGLM conditional model coefficients	Euclidean distances between the conditional coefficients of the zero-inflated generalised models for each species
Classical multi-dimensional scaling	Euclidean distances between coordinates derived from classical multi-dimensional scaling

3.Results

Figures 3.1, 3.3 and 3.4 show that the guilds/taxa groups were dispersed throughout the similarity structure. The within guild/ taxa group dissimilarity was particularly stark between the rorquals (blue rectangle; figures 3.1 and 3.4a) and deep-diving odontocetes (green rectangle; figures 3.1 and 3.4a).

Figure 3.1 Biplot of principle components 1 and 2, of coefficients from the conditional models. Colour coded by the cluster to which the *k* means cluster algorithm assigned each species. Eigen vectors (direction of the variable plane through the matrix) of the variables are represented by the direction of the black arrows (each labelled with variable name in black) and the Eigen values (loading, or weighting of the variable) of the variables are represented by the length of the black arrows (each labelled with variable name in black). The scores of species are represented by positioning of the points (labelled with species abbreviation). Blue rectangles highlight rorquals, green rectangles highlight deep-diving odontocetes.

Figures 3.1 and 3.4a show that the minke whale (MINW) and harbour porpoise (HRBP) are close together within the similarity structure, and the combination of relationships with

environmental variables that explain their uniqueness to the other species, are also the combinations that make the minke whale and harbour porpoise similar to one another. The K-means clustering analysis identified a large cluster of 17 species and other than a cluster containing the Rissos dolphin and the Orca, the remainder of the clusters only contained one species. This was because the scale of the slope estimates for the 6 species not in this cluster were so much larger than the other species such that comparitively, the species with smaller slope estimates appeared to be similar. Because of this, the large group was taken as a subset and re-analysed to investigate if there were any other patterns present at the scale of those species. A taxa-based dissimilarity gradient can be observed in figure 3.2, where highly similar species were mostly seabirds, and progressing along the gradient of increasing dissimilarity, delphinids overlapped with seabirds, then the non-delphinid cetaceans had the greatest dissimilarity.

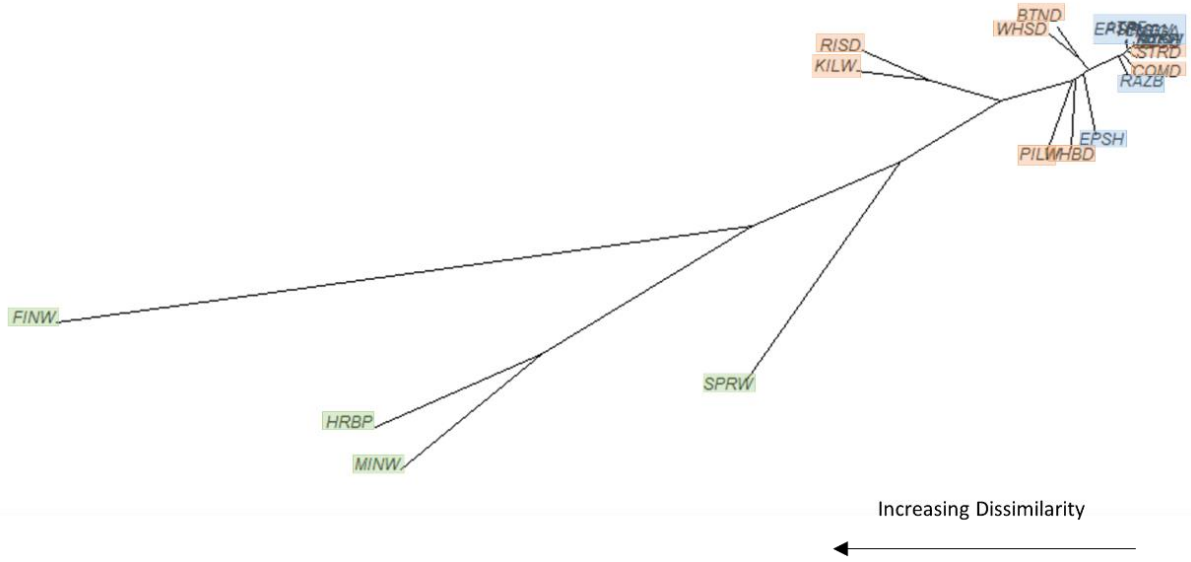

Figure 3.2 Unrooted dendrogram of hierarchical clustering. Unrooted dendrogram quantitatively derived from agglomerative hierarchical clustering of species ZIGLM conditional coefficients. Black arrow denotes increasing dissimilarity between species from right to left (length of arrow is arbitrary). Green shading highlights non-delphinid cetaceans, orange shading highlights delphinids and blue shading highlights seabirds.

Within the subset analysis, there was greatest dispersion throughout the similarity structure between the small-sized delphinids (green highlight; figures 3.3 and 3.4b) and auks (orange highlight; figures 3.3 and 3.4b). Within the gulls (yellow highlight; figures 3.3 and 3.4b), there was high similarity between the herring gull (HRGL) and black-legged kittiwake

(BLKW), but the lesser black-backed gull (LBGL) was dissimilar to the other gulls. Within the procellariiformes (purple highlight; figures 3.3 and 3.4b), there was high similarity between the manx shearwater (MXSH) and northern fulmar (NTFU), and the European storm petrel (EPSP) was more distant. The guillemot (CMGM), kittiwake (BLKW) and herring gull (HRGL) were highly similar to eachother, as were the gannet (NTGA), northern fulmar (NTFU) and manx shearwater (MXSH) to one another (figures 3.3 and 3.4b).

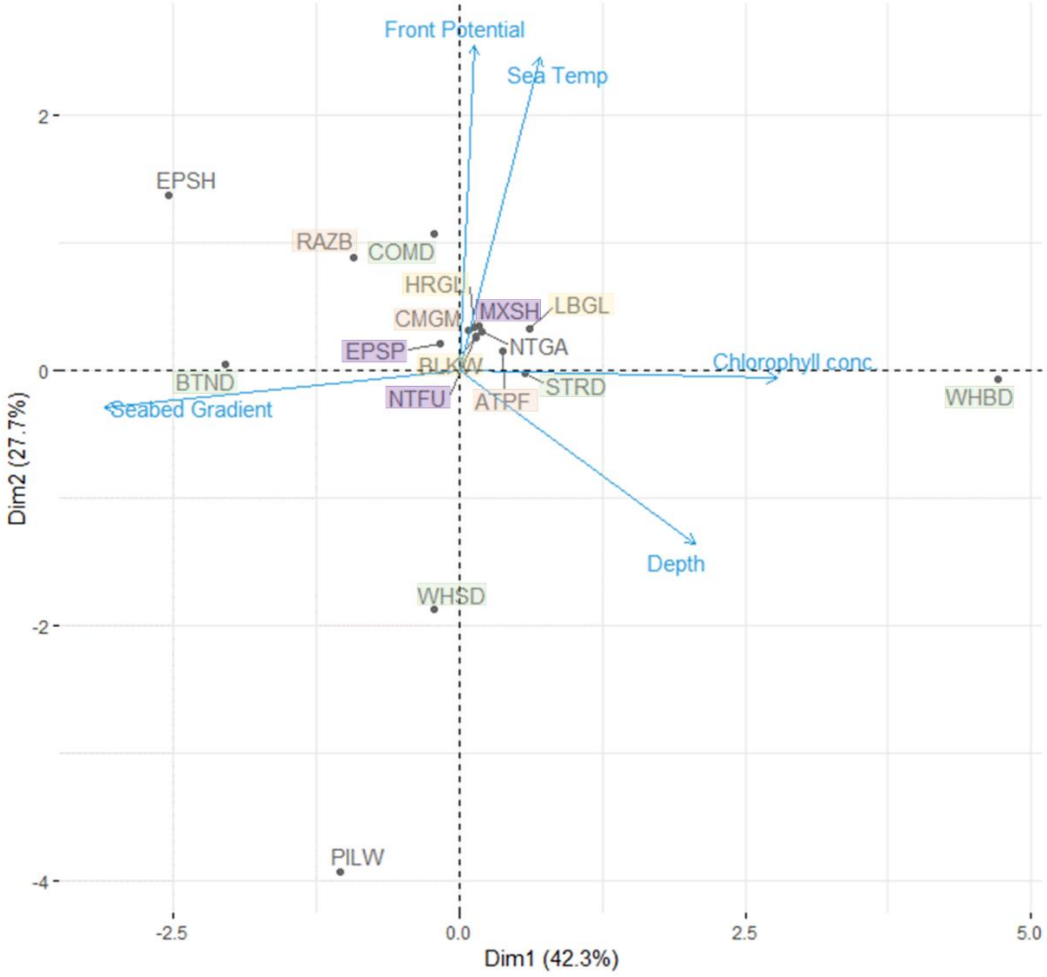

Figure 3.3 Biplot of principle components 1 and 2, of coefficients from the conditional models from the subset analysis of k means cluster 3. Eigen vectors (direction of the variable plane through the matrix) of the variables are represented by the direction of the black arrows (each labelled with variable name in black) and the Eigen values (loading, or weighting of the variable) of the variables are represented by the length of the blue arrows (each labelled with variable name in blue). The scores of species are represented by the grey points (labelled with species abbreviation). The scores of species are represented by positioning of the points (labelled with species abbreviation). Shaded rectangles highlight species groups, orange: auks, green: small-sized delphinids, yellow: gulls, purple: procellariiformes.

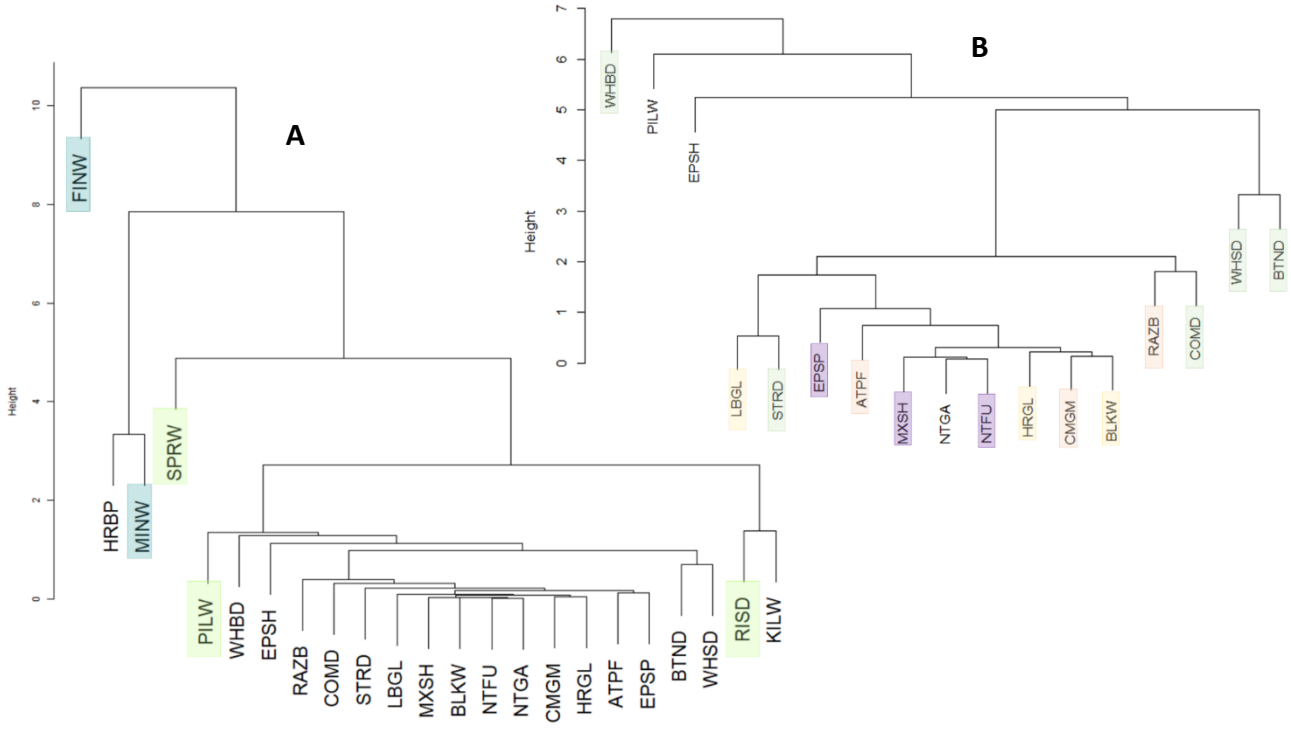

Figure 3.4 Dendrograms of hierarchical clustering of species ZIGLM conditional coefficients. Figure A is clustering of all species and figure B is the subset clustering. Shaded rectangles highlight species groups; in figure A, blue : rorquals and green: deep-diving odontocete, in figure B, orange: auks, green: small-sized delphinids, yellow: gulls, purple: procellariiformes.

The majority of seabirds and cetaceans abundance had the same direction of correlation with the dynamic variables: positive correlation with fronts and negative correlation with sea temperature and chlorophyll (table 3.1). However, the majority of seabirds and cetaceans' abundances were oppositely correlated with the static parameters: majority of seabirds were negatively correlated with seabed gradient and depth, whereas the majority of cetaceans were positively correlated (table 3.1). Depth was the only parameter with seabird coefficients over the 75th percentile (razorbill and European shag) and the most cetaceans below the 25th percentile (common, Risso's and striped dolphins) (table 3.1). Sea temperature was the only parameter where no cetacean coefficients were below the 25th percentile (table 3.1). For the seabirds, the order of the most important variables was: (i) depth, (ii) sea temperature, (iii) fronts, then (iv) both chlorophyll and seabed gradient equally, the order was opposite for the least important variables of seabirds (table 3.1). For cetaceans, the order of the most important variables was (i) fronts, (ii) depth, (iii) both sea

temperature and chlorophyll equally, then (iv) seabed gradient (table 3.1). The order of the least important variables for cetaceans was (i) depth, (ii) both chlorophyll and seabed gradient equally, then (iii) both fronts and sea temperature equally (table 3.1).

Fronts was the most important variable to the cetaceans that are predominantly found on the shelf edge and oceanic waters: two of the deep diving odontocetes (pilot whale and sperm whale), striped dolphin (all negatively correlated with fronts) and fin whale (positively correlated) (table 3.1). The most important variable for the predominantly neritic cetaceans (minke whale, white-beaked dolphin and harbour porpoise) was water depth, with which the white-beaked dolphin was negatively correlated (table 3.1). The only cetaceans with chlorophyll as the most important variable (Risso's and bottlenose dolphin) were negatively correlated (table 3.1). The most important variable for 3 of the deep diving seabirds was depth (guillemot, razorbill and shag), whereas sea temperature was most important to the puffin (table 3.1).

Table 3.1 Summary of conditional model slope estimates. Bold text highlights where species are above the 75th percentile. '<25th' identifies that the species absolute value is lower than the 25th percentile of all species absolute values for the corresponding predictor. '>75th' means that the species absolute value is greater than the 75th percentile of all species absolute values for the corresponding predictor, 'IQR' denotes the interquartile range. When the value contains '+', the abundance of that species increases linearly with an increase in the value of the corresponding predictor. When the value contains '-', the abundance of that species decreases linearly with an increase in the value of the corresponding predictor. Dark grey shading highlights the parameter with the steepest slope estimate compared to the other parameters for the species, light grey shading highlights the parameter with the shallowest slope estimate for the species.

	Species	Guild/taxa group	Sea Temp.	Thermal fronts	Chlorophyll	Seabed Gradient	Depth
Seabirds	Atlantic puffin	Auk	IQR -	IQR +	IQR +	IQR -	IQR -
	Common guillemot	Auk	IQR -	IQR +	IQR -	IQR -	IQR -
	Razorbill	Auk	<25th +	IQR +	IQR -	IQR +	**>75th -**
	Black-legged kittiwake	Gull	<25th -	<25th +	IQR -	<25th -	<25th -
	Herring gull	Gull	<25th -	<25th +	<25th -	IQR -	IQR -
	Lesser black-backed gull	Gull	IQR +	IQR -	IQR +	<25th -	IQR -
	European storm petrel	Procellariiform	IQR -	IQR -	IQR -	IQR -	IQR -
	Manx shearwater	Procellariiform	<25th +	<25th +	<25th +	<25th +	IQR -
	Northern Fulmar	Procellariiform	<25th -	<25th +	<25th -	<25th +	<25th -
	European shag		IQR -	IQR +	<25th +	IQR +	**>75th -**
	Northern Gannet		<25th -	<25th +	<25th +	<25th -	<25th -
Cetaceans	Pilot whale	Deep diving odontocete	**>75th -**	**>75th -**	IQR -	**>75th +**	IQR +
	Risso's dolphin	Deep diving odontocete	IQR -	**>75th +**	**>75th -**	IQR +	<25th +
	Sperm whale	Deep diving odontocete	**>75th -**	**>75th -**	**>75th +**	**>75th +**	**>75th +**
	Fin whale	Rorqual	**>75th +**	**>75th +**	**> 75th -**	IQR +	**>75th +**
	Minke whale	Rorqual	**>75th -**	**>75th +**	IQR -	**>75th +**	**>75th -**
	Bottlenose dolphin	Small-sized delphinid	IQR -	IQR +	IQR -	IQR +	IQR +
	Common dolphin	Small-sized delphinid	IQR +	IQR +	IQR -	<25th -	<25th +
	Striped dolphin	Small-sized delphinid	IQR +	IQR -	IQR +	IQR +	<25th +
	White-beaked dolphin	Small-sized delphinid	IQR -	<25th +	**>75th +**	**>75th -**	IQR +
	White-sided dolphin	Small-sized delphinid	**>75th -**	IQR +	<25th -	IQR -	IQR +
	Harbour porpoise		IQR -	IQR +	**>75th +**	**>75th +**	**> 75th -**
	Orca		**>75th -**	**>75th +**	**>75th -**	**>75th +**	IQR +

The strong positive correlations between the analyses and the dissimilarity matrix of species based on the ZIGLM conditional coefficients (table 3.2) validates the latent similarity structure persistent in the different analysis.

Table 3.2 Pearson product-moment correlation coefficient matrix of cophenetic distances derived from the agglomerative hierarchical clustering analysis (HClust. cophenetic dist.), Euclidean distances between the observation (species) scores from principle dimensions 1 and 2 from principle component analysis (Euclid dist. between pc1 and pc2 scores) and the Euclidean distances between the conditional coefficients of the zero-inflated generalised mixed models for each species (Euclid dist. between ZIGLM coefficients (conditional) for each species) and the Euclidean distances between coordinates derived from classical multi-dimensional scaling (Euclid dist. between coordinates from classical MDS).

	HClust. cophenetic dist.	Euclid dist. between pc1 and pc2 scores	Euclid dist. between ZIGLM coefficients (conditional) for each species	Euclid dist. between coordinates from classical MDS
HClust. cophenetic dist.	-			
Euclid dist. between pc1 and pc2 scores	0.963	-		
Euclid dist. between ZIGLM coefficients (conditional) for each species	0.976	0.984	-	
Euclid dist. between coordinates from classical MDS	0.963	1	0.984	-

4.Discussion

This study has identified a similarity structure amongst some of the seabird and cetacean community in the northeast Atlantic. On a coarse scale, the identified similarity structure followed a taxa-based dissimilarity gradient, where highly similar species were mostly seabirds, and progressing along the gradient of increasing dissimilarity, delphinids overlapped with seabirds, then the non-delphinid cetaceans had the greatest dissimilarity. The scale at which the non-delphinid cetaceans were dissimilar resulted in the dissimilarity of the seabirds and delphinids being negligible, resulting in a nested similarity structure that is observable when the non-delphinid cetaceans and the orca and Risso's dolphin are removed. Across both structures, there is a common theme of dissimilarity between species in the same guild, and similarity between sympatric species from separate guilds, and not closely related taxa.

The dissimilarity gradient largely reflected steepness of gradient of correlation with the environmental parameters, which could be expected to occur if species at one end of the gradient had a relatively low abundance in the study area and the other end of the gradient had a relatively high abundance. However, there was a mixture of species across this gradient with varying abundance in the study area, for example, species at the dissimilar end of the gradient includes the harbour porpoise, the most abundant cetacean in the study area (Hammond *et al.*, 2013), and the sperm whale and fin whale, which have a relatively low abundance in the study area (K. Macleod *et al.*, 2009; Rogan *et al.*, 2017). Furthermore, at the other end of the gradient are species with relatively high abundance such as the guillemot (Mitchell *et al.*, 2004), and species with relatively low abundance, such as the European storm petrel (Mitchell *et al.*, 2004). Another potential explanation could be annual variation in the presence of the species and similarity of the distribution across the seasons. However, this was also mixed across the dissimilarity gradient, for example, species that have a consistent year-round presence and have comparatively low variation in range across the seasons, such as the harbour porpoise (Laran, Pettex, David *et al.*, 2017) and European shag (Acker *et al.*, 2020) were spread across the dissimilarity gradient, and migratory species with low abundance in the study area at some parts of the year, such as the fin whales

(Laran, Pettex, David *et al.*, 2017; Gauffier *et al.*, 2020) and Manx shearwater (Guilford *et al.*, 2009), were at either end of the dissimilarity gradient.

A weak correlation between species distribution and the environmental parameters could occur if multiple environmental gradients were crossed, which could be more common amongst central place foragers, for example, seabirds during the breeding season (Patrick *et al.*, 2014). Another instance where this might also apply is when intraspecific habitat partitioning occurs within a range that encompasses multiple populations of a species. Intraspecific habitat partitioning has been found in many of the species in this study, particularly between male and female (Edwards *et al.*, 2016; Clark *et al.*, 2021), which, could result in more environmental gradients being crossed by that species if both genders were encompassed in the spatial range of the study. Within this study area, both genders of the seabirds are present, but relationships between foraging behaviours and habitat can be different between the genders for some species such as gannets (Cox *et al.*, 2016), which could result in more environmental gradients being represented by the species. Another example is the use of a dual foraging strategy by Manx shearwaters at the Skomer Island colony during the breeding season, where short foraging trips to the Celtic Sea front were used for chick provisioning, and longer foraging trips to the north and west of the Irish Sea front for maintaining personal body condition (Shoji *et al.*, 2015). Whilst both types of foraging trip were to fronts, there is potential for other environmental gradients to be crossed with this dual foraging strategy. Furthermore, high abundances of some seabirds in different habitats can occur where species such as Manx shearwaters raft in the sea nearby their breeding colony, often in large numbers (Richards *et al.*, 2019), which is a different type of habitat to areas where most intense foraging activity occurs. Furthermore, density-dependent competition results in foraging habitat partitioning between neighbouring colonies of conspecifics for a variety of seabirds, such as gannets (Wakefield *et al.*, 2013), lesser black-backed gulls (Corman *et al.*, 2016), kittiwakes and guillemots (Wakefield *et al.*, 2017), which could also result in more environmental gradients being crossed. At the other end of the taxa-based dissimilarity gradient, latitudinal partitioning can occur between genders of many of the non-delphinid cetaceans (Born *et al.*, 2003; Teloni *et al.*, 2008; Laidre *et al.*, 2009), so counts of these species within the northeast Atlantic could be more composed of one of the genders, which could result in less environmental gradients being

represented by the species. For example, mature male sperm whales mainly occur at higher latitudes than their conspecifics (Teloni *et al.*, 2008).

There was dissimilarity within guilds, which was particularly pronounced among auks, small-sized delphinids, rorquals, *Larus* gulls and deep-diving odontocetes. Niche partitioning has been found to occur within these guilds in numerous fine-scale studies, for example spatial partitioning of foraging areas between sympatric auks (Linnebjerg *et al.*, 2013; Symons, 2018; Gulka *et al.*, 2019; Delord *et al.*, 2020) and Larus gulls (Kubetzki & Garthe, 2003). Habitat partitioning within the small-sized delphinid guild has also been observed, for example, between white-sided and common dolphins (Gowans & Whitehead, 1995), common and striped dolphins (Giménez *et al.*, 2017), white-beaked and white-sided dolphins (MacLeod *et al.*, 2007), and trophic niche partitioning between the white-beaked and white-sided dolphins (Das *et al.*, 2003). Fine-scale spatial partitioning and trophic niche partitioning between the rorquals has also been found (Ingram *et al.*, 2007; Ryan *et al.*, 2013; Gavrilchuk *et al.*, 2014). The dissimilarity between the deep-diving odontocetes in the current study reflects observations of habitat and trophic niche partitioning between these species in literature (Azzellino *et al.*, 2008; Spitz *et al.*, 2011; Giorli *et al.*, 2016). Policy makers, planning authorities and conservationists frequently use species distribution models (SDMs) in planning and decision-making processes to predict the current and/or future distribution of a species (Mannocci *et al.*, 2017). However, ecological processes such as those observed in this study are rarely incorporated, potentially due to lack of data, reliable quantification of the processes and a lack of clarity on how relevant the processes are to the scenario. The results found here indicate that these processes, that are also observed in fine scale studies, could potentially be occurring on a larger scale.

There was a similarity pattern of species that share similar diets and occur sympatrically throughout parts of their range, but were from different guilds. For example, the northern fulmar is a surface feeder, the Manx shearwater is a pursuit plunger, and northern gannet a plunge diver (Furness & Tasker, 2000), yet they showed similarity. Despite sharing prey resources, aspects of the ecology of species showing similarity could result in comparatively low competitive pressure, potentially explaining how their relationships between distribution and environmental parameters could be relatively similar. The high similarity

between the gannet, fulmar and shearwater is largely due to their particularly weak relationships with environmental parameters in this study, which could be related to potentially being observed crossing many environmental gradients, as they are less constrained by central place foraging than the other seabirds in the study, frequently travelling over 50 km from their nests with maximum ranges over 330 km (Furness & Tasker, 2000; Thaxter *et al.*, 2012). The similarity could also be because of lack of competition, of the species in the current study, (Furness & Tasker, 2000) considered the gannet and fulmar (along with the herring gull and storm petrel) to have the greatest plasticity in diet and/or foraging methods, and the shearwater slightly less varied methods of foraging and/or prey types.

The guillemot, kittiwake and herring gull are the only species in this study with matching direction and similar magnitude of correlation between distribution and the parameters. The guillemot and kittiwake were more similar to each other than the herring gull. The guillemot and kittiwake are similar in that they share the same diet, as their main prey type is sandeels and other forage fish. They are both heavily dependent on sandeels, such that their breeding productivity has been linked to population dynamics of sandeels (Frederiksen *et al.*, 2006). They are also similar in that they have similar foraging ranges from the colony (Furness & Tasker, 2000; Thaxter *et al.*, 2012), their at-sea distribution overlaps (Waggitt *et al.*, 2020), their colonies can be adjacent to one-another (Newell *et al.*, 2015), and they are both present in the study area during the non-breeding season (Lambert, Pettex *et al.*, 2017). However, whilst they target the same prey and have similar ranges, their foraging behaviours are vastly different, as the kittiwake is a surface feeder, and the guillemot is a pursuit diver (Camphuysen & Webb, 1999). As their methods of catching prey greatly differ, it could be expected that they would need different physical environments for optimising efficiency of prey capture, specific to their behaviours. However, they are frequently observed in the same multi-species feeding aggregations, as the guillemots facilitate kittiwakes in capturing prey (Skov *et al.*, 2000; Camphuysen *et al.*, 2006). Camphuysen and Webb (Camphuysen & Webb, 1999) suggested that facilitation by guillemots could be a driver of kittiwake distribution, that auks could determine kittiwake foraging range extent, and that this mechanism influencing kittiwake distribution is greatly underestimated. The expected result from this theory would be that the guillemot and kittiwake have similar

relationships between their distribution and environment, which is present in the results of this study.

The kittiwake facilitates herring gulls in locating prey patches, described as 'catalysts' in multi-species feeding aggregations due to their high visibility (Camphuysen & Webb, 1999; Anderwald *et al.*, 2011). The behaviours of herring gulls can break up the multi-species feeding aggregations, by sitting in the centre of the prey patch, blocking the other surface feeders, where they often remain until another aggregation is visible (Camphuysen & Webb, 1999). Since many kittiwake populations are declining (Frederiksen, 2010), it is important to have a clear understanding of the processes influencing their distribution. Future research must be undertaken to identify if facilitation by feeding guillemots influences kittiwake distribution, and if this is the case, then it is important to understand the extent of this effect.

The minke whale and harbour porpoise were found to be similar in this study however, unlike the possible explanation for similarity between the guillemot and kittiwake, it is highly unlikely that facilitation occurs between the minke whale and harbour porpoise. Despite their range and dietary overlap, the similarity between the minke whale and harbour porpoise could be explained by lack of competitive exclusion due to their different foraging strategies (Johnston & Berta, 2011; Kot *et al.*, 2014). Furthermore, their solitary nature (Sigurjónsson *et al.*, 1991) could be less exclusionary to each other at prey patches.

4.1 Critical appraisal of the methods

Using linear models to model non-linear data results in information loss, however, it was outside of the scope of the project to develop statistical methods to enable a quantifiable comparison of the species relationships of non-linear models, which is why generalised linear models were chosen. Further improvement to the models would be incorporating spatial and temporal autocorrelation structures, however there was not enough time to run these models. Slope estimates used in the similarity analysis were scaled to allow comparison of slope estimates amongst models, however, this did not account for skewness of the different species abundance data.

This could be problematic, for instance, scaling slope estimates to the maximum value of right-skewed data will result in a shallower slope estimate than that of similarly correlated data with a more normal distribution. Whilst a square root transformation of the count data would reduce right-skewedness, this can be problematic as transformations alter the relationship between the response and explanatory variables (Zuur *et al.*, 2009). A more robust approach would be to account for right skewedness of the response variable in scaling the slope estimates, by using the 75th percentile of the response variable rather than the maximum value when scaling.

To test this theory, this and the original scaling methods were applied to a conditional coefficient of two species, (one heavily skewed, and the other more normally distributed), the outcome was that the relative difference between slope estimate scaled using 75th percentile of *y* was slightly smaller than when the slope estimate was scaled using maximum *y*, however the extent that it could affect interpretability of the similarity structure was sufficiently negligible. Furthermore, count data for most of the species are right skewed, therefore the effect of skewedness on coefficient scaling is relatively consistent and patterns of similarity are still interpretable.

4.2 Conclusion

The scale of the relationship between species abundance and their environment was distinct between taxa, as non-delphinid cetaceans had much stronger correlations than delphinids and seabirds. Furthermore, species with resource overlap that were not closely related or from the same guilds, showed similarity and there was a pattern of dissimilarity between species that were closely related or sharing guilds, which reflected patterns expected from species interactions such as habitat partitioning and coexistence. The relationships between distribution and environmental parameters of many marine top predators cannot be grouped together purely based on them being closely related or sharing guilds. Future research directions arisen from this study includes identifying underlying mechanisms driving this similarity structure and exploring whether interspecific interactions have a role.

5.References

Acker, P., Daunt, F., Wanless, S., Burthe, S.J., Newell, M.A., Harris, M.P., Grist, H., Sturgeon, J., Swann, R.L., Gunn, C., Payo-Payo, A., and Reid, J.M. (2020). Strong survival selection on seasonal migration versus residence induced by extreme climatic events. *Journal of Animal Ecology* 90, 796–808.

Anderwald, P., Evans, P., Gygax, L., and Hoelzel, A. (2011). Role of feeding strategies in seabird–minke whale associations. *Marine Ecology Progress Series* 424, 219–227.

Anderwald, P., Evans, P.G.H., Dyer, R., Dale, A., Wright, P.J., and Hoelzel, A.R. (2012). Spatial scale and environmental determinants in minke whale habitat use and foraging. *Marine Ecology Progress Series* 450, 259–274.

Azzellino, A., Gaspari, S., Airoldi, S., and Nani, B. (2008). Habitat use and preferences of cetaceans along the continental slope and the adjacent pelagic waters in the western Ligurian Sea. *Deep-Sea Research: Part I* 55, 296–323.

Bailey, H., Brookes, K.L., and Thompson, P.M. (2014). Assessing environmental impacts of offshore wind farms: lessons learned and recommendations for the future. *Aquatic Biosystems* 10:8.

Bailey, H., Senior, B., Simmons, D., Rusin, J., Picken, G., and Thompson, P.M. (2010). Assessing underwater noise levels during pile-driving at an offshore windfarm and its potential effects on marine mammals. *Marine Pollution Bulletin* 60, 888–897.

Baines, M., Reichelt, M., and Griffin, D. (2017). An autumn aggregation of fin (Balaenoptera physalus) and blue whales (B. musculus) in the Porcupine Seabight, southwest of Ireland. *Deep Sea Research Part II: Topical Studies in Oceanography* 141, 168–177.

Baltzer, J., Maurer, N., Schaffeld, T., Ruser, A., Schnitzler, J.G., and Siebert, U. (2020). Effect ranges of underwater noise from anchor vibration operations in the Wadden Sea. *Journal of Sea Research* 162, 101912.

Baptist, M., van Bemmelen, R., Leopold, M., de Haan, D., Flores, H., Couperus, B., Fassler, S., and Geelhoed, S. (2019). Self-foraging vs facilitated foraging by Lesser Black-backed Gull (Larus fuscus) at the Frisian Front, the Netherlands. *Bulletin of Marine Science* 95, 29–43.

Baum, J.K., and Worm, B. (2009). Cascading top-down effects of changing oceanic predator abundances. *Journal of Animal Ecology* 78, 699–714.

Bearzi, G., Politi, E., Agazzi, S., and Azzellino, A. (2006). Prey depletion caused by overfishing and the decline of marine megafauna in eastern Ionian Sea coastal waters (central Mediterranean). *Biological Conservation* 127, 373–382.

Berrow, S., Volkenandt, M., O'connor, I., Guarini, J.-M., and O'donnell, C. (2015). Fine-scale spatial association between baleen whales and forage fish in the Celtic Sea. *Article in Canadian Journal of Fisheries and Aquatic Sciences* 73, 197–204.

Booth, C.G., Embling, C., Gordon, J., Calderan, S. V., and Hammond, P.S. (2013). Habitat preferences and distribution of the harbour porpoise Phocoena phocoena west of Scotland. *Marine Ecology Progress Series* 478, 273–285.

Born, E.W., Outridge, P., Riget, F.F., Hobson, K.A., Dietz, R., Øien, N., and Haug, T. (2003). Population substructure of North Atlantic minke whales (Balaenoptera acutorostrata) inferred from regional variation of elemental and stable isotopic signatures in tissues. *Journal of Marine Systems* 43, 1–17.

Broennimann, O., Fitzpatrick, M.C., Pearman, P.B., Petitpierre, B., Pellissier, L., Yoccoz, N.G., Thuiller, W., Fortin, M.J., Randin, C., Zimmermann, N.E., Graham, C.H., and Guisan, A. (2012). Measuring ecological niche overlap from occurrence and spatial environmental data. *Global Ecology and Biogeography* 21, 481–497.

Brooks, M.E., Kristensen, K., van Benthem, K.J., Magnusson, A., Berg, C.W., Nielsen, A., Skaug, H.J., Mächler, M., and Bolker, B.M. (2017). glmmTMB balances speed and flexibility among packages for zero-inflated generalized linear mixed modeling. *R Journal* 9, 378–400.

Burke, C.M., and Montevecchi, W.A. (2009). The foraging decisions of a central place foraging seabird in response to fluctuations in local prey conditions. *Journal of Zoology* 278, 354–361.

Burthe, S.J., Wanless, S., Newell, M.A., Butler, A., and Daunt, F. (2014). Assessing the vulnerability of the marine bird community in the western North Sea to climate change and other anthropogenic impacts. *Marine Ecology Progress Series* 507, 277–295.

Camphuysen, C., Scott, B., and Wanless, S. (2006). Distribution and foraging interactions of seabirds and marine mammals in the North Sea: a metapopulation analysis. In I. L. Boyd, S. Wanless, & C. J. Camphuysen (Eds.), *Top Predators in Marine Ecosystems: Their Role in Monitoring and Management* (pp. 82–97). Cambridge University Press.

Camphuysen, C., and Webb, A. (1999). Multi-species feeding associations in North Sea seabirds: jointly exploiting a patchy environment. *Ardea* 87, 1999.

Cañadas, A., Sagarminaga, R., and García-Tiscar, S. (2002). Cetacean distribution related with depth and slope in the Mediterranean waters off southern Spain. *Deep-Sea Research Part I: Oceanographic Research Papers* 49, 2053–2073.

Canning, S., Santos, B., Reid, R., Evans, P., Sabin, R., Bailey, N., and Pierce, G. (2008). Seasonal distribution of white-beaked dolphins (Lagenorhynchus albirostris) in UK waters with new information on diet and habitat use. *Journal of the Marine Biological Association of the United Kingdom* 88, 1159–1166.

Carroll, R.L. (2001). The origin and early radiation of terrestrial vertebrates. *Journal of Paleontology* 75, 1202–1213.

Certain, G., Masse, J., Van Canneyt, O., Petitgas, P., Doremus, G., Santos, M., and Ridoux, V. (2011). Investigating the coupling between small pelagic fish and marine top predators using data collected from ecosystem-based surveys. *Marine Ecology Progress Series* 422, 23–39.

Clark, B., Cox, S., Atkins, K., Bearhop, S., Bicknell, A., Bodey, T., Cleasby, I., Grecian, W., Hamer, K., Loveday, B., Miller, P., Morgan, G., Morgan, L., Newton, J., Patrick, S., Scales, K., Sherley, R., Vigfúsdóttir, F., Wakefield, E., and Votier, S. (2021). Sexual segregation of gannet foraging over 11 years: movements vary but isotopic differences remain stable. *Marine Ecology Progress Series* 661, 1–16.

Corman, A.M., Mendel, B., Voigt, C.C., and Garthe, S. (2016). Varying foraging patterns in response to competition? A multicolony approach in a generalist seabird. *Ecology and Evolution* 6, 974–86.

Cotté, C., Guinet, C., Taupier-Letage, I., and Petiau, E. (2010). Habitat use and abundance of striped dolphins in the western Mediterranean Sea prior to the morbillivirus epizootic resurgence. *Endangered Species Research* 12, 203–214.

Couperus, A.S. (1997). Interactions Between Dutch Midwater Trawl and Atlantic White-sided Dolphins (Lagenorhynchus acutus) Southwest of Ireland. *Journal of Northwest Atlantic Fishery Science* 22, 209–218.

Cox, S.L., Embling, C.B., Hosegood, P.J., Votier, S.C., and Ingram, S.N. (2018). Oceanographic drivers of marine mammal and seabird habitat-use across shelf-seas: A guide to key features and recommendations for future research and conservation management. *Estuarine, Coastal and Shelf Science* 212, 294–310.

Cox, S.L., Votier, S.C., Miller, P.I., Embling, C.B., Scales, K.L., Bicknell, A.W.J., Hosegood, P.J., Morgan, G., and Ingram, S.N. (2016). Seabird diving behaviour reveals the functional significance of shelf-sea fronts as foraging hotspots. *Royal Society Open Science* 3: 160317.

Das, K., Lepoint, G., Leroy, Y., and Bouquegneau, J. (2003). Marine mammals from the southern North Sea: feeding ecology data from δ13C and δ15N measurements. *Marine Ecology Progress Series* 263, 287–298.

Davis, M.B., and Guderley, H. (1990). Biochemical adaptations to diving in the common murre, Uria aalge, and the Atlantic puffin, Fratercula arctica. *Journal of Experimental Zoology* 253, 235–244.

de Stephanis, R., Cornulier, T., Verborgh, P., Salazar Sierra, J., Gimeno, N., and Guinet, C. (2008). Summer spatial distribution of cetaceans in the Strait of Gibraltar in relation to the oceanographic context. *Marine Ecology Progress Series* 353, 275–288.

Delord, K., Barbraud, C., Pinaud, D., and Letournel, B. (2020). Movements of three alcid species breeding sympatrically in Saint Pierre and Miquelon, northwestern Atlantic Ocean. *Journal of Ornithology* 161, 359–371.

DeMaster, D.P., Fowler, C.W., Perry, S.L., and Richlen, M.F. (2001). Predation and Competition: The Impact of Fisheries on Marine-Mammal Populations Over the next one Hundred Years. *Journal of Mammalogy* 82, 641–651.

Doniol-Valcroze, T., Berteaux, D., Larouche, P., and Sears, R. (2007). Influence of thermal fronts on habitat selection by four rorqual whale species in the Gulf of St. Lawrence. *Marine Ecology Progress Series* 335, 207–216.

Edwards, E.W.J., Quinn, L.R., and Thompson, P.M. (2016). State-space modelling of geolocation data reveals sex differences in the use of management areas by breeding northern fulmars. *Journal of Applied Ecology* 53, 1880–1889.

Embling, C.B., Illian, J., Armstrong, E., van der Kooij, J., Sharples, J., Camphuysen, C.J., and Scott, B.E. (2012). Investigating fine-scale spatio-temporal predator–prey patterns in dynamic marine ecosystems: a functional data analysis approach. *Journal of Applied Ecology* 49, 481–492.

Embling, C.B., Sharples, J., Armstrong, E., Palmer, M.R., and Scott, B.E. (2013). Fish behaviour in response to tidal variability and internal waves over a shelf sea bank. *Progress in Oceanography* 117, 106–117.

Esteban, R., Verborgh, P., Gauffier, P., Giménez, J., Afán, I., Cañadas, A., García, P., Murcia, J.L., Magalhães, S., Andreu, E., and de Stephanis, R. (2014). Identifying key habitat and seasonal patterns of a critically endangered population of killer whales. *Journal of the Marine Biological Association of the United Kingdom* 94, 1317–1325.

Fayet, A.L., Clucas, G. V., Anker-Nilssen, T., Syposz, M., and Hansen, E.S. (2021). Local prey shortages drive foraging costs and breeding success in a declining seabird, the Atlantic puffin. *Journal of Animal Ecology* 90, 1152–1164.

Frederiksen, M. (2010). Appendix 1: Seabirds in the North East Atlantic. A review of status, trends and anthropogenic impact. *TemaNord* 587, 47–122.

Frederiksen, M., Edwards, M., Richardson, A.J., Halliday, N.C., and Wanless, S. (2006). From plankton to top predators: bottom-up control of a marine food web across four trophic levels. *Journal of Animal Ecology* 75, 1259–1268.

Friedlaender, A.S., Bowers, M.T., Cade, D., Hazen, E.L., Stimpert, A.K., Allen, A.N., Calambokidis, J., Fahlbusch, J., Segre, P., Visser, F., Southall, B.L., and Goldbogen, J.A. (2020). The advantages of diving deep: Fin whales quadruple their energy intake when targeting deep krill patches. *Functional Ecology* 34, 497–506.

Furness, R.W., and Tasker, M.L. (2000). Seabird-fishery interactions: quantifying the sensitivity of seabirds to reductions in sandeel abundance, and identification of key

areas for sensitive seabirds in the North Sea. *Marine Ecology Progress Series* 202, 253–264.

Garthe, S., Guse, N., Montevecchi, W.A., Rail, J.F., and Grégoire, F. (2014). The daily catch: Flight altitude and diving behavior of northern gannets feeding on Atlantic mackerel. *Journal of Sea Research* 85, 456–462.

Gauffier, P., Borrell, A., Silva, M.A., Víkingsson, G.A., López, A., Giménez, J., Colaço, A., Halldórsson, S.D., Vighi, M., Prieto, R., de Stephanis, R., and Aguilar, A. (2020). Wait your turn, North Atlantic fin whales share a common feeding ground sequentially. *Marine Environmental Research* 155, 104884.

Gavrilchuk, K., Lesage, V., Ramp, C., Sears, R., Bérubé, M., Bearhop, S., and Beauplet, G. (2014). Trophic niche partitioning among sympatric baleen whale species following the collapse of groundfish stocks in the Northwest Atlantic. *Marine Ecology Progress Series* 497, 285–301.

Gilles, A., Adler, S., Kaschner, K., Scheidat, M., and Siebert, U. (2011). Modelling harbour porpoise seasonal density as a function of the German Bight environment: Implications for management. *Endangered Species Research* 14, 157–169.

Giménez, J., Cañadas, A., Ramírez, F., Afán, I., García-Tiscar, S., Fernández-Maldonado, C., José Castillo, J., and de Stephanis, R. (2017). Intra-and interspecific niche partitioning in striped and common dolphins inhabiting the southwestern Mediterranean Sea. *Marine Ecology Progress Series* 567, 199–210.

Giorli, G., Neuheimer, A., and Au, W. (2016). Spatial variation of deep diving odontocetes' occurrence around a canyon region in the Ligurian Sea as measured with acoustic techniques. *Deep Sea Research Part I: Oceanographic Research Papers* 116, 88–93.

Godsoe, W. (2014). Inferring the similarity of species distributions using Species' Distribution Models. *Ecography* 37, 130–136.

Gowans, S., and Whitehead, H. (1995). Distribution and habitat partitioning by small odontocetes in the Gully, a submarine canyon on the Scotian Shelf. *Canadian Journal of Zoology* 73, 1599–1608.

Grémillet, D., and Boulinier, T. (2009). Spatial ecology and conservation of seabirds facing global climate change: a review. *Marine Ecology Progress Series* 391, 121–137.

Grémillet, D., Péron, C., Kato, A., Amélineau, F., Ropert-Coudert, Y., Ryan, P.G., and Pichegru, L. (2016). Starving seabirds: unprofitable foraging and its fitness consequences in Cape gannets competing with fisheries in the Benguela upwelling ecosystem. *Marine Biology* 163: 35, 1–11.

Griffiths, J. (2015). *The definition of bottlenose dolphin specific MPAs: Habitat modelling of the English Channel and Bay of Biscay using data from platforms of opportunity*. Plymouth University. https://doi.org/10.13140/RG.2.1.4792.4560

Guilford, T., Meade, J., Willis, J., Phillips, R.A., Boyle, D., Roberts, S., Collett, M., Freeman, R., and Perrins, C.M. (2009). Migration and stopover in a small pelagic seabird, the Manx shearwater Puffinus puffinus: Insights from machine learning. *Proceedings of the Royal Society B: Biological Sciences* 276, 1215–1223.

Gulka, J., Ronconi, R.A., and Davoren, G.K. (2019). Spatial segregation contrasting dietary overlap: niche partitioning of two sympatric alcids during shifting resource availability. *Marine Biology* 166, 115.

Hammond, P.S., Macleod, K., Berggren, P., Borchers, D.L., Burt, L., Cañadas, A., Desportes, G., Donovan, G.P., Gilles, A., Gillespie, D., Gordon, J., Hiby, L., Kuklik, I., Leaper, R., Lehnert, K., Leopold, M., Lovell, P., Øien, N., Paxton, C.G.M., Ridoux, V., Rogan, E., Samarra, F., Scheidat, M., Sequeira, M., Siebert, U., Skov, H., Swift, R., Tasker, M.L., Teilmann, J., Van Canneyt, O., and Vázquez, J.A. (2013). Cetacean abundance and distribution in European Atlantic shelf waters to inform conservation and management. *Biological Conservation* 164, 107–122.

Hardin, J.W., and Hilbe, J.M. (2007). *Generalized linear models and extensions* (2nd ed.). Stata Press.

Hastie, G.D., Wilson, B., Wilson, L.J., Parsons, K.M., and Thompson, P.M. (2004). Functional mechanisms underlying cetacean distribution patterns: Hotspots for bottlenose dolphins are linked to foraging. *Marine Biology* 144, 397–403.

Hedges, S.B., Parker, P.H., Sibley, C.G., and Kumar, S. (1996). Continental breakup and the ordinal diversification of birds and mammals. *Nature* 381, 226–229.

Heithaus, M.R., Frid, A., Wirsing, A.J., and Worm, B. (2008). Predicting ecological consequences of marine top predator declines. *Trends in Ecology & Evolution* 23, 202–210.

Herr, H., Fock, H.O., and Siebert, U. (2009). Spatio-temporal associations between harbour porpoise Phocoena phocoena and specific fisheries in the German Bight. *Biological Conservation* 142, 2962–2972.

Ingram, S., Walshe, L., Johnston, D., and Rogan, E. (2007). Habitat partitioning and the influence of benthic topography and oceanography on the distribution of fin and minke whales in the Bay of Fundy, Canada. *Journal of the Marine Biological Association of the United Kingdom* 87, 149–156.

Jansen, O.E., Leopold, M.F., Meesters, E.H. w. g., and Smeenk, C. (2010). Are white-beaked dolphins Lagenorhynchus albirostris food specialists? Their diet in the southern North Sea. *Journal of the Marine Biological Association of the United Kingdom* 90, 1501–1508.

Johnston, C., and Berta, A. (2011). Comparative anatomy and evolutionary history of suction feeding in cetaceans. *Marine Mammal Science* 27, 493–513.

Jones, A.R., Hosegood, P., Wynn, R.B., De Boer, M.N., Butler-Cowdry, S., and Embling, C.B.

(2014). Fine-scale hydrodynamics influence the spatio-temporal distribution of harbour porpoises at a coastal hotspot. *Progress in Oceanography* 128, 30–48.

Kahane-Rapport, S.R., Savoca, M.S., Cade, D.E., Segre, P.S., Bierlich, K.C., Calambokidis, J., Dale, J., Fahlbusch, J.A., Friedlaender, A.S., Johnston, D.W., Werth, A.J., and Goldbogen, J.A. (2020). Lunge filter feeding biomechanics constrain rorqual foraging ecology across scale. *Journal of Experimental Biology* 223: jeb224196.

Kneitel, J.M., and Chase, J.M. (2004). Trade-offs in community ecology: Linking spatial scales and species coexistence. *Ecology Letters* 7, 69–80.

Kooyman, G.., and Ponganis, P.. (1998). The physiological basis of diving to depth: birds and mammals. *Annual Review of Physiology* 60, 19–32.

Kot, B.W., Sears, R., Zbinden, D., Borda, E., and Gordon, M.S. (2014). Rorqual whale (Balaenopteridae) surface lunge-feeding behaviors: Standardized classification, repertoire diversity, and evolutionary analyses. *Marine Mammal Science* 30, 1335–1357.

Kubetzki, U., and Garthe, S. (2003). Distribution, diet and habitat selection by four sympatrically breeding gull species in the south-eastern North Sea. *Marine Biology* 143, 199–207.

Laidre, K.L., Heagerty, P.J., Heide-Jørgensen, M.P., Witting, L., and Simon, M. (2009). Sexual segregation of common minke whales (Balaenoptera acutorostrata) in Greenland, and the influence of sea temperature on the sex ratio of catches. *ICES Journal of Marine Science* 66, 2253–2266.

Lambert, C., Laran, S., David, L., Dorémus, G., Pettex, E., Van Canneyt, O., and Ridoux, V. (2017). How does ocean seasonality drive habitat preferences of highly mobile top predators? Part I: The north-western Mediterranean Sea. *Deep Sea Research Part II: Topical Studies in Oceanography* 141, 115–132.

Lambert, C., Mannocci, L., Lehodey, P., and Ridoux, V. (2014). Predicting Cetacean Habitats from Their Energetic Needs and the Distribution of Their Prey in Two Contrasted Tropical Regions. *PLoS ONE* 9, e105958.

Lambert, C., Pettex, E., Dorémus, G., Laran, S., Stéphan, E., Canneyt, O. Van, and Ridoux, V. (2017). How does ocean seasonality drive habitat preferences of highly mobile top predators? Part II: The eastern North-Atlantic. *Deep Sea Research Part II: Topical Studies in Oceanography* 141, 133–154.

Laran, S., Pettex, E., Authier, M., Blanck, A., David, L., Dorémus, G., Falchetto, H., Monestiez, P., Van Canneyt, O., and Ridoux, V. (2017). Seasonal distribution and abundance of cetaceans within French waters- Part I: The North-Western Mediterranean, including the Pelagos sanctuary. *Deep-Sea Research Part II: Topical Studies in Oceanography* 141, 20–30.

Laran, S., Pettex, E., David, L., Dorémus, G., Falchetto, H., Monestiez, P., and Van Canneyt, O. (2017). Seasonal distribution and abundance of cetaceans within French waters-Part I: The North-Western Mediterranean, including the Pelagos sanctuary. *Deep Sea Research Part II: Topical Studies in Oceanography* 141, 20–30.

Le Rest, K., Certain, G., Debétencourt, B., and Bretagnolle, V. (2016). Spatio-temporal modelling of auk abundance after the Erika oil spill and implications for conservation. *Journal of Applied Ecology* 53, 1862–1870.

Leonard, D.M., and Øien, N.I. (2020). Estimated abundances of cetacean species in the Northeast Atlantic from two multiyear surveys conducted by Norwegian vessels between 2002–2013. *NAMMCO Scientific Publications* 11.

Linnebjerg, J.F., Fort, J., Guilford, T., Reuleaux, A., Mosbech, A., and Frederiksen, M. (2013). Sympatric Breeding Auks Shift between Dietary and Spatial Resource Partitioning across the Annual Cycle. *PLOS ONE* 8, e72987.

Macleod, C.D., Bannon, S.M., Pierce, G.J., Schweder, C., Learmonth, J.A., Herman, J.S., and Reid, R.J. (2005). Climate change and the cetacean community of north-west Scotland. *Biological Conservation* 124, 477–483.

MacLeod, C.D., Weir, C.R., Pierpoint, C., and Harland, E.J. (2007). The habitat preferences of marine mammals west of Scotland (UK). *Journal of the Marine Biological Association of the UK* 87, 157.

Macleod, K., Burt, L., Cañadas, A., Lens, S., Rogan, E., Santos, B., Uriarte, A., Van Canneyt, O., Vazquez, J.A., and Hammond, P. (2009). Distribution and Abundance of Fin whales and other baleen whales in the European Atlantic. *In: Commission, I.W. (Ed.), SC/61/RMP10*.

Macleod, K., Fairbairns, R., Gill, A., Fairbairns, B., Gordon, J., Blair-Myers, C., and Parsons, E.C.M. (2004). Seasonal distribution of minke whales Balaenoptera acutorostrata in relation to physiography and prey off the Isle of Mull, Scotland. *Marine Ecology Progress Series* 277, 263–274.

Macleod, K., Simmonds, M., and Murray, E. (2003). Summer distribution and relative abundance of cetacean populations off north-west Scotland. *Journal of the Marine Biological Association of the United Kingdom* 83, 1187–1192.

Mann, J., and Karniski, C. (2017). Diving beneath the surface: long-term studies of dolphins and whales. *Journal of Mammalogy* 98, 621–630.

Mannocci, L., Boustany, A.M., Roberts, J.J., Palacios, D.M., Dunn, D.C., Halpin, P.N., Viehman, S., Moxley, J., Cleary, J., Bailey, H., Bograd, S.J., Becker, E.A., Gardner, B., Hartog, J.R., Hazen, E.L., Ferguson, M.C., Forney, K.A., Kinlan, B.P., Oliver, M.J., Perretti, C.T., Ridoux, V., Teo, S.L.H., and Winship, A.J. (2017). Temporal resolutions in species distribution models of highly mobile marine animals: Recommendations for ecologists and managers. *Diversity and Distributions* 23, 1098–1109.

Mannocci, L., Roberts, J.J., Pedersen, E.J., and Halpin, P.N. (2020). Geographical differences in habitat relationships of cetaceans across an ocean basin. *Ecography* 43, 1–10.

Maravelias, C.D., Reid, D.G., and Swartzman, G. (2000). Seabed substrate, water depth and zooplankton as determinants of the prespawning spatial aggregation of North Atlantic herring. *Marine Ecology Progress Series* 195, 249–259.

Martin, A.D., Quinn, K.M., and Park, J.H. (2011). MCMCpack: Markov chain Monte Carlo in R. *JSS Journal of Statistical Software* 42.

McClellan, C.M., Brereton, T., Dell'Amico, F., Johns, D.G., Cucknell, A.-C., Patrick, S.C., Penrose, R., Ridoux, V., Solandt, J.-L., Stephan, E., Votier, S.C., Williams, R., and Godley, B.J. (2014). Understanding the Distribution of Marine Megafauna in the English Channel Region: Identifying Key Habitats for Conservation within the Busiest Seaway on Earth. *PLoS ONE* 9, e89720.

Mccurry, M.R., Fitzgerald, E.M.G., Evans, A.R., Adams, J.W., and Mchenry, C.R. (2017). Skull shape reflects prey size niche in toothed whales. *Biological Journal of the Linnean Society* 121, 936–946.

Mirceta, S., Signore, A. V., Burns, J.M., Cossins, A.R., Campbell, K.L., and Berenbrink, M. (2013). Evolution of mammalian diving capacity traced by myoglobin net surface charge. *Science* 340: 1234192.

Mitchell, P., Newton, S., Ratcliffe, N., and Dunn, T. (2004). *Seabird Populations of Britain and Ireland: results of the Seabird 2000 census (1998-2002)*. *Published by T and A.D. Poyser, London.* T and A.D. Poyser, London.

Moore, S.E., and Kuletz, K.J. (2019). Marine birds and mammals as ecosystem sentinels in and near Distributed Biological Observatory regions: An abbreviated review of published accounts and recommendations for integration to ocean observatories. *Deep-Sea Research Part II: Topical Studies in Oceanography* 162, 211–217.

Murtagh, F., and Legendre, P. (2014). Ward's Hierarchical Agglomerative Clustering Method: Which Algorithms Implement Ward's Criterion? *Journal of Classification 2014 31:3* 31, 274–295.

Newell, M., Wanless, S., Harris, M.P., and Daunt, F. (2015). Effects of an extreme weather event on seabird breeding success at a North Sea colony. *Marine Ecology Progress Series* 532, 257–268.

Nichol, L.M. (1990). *Seasonal movements and foraging behaviour of resident killer whales (Orcinus orca) in relation to the inshore distribution of salmon (Oncarhynchus spp.) in British Columbia*. University of British Columbia. https://doi.org/10.14288/1.0098406

Nøttestad, L., Krafft, B.A., Anthonypillai, V., Bernasconi, M., Langård, L., Mørk, H.L., and Fernö, A. (2015). Recent changes in distribution and relative abundance of cetaceans in the Norwegian Sea and their relationship with potential prey. *Frontiers in Ecology and*

Evolution 2, 83.

Pacariz, S. V., Hátún, H., Jacobsen, J.A., Johnson, C., Eliasen, S., and Rey, F. (2016). Nutrient-driven poleward expansion of the Northeast Atlantic mackerel (Scomber scombrus) stock: A new hypothesis. *Elementa: Science of the Anthropocene* 4, 105.

Paredes, R., Harding, A.M.A., Irons, D.B., Roby, D.D., Suryan, R.M., Orben, R.A., Renner, H., Young, R., and Kitaysky, A. (2012). Proximity to multiple foraging habitats enhances seabirds' resilience to local food shortages. *Marine Ecology Progress Series* 471, 253–269.

Paredes, R., Orben, R.A., Suryan, R.M., Irons, D.B., Roby, D.D., Harding, A.M.A., Young, R.C., Benoit-Bird, K., Ladd, C., Renner, H., Heppell, S., Phillips, R.A., and Kitaysky, A. (2014). Foraging Responses of Black-Legged Kittiwakes to Prolonged Food-Shortages around Colonies on the Bering Sea Shelf. *PLoS ONE* 9, e92520.

Patrick, S.C., Bearhop, S., Grémillet, D., Lescroël, A., Grecian, W.J., Bodey, T.W., Hamer, K.C., Wakefield, E., Le Nuz, M., and Votier, S.C. (2014). Individual differences in searching behaviour and spatial foraging consistency in a central place marine predator. *Oikos* 123, 33–40.

Petalas, C., Lazarus, T., Lavoie, R.A., Elliott, K.H., and Guigueno, M.F. (2021). Foraging niche partitioning in sympatric seabird populations. *Scientific Reports* 11, 2493.

Pierce, G.J., Santos, M.B., Reid, R.J., Patterson, I.A.P., and Ross, H.M. (2004). Diet of minke whales Balaenoptera acutorostrata in Scottish (UK) waters with notes on strandings of this species in Scotland 1992–2002. *Journal of the Marine Biological Association of the United Kingdom* 84, 1241–1244.

Pirotta, E., Matthiopoulos, J., MacKenzie, M., Scott-Hayward, L., and Rendell, L. (2011). Modelling sperm whale habitat preference: a novel approach combining transect and follow data. *Marine Ecology Progress Series* 436, 257–272.

Praca, E., and Gannier, A. (2008). Ecological niches of three teuthophageous odontocetes in the northwestern Mediterranean Sea. *Ocean Science* 4, 49–59.

Pyron, R.A., Costa, G.C., Patten, M.A., and Burbrink, F.T. (2015). Phylogenetic niche conservatism and the evolutionary basis of ecological speciation. *Biological Reviews* 90, 1248–1262.

R Core Team. (2018). R: A language and environment for statistical computing. Vienna, Austria: R Foundation for Statistical Computing. URL http://www.R-project.org/.

Reeves, R., McClellan, K., and Werner, T. (2013). Marine mammal bycatch in gillnet and other entangling net fisheries, 1990 to 2011. *Endangered Species Research* 20, 71–97.

Richards, C., Padget, O., Guilford, T., and Bates, A.E. (2019). Manx shearwater (Puffinus puffinus) rafting behaviour revealed by GPS tracking and behavioural observations.

PeerJ 7: e7863.

Ritchie, M. (2002). Competition and Coexistence of Mobile Animals. In U. Sommer & B. Worm (Eds.), *Competition and Coexistence. Ecological Studies (Analysis and Synthesis)* (Vol. 161, pp. 109–131). Springer, Berlin, Heidelberg.

Rogan, E., Cañadas, A., Macleod, K., Santos, M.B., Mikkelsen, B., Uriarte, A., Van Canneyt, O., Vázquez, J.A., and Hammond, P.S. (2017). Distribution, abundance and habitat use of deep diving cetaceans in the North-East Atlantic. *Deep Sea Research Part II: Topical Studies in Oceanography* 141, 8–19.

Røjbek, M.C., Tomkiewicz, J., Jacobsen, C., and Støttrup, J.G. (2014). Forage fish quality: seasonal lipid dynamics of herring (Clupea harengus L.) and sprat (Sprattus sprattus L.) in the Baltic Sea. *ICES Journal of Marine Science* 71, 56–71.

Romero-Romero, S., Choy, C.A., Hannides, C.C.S., Popp, B.N., and Drazen, J.C. (2019). Differences in the trophic ecology of micronekton driven by diel vertical migration. *Limnology and Oceanography* 64, 1473–1483.

Ryan, C., McHugh, B., Trueman, C., Sabin, R., Deaville, R., Harrod, C., Berrow, S., and O'Connor, I. (2013). Stable isotope analysis of baleen reveals resource partitioning among sympatric rorquals and population structure in fin whales. *Marine Ecology Progress Series* 479, 251–261.

Santos, M.B., Pierce, G.J., Learmonth, J.A., Reid, R.J., Ross, H.M., Patterson, I.A.P., Reid, D.G., and Beare, D. (2004). VARIABILITY IN THE DIET OF HARBOR PORPOISES (PHOCOENA PHOCOENA) IN SCOTTISH WATERS 1992–2003. *Marine Mammal Science* 20, 1–27.

Sato, K., Watanuki, Y., Takahashi, A., Miller, P.J.., Tanaka, H., Kawabe, R., Ponganis, P.J., Handrich, Y., Akamatsu, T., Watanabe, Y., Mitani, Y., Costa, D.P., Bost, C.-A., Aoki, K., Amano, M., Trathan, P., Shapiro, A., and Naito, Y. (2007). Stroke frequency, but not swimming speed, is related to body size in free-ranging seabirds, pinnipeds and cetaceans. *Proceedings of the Royal Society B: Biological Sciences* 274, 471–477.

Scales, K.L., Miller, P.I., Hawkes, L.A., Ingram, S.N., Sims, D.W., and Votier, S.C. (2014). On the front line: Frontal zones as priority at-sea conservation areas for mobile marine vertebrates. *Journal of Applied Ecology* 51, 1575–1583.

Shoji, A., Stéphane Aris-Brosou, S., Fayet, A., Padget, O., Perrins, C., and Guilford, T. (2015). Dual foraging and pair coordination during chick provisioning by Manx shearwaters: empirical evidence supported by a simple model. *The Journal of Experimental Biology* 218, 2116–2123.

Sigurjónsson, J., Gunnlaugsson, T., Ensor, P., Newcomer, M., and Víkingsson, G. (1991). North Atlantic sightings survey 1989 (NASS-89): Shipboard surveys in Icelandic and adjacent waters July-August 1989.(IWC SC/42/0-21). *Report on International Whale Communication* 41, 559–572.

Skov, H., Durinck, J., and Andell, P. (2000). Associations between wintering avian predators and schooling fish in the Skagerrak-Kattegat suggest reliance on predictable aggregations of herring Clupea harengus. *Journal of Avian Biology* 31, 135–143.

Skov, H., and Thomsen, F. (2008). Resolving fine-scale spatio-temporal dynamics in the harbour porpoise Phocoena phocoena. *Marine Ecology Progress Series* 373, 173–186.

Spitz, J., Cherel, Y., Bertin, S., Kiszka, J., Dewez, A., and Ridoux, V. (2011). Prey preferences among the community of deep-diving odontocetes from the Bay of Biscay, Northeast Atlantic. *Deep-Sea Research Part I: Oceanographic Research Papers* 58, 273–282.

Spitz, J., Ridoux, V., Trites, A.W., Laran, S., and Authier, M. (2018). Prey consumption by cetaceans reveals the importance of energy-rich food webs in the Bay of Biscay. *Progress in Oceanography* 166, 148–158.

Spitz, J., Trites, A.W., Becquet, V., Brind'Amour, A., Cherel, Y., Galois, R., and Ridoux, V. (2012). Cost of Living Dictates what Whales, Dolphins and Porpoises Eat: The Importance of Prey Quality on Predator Foraging Strategies. *PLoS ONE* 7, e50096.

Sveegaard, S., Andreasen, H., Mouritsen, K.N., Jeppesen, J.P., Teilmann, J., and Kinze, C.C. (2012). Correlation between the seasonal distribution of harbour porpoises and their prey in the Sound, Baltic Sea. *Marine Biology* 159, 1029–1037.

Symons, S. (2018). *Ecological segregation between two closely related species: exploring Atlantic puffin and razorbill foraging hotspots.* University of New Brunswick.

Teloni, V., Johnson, M., Miller, P., and Madsen, P. (2008). Shallow food for deep divers: Dynamic foraging behavior of male sperm whales in a high latitude habitat. *Journal of Experimental Marine Biology and Ecology* 354, 119–131.

Thaxter, C.B., Lascelles, B., Sugar, K., Cook, A.S.C.P., Roos, S., Bolton, M., Langston, R.H.W., and Burton, N.H.K. (2012). Seabird foraging ranges as a preliminary tool for identifying candidate Marine Protected Areas. *Biological Conservation* 156, 53–61.

Townsend, C.R., Begon, M., and Harper, J.L. (2008). *Essentials of Ecology* (Third). Blackwell Publishing.

van der Kooij, J., Scott, B.E., and Mackinson, S. (2008). The effects of environmental factors on daytime sandeel distribution and abundance on the Dogger Bank. *Journal of Sea Research* 3, 201–209.

Víkingsson, G.A., Pike, D.G., Valdimarsson, H., Schleimer, A., Gunnlaugsson, T., Silva, T., Elvarsson, B.P., Mikkelsen, B., Øien, N., Desportes, G., Bogason, V., and Hammond, P.S. (2015). Distribution, abundance, and feeding ecology of baleen whales in Icelandic waters: Have recent environmental changes had an effect? *Frontiers in Ecology and Evolution* 3.

Visser, F., Hartman, K.L., Pierce, G.J., Valavanis, V.D., and Huisman, J. (2011). Timing of

migratory baleen whales at the azores in relation to the north atlantic spring bloom. *Marine Ecology Progress Series* 440, 267–279.

Waggitt, J.J., Evans, P.G.H., Andrade, J., Banks, A.N., Boisseau, O., Bolton, M., Bradbury, G., Brereton, T., Camphuysen, C.J., Durinck, J., Felce, T., Fijn, R.C., Garcia-Baron, I., Garthe, S., Geelhoed, S.C. V., Gilles, A., Goodall, M., Haelters, J., Hamilton, S., Hartny-Mills, L., Hodgins, N., James, K., Jessopp, M., Kavanagh, A.S., Leopold, M., Lohrengel, K., Louzao, M., Markones, N., Martínez-Cedeira, J., Cadhla, O.Ó., Perry, S.L., Pierce, G.J., Ridoux, V., Robinson, K.P., Santos, M.B., Saavedra, C., Skov, H., Stienen, E.W.M., Sveegaard, S., Thompson, P., Vanermen, N., Wall, D., Webb, A., Wilson, J., Wanless, S., and Hiddink, J.G. (2020). Distribution maps of cetacean and seabird populations in the North-East Atlantic. *Journal of Applied Ecology* 57, 253–269.

Wakefield, E.D., Bodey, T.W., Bearhop, S., Blackburn, J., Colhoun, K., Davies, R., Dwyer, R.G., Green, J.A., Grémillet, D., Jackson, A.L., Jessopp, M.J., Kane, A., Langston, R.H.W., Lescroël, A., Murray, S., Le Nuz, M., Patrick, S.C., Péron, C., Soanes, L.M., Wanless, S., Votier, S.C., and Hamer, K.C. (2013). Space partitioning without territoriality in gannets. *Science* 341, 68–70.

Wakefield, E.D., Owen, E., Baer, J., Carroll, M.J., Daunt, F., Dodd, S.G., Green, J.A., Guilford, T., Mavor, R.A., Miller, P.I., Newell, M.A., Newton, S.F., Robertson, G.S., Shoji, A., Soanes, L.M., Votier, S.C., Wanless, S., and Bolton, M. (2017). Breeding density, fine-scale tracking, and large-scale modeling reveal the regional distribution of four seabird species. *Ecological Applications* 27, 2074–2091.

Wall, D., O'Brien, J., Meade, J., and Allen, B.M. (2006). Summer distribution and relative abundance of cetaceans off the west coast of Ireland. *Biology and Environment* 106, 135–142.

Wanless, S., Harris, M., Redman, P., and Speakman, J. (2005). Low energy values of fish as a probable cause of a major seabird breeding failure in the North Sea. *Marine Ecology Progress Series* 294, 1–8.

Weir, C., Stockin, K., and Pierce, G. (2007). Spatial and temporal trends in the distribution of harbour porpoises, white-beaked dolphins and minke whales off Aberdeenshire (UK), north-western North Sea. *Journal of the Marine Biological Association of the United Kingdom* 87, 327–338.

Wilson, J.B. (1999). Guilds, functional types and ecological groups. *Oikos* 86, 507–522.

Wong, S.N.., Ronconi, R.A., and Gjerdrum, C. (2018). Autumn at-sea distribution and abundance of phalaropes Phalaropus and other seabirds in the lower Bay of Fundy, Canada. *Marine Ornithology* 46, 1–10.

Wong, S.N.P., and Whitehead, H. (2014). Seasonal occurrence of sperm whales (Physeter macrocephalus) around Kelvin Seamount in the Sargasso Sea in relation to oceanographic processes. *Deep-Sea Research Part I* 91, 10–16.

Woodward, B.L., Winn, J.P., and Fish, F.E. (2006). Morphological specializations of baleen whales associated with hydrodynamic performance and ecological niche. *Journal of Morphology* 267, 1284–1294.

Zuur, A.F., Ieno, E.N., Walker, N., Saveliev, A.A., and Smith, G.M. (2009). *Mixed effects models and extensions in ecology with R*. Springer.

6.Appendices

Appendix 1: Methodology

1.1 Environmental parameters

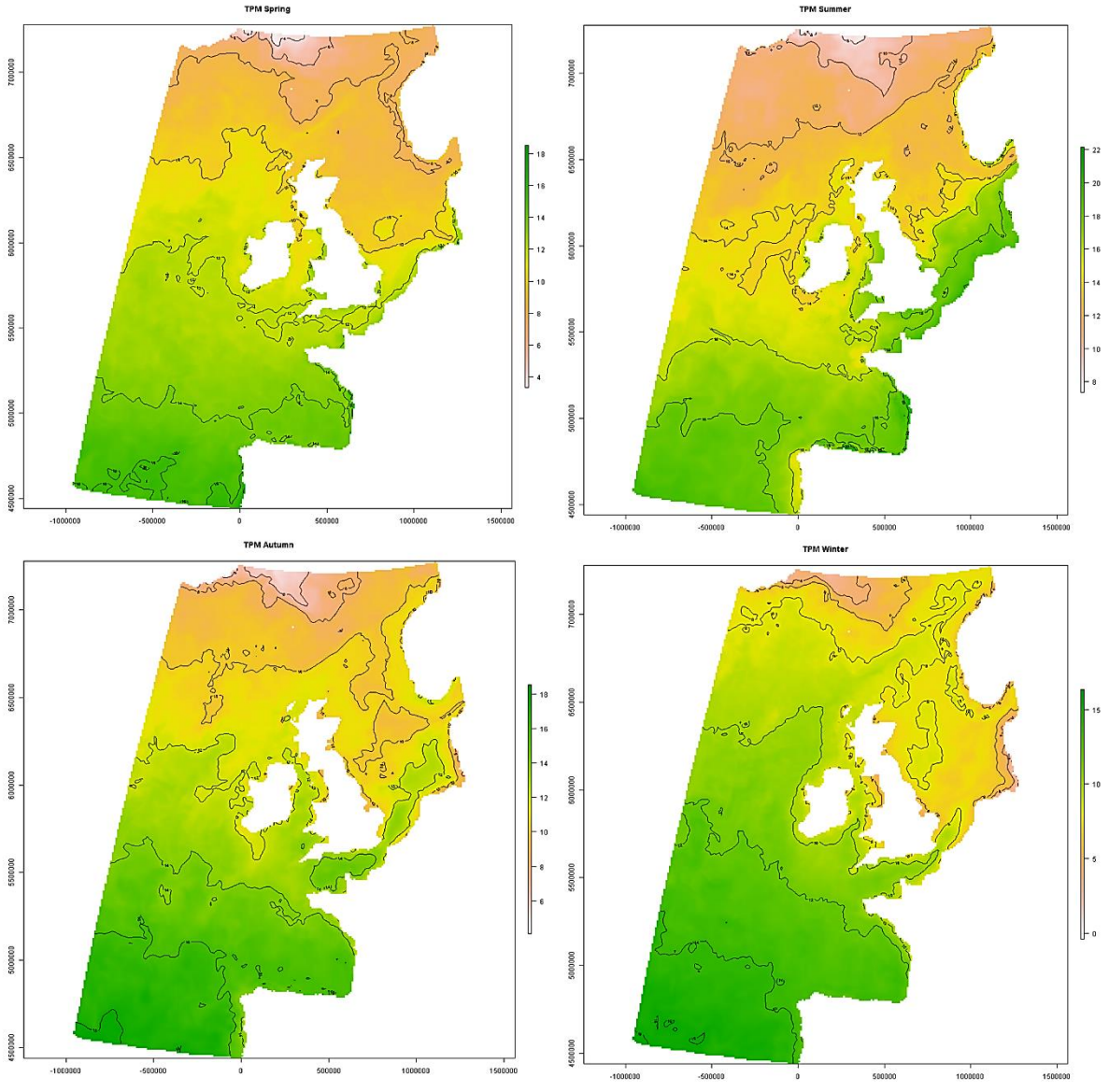

Figure 6.1.1. *Mean potential temperature (Celsius) between 0 and 150m from surface (modelled) per season (parameter code: TPM)*. Top left: spring, top right: summer, bottom left: autumn, bottom right: winter.

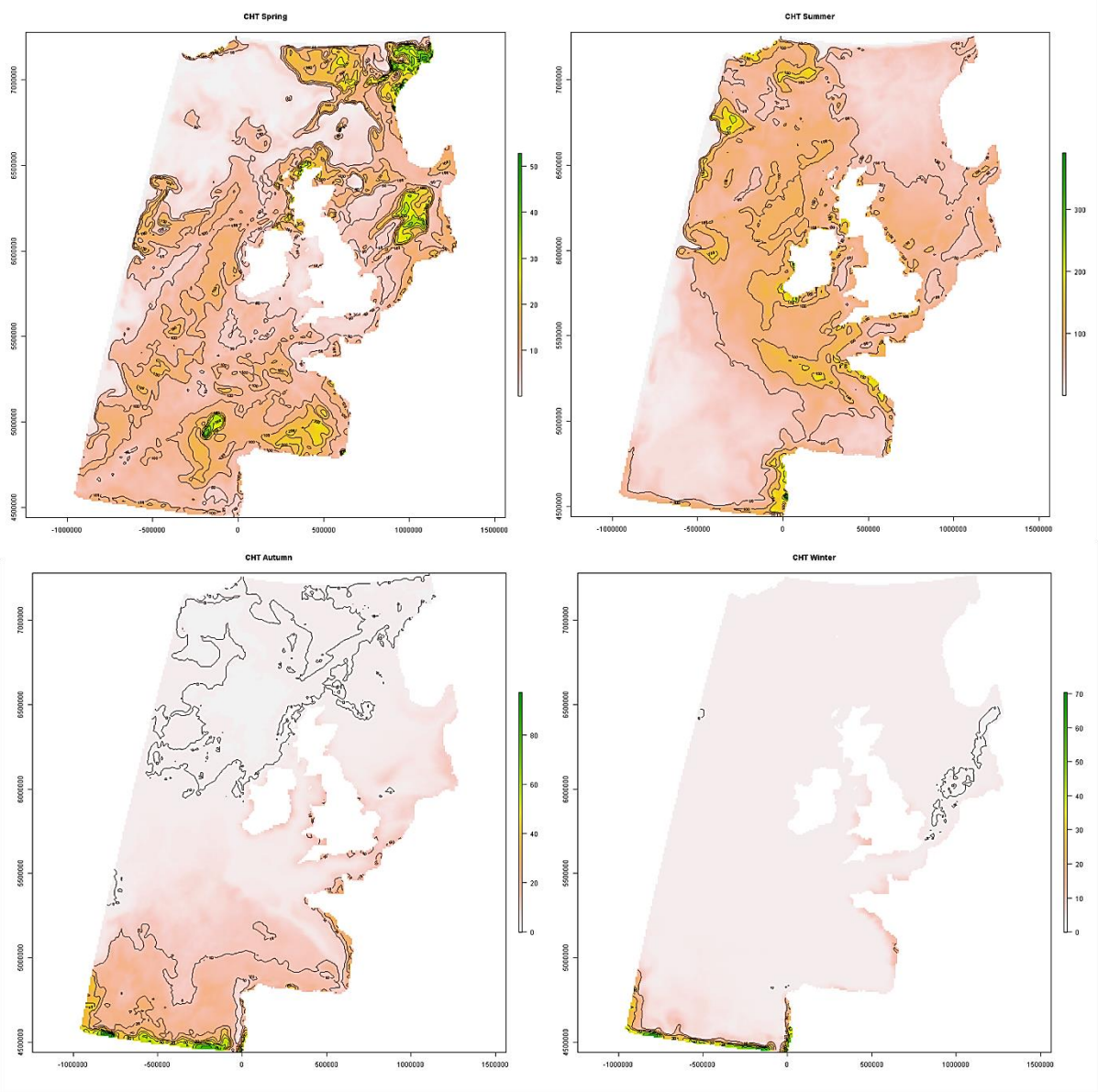

Figure 6.1.2. *Total Chlorophyll (mg) depth summed between 0 and 150m from surface (modelled) (parameter code: CHT).* Top left: spring, top right: summer, bottom left: autumn, bottom right: winter.

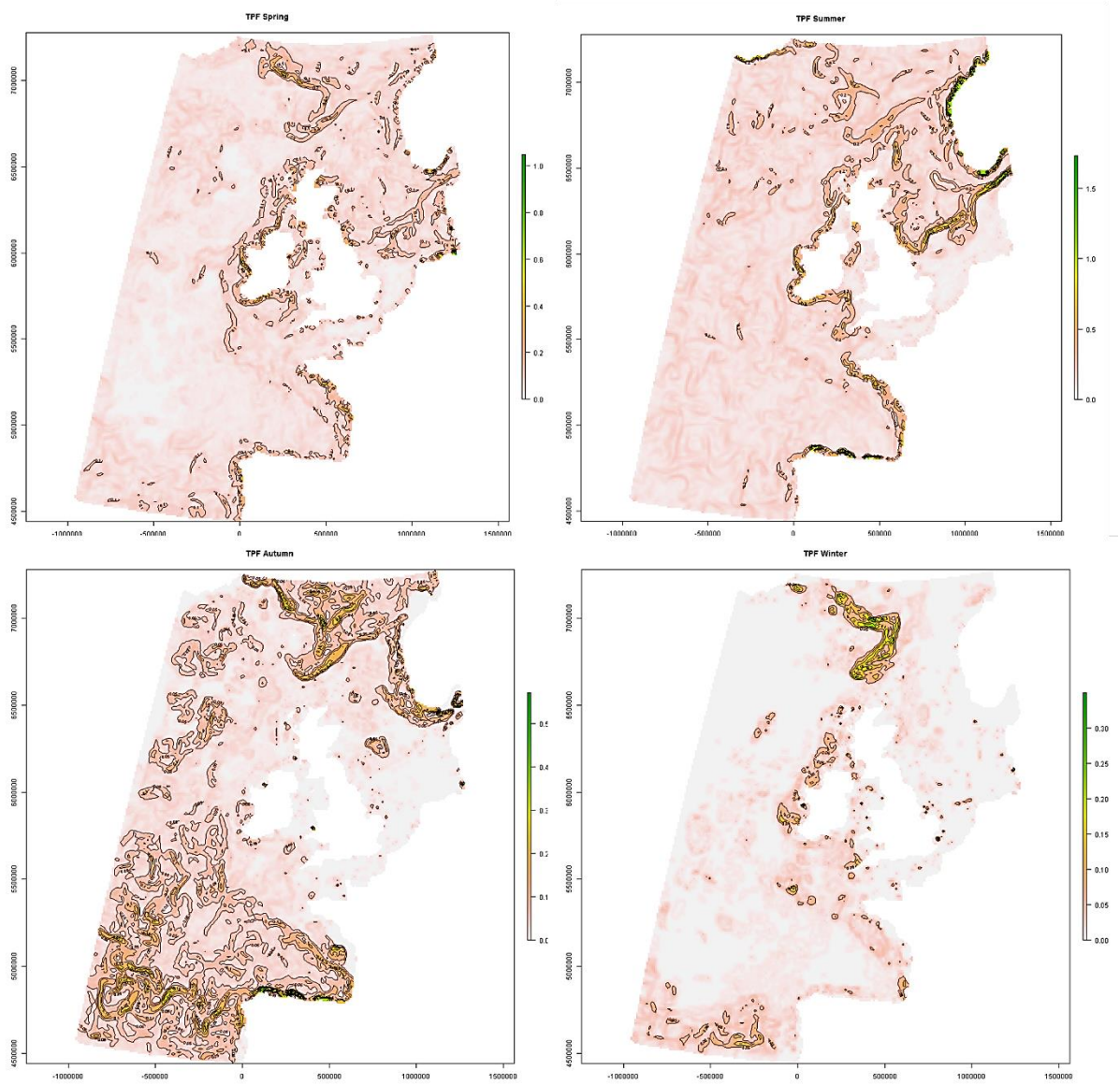

Figure 6.1.3. *Thermal stratification gradient (unitless) (parameter code: TPF)*. Higher values indicate greater frontal activity Top left: spring, top right: summer, bottom left: autumn, bottom right: winter.

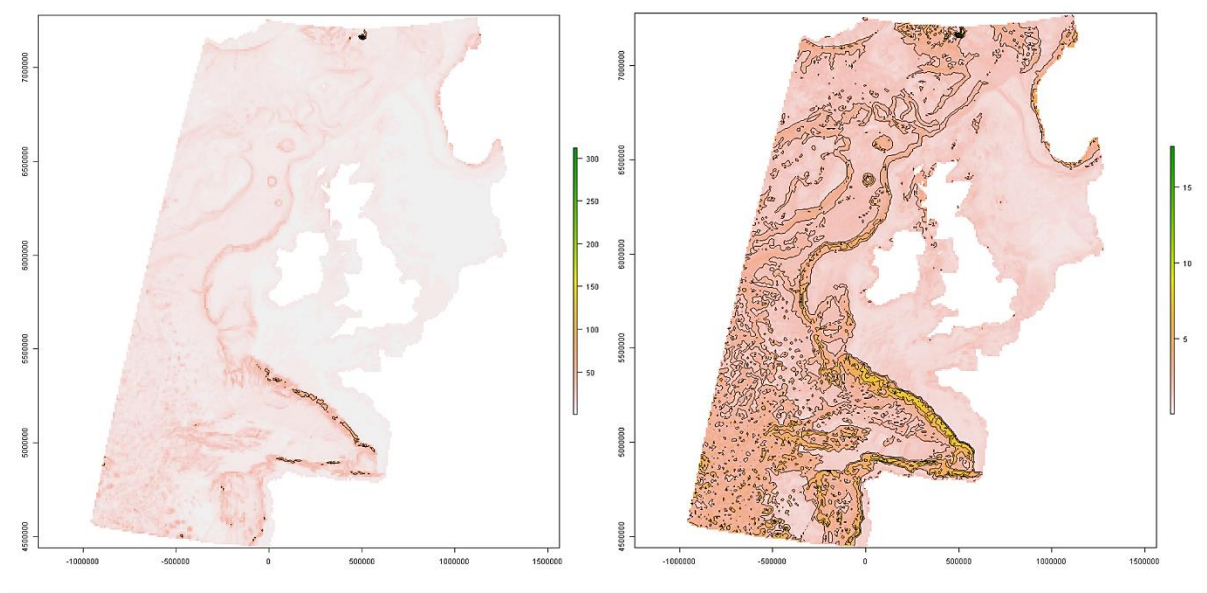

Figure 6.1.4. *Seabed gradient, and square root transformed seabed gradient (parameter code: FEA).* Depth gradient (m) calculated using terrain ruggedness index. Seabed gradient (left), square root transformed seabed gradient (right).

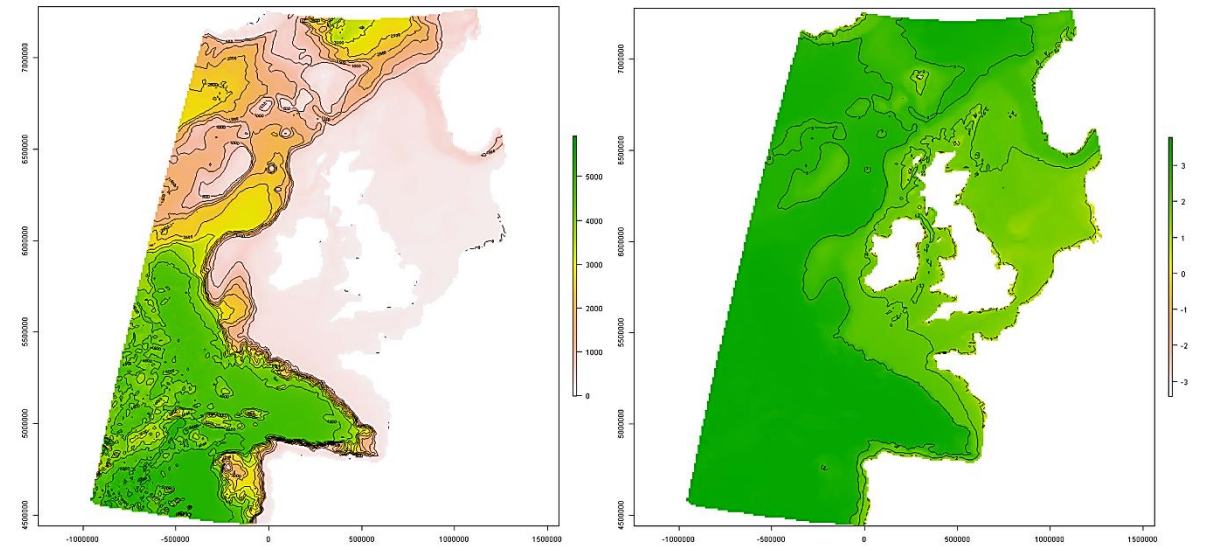

Figure 6.1.5. *Depth (m), and log10 transformed depth (m) (parameter code: BAT).* Depth (m) (left), log10 transformed water depth (right).

Appendix 2: Results

Table 6.2.1. *Table of k fold cross validation mean squared errors and Durbin-Watson residuals statistic.*

Species	*k* 1 (MSE)	*k* 2 (MSE)	*k* 3 (MSE)	*k* 4 (MSE)	*k* 5 (MSE)	mean of *k* 1-5 MSEs	Durbin-Watson (residuals)
Puffin	257.61	37.88	75.33	99.2	16.16	97.24	1.64
black-legged kittiwake	3974.56	1055.15	900.41	1757.98	140.73	1565.77	1.97
bottlenose dolphin	2.47	1.58	1.47	1.34	0.8	1.53	1.8
common guillemot	3178.47	915.93	1097.99	1230.71	248.27	1334.27	1.76
Common Dolphin	142.78	65.12	47.92	79.16	27.74	72.54	1.94
European shag	11.03	2.58	2	5.36	0.66	4.33	1.8
European Storm petrel	32	7.15	10.52	13.95	2.57	13.24	1.95
Fin whale						0.03	1.8
harbour porpoise						1.68	1.86
herring gull	999.68	201.22	262.96	404.53	56.45	384.97	1.92
Lesser Black Backed Gull	638	195	183	278	52	269	1.93
Manx Shearwater	2951	1203	781	1111	56	1220	1.88
Minke Whale							1.93
Northern Fulmar	23678	5829	3994	11484	433	9083	1.89
Northern Gannet	1429.14	430.93	270.02	714.29	106.26	590.13	1.85
Orca	0.05	0.02	0.01	0.03	0.02	0.03	2.002
Pilot Whale	2.34	0.7	0.87	1.51	0.59	1.2	1.97
Razorbill	146.67	39.52	48.79	60.73	16.07	62.35	1.86
Risso's Dolphin	0.23	0.08	0.09	0.12	0.05	0.11	1.95
Sperm Whale						0.01	2
Striped Dolphin	5.53	1.9	1.96	3	1.06	2.69	1.98
White-beaked Dolphin	0.94	0.37	0.44	0.59	0.31	0.53	1.9
White-sided Dolphin	18.56	3.49	1.81	9.66	1.39	6.98	2

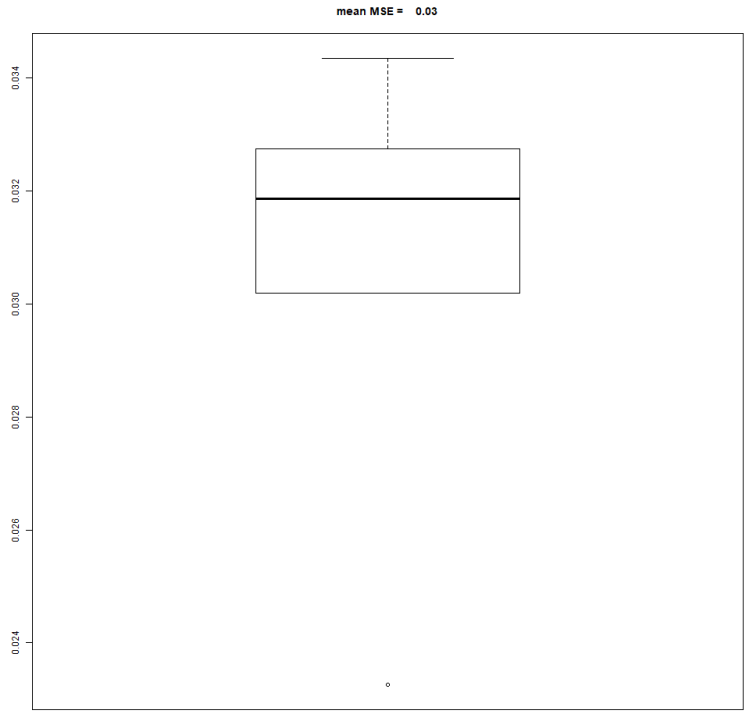

Figure 6.2.1. *Boxplots of averages of fin whale model K fold cross validation mean squared errors*

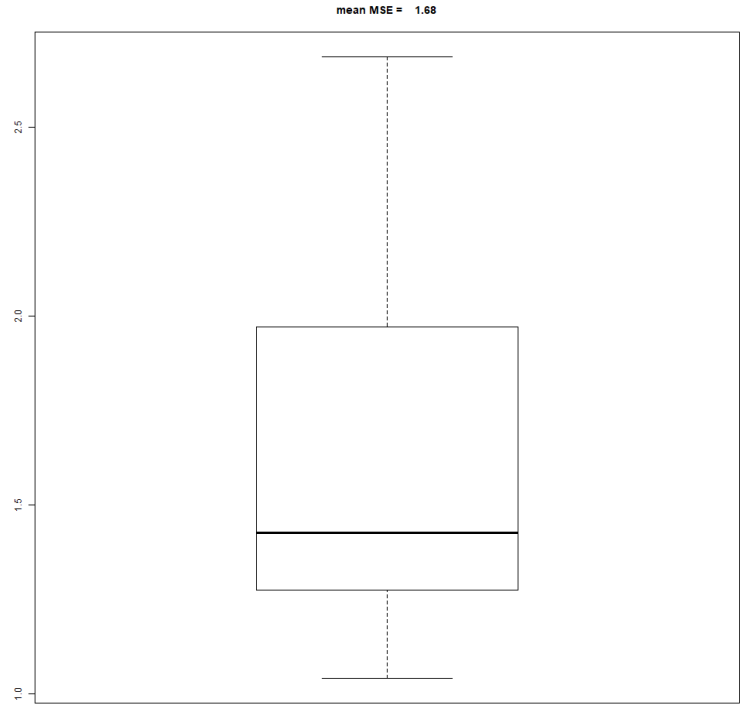

Figure 6.2.2. *Boxplots of averages of harbour porpoise model K fold cross validation mean squared errors*

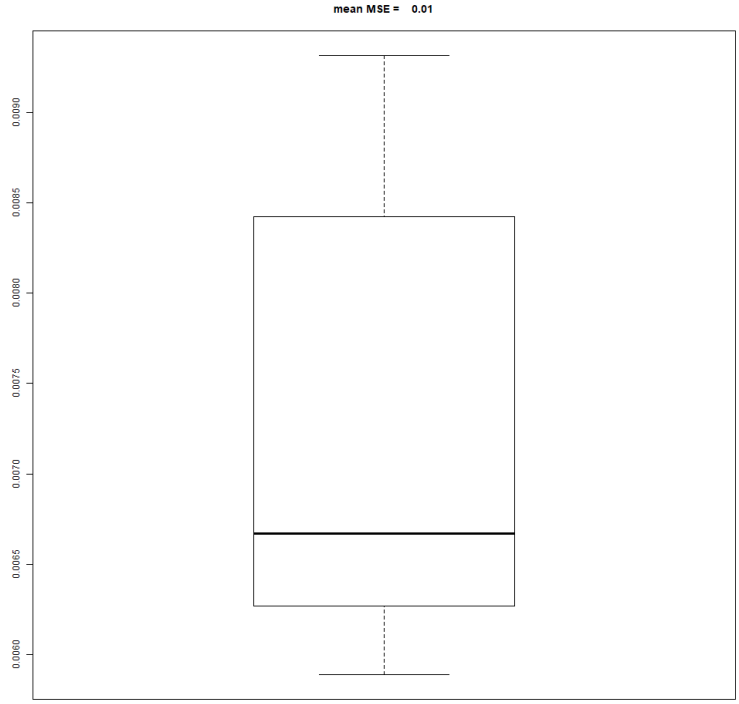

Figure 6.2.3. *Boxplots of averages of sperm whale model K fold cross validation mean squared errors*

2.1 Coefficient Validation

Table 6.2.2. *Table of conditional model parameters where coefficients p value were greater than 0.05, wide standard error of slope estimate, or predicted coefficients from RW Metropolis sampling overlapping zero.*

Species	Variable	p	m% of SE
Razorbill	TPM	0.19	73
Sperm whale	TPM		
White-beaked dolphin	TPM		
European shag	TPF	0.047	51
Storm petrel	TPF	0.038	48
Herring gull	TPF	0.08	55
Sperm whale	TPF		
White-beaked dolphin	TPF		
White-sided dolphin	TPF		
European shag	CHT	4.33	13
Orca	CHT	0.278	91
Pilot whale	CHT	0.78	27
Sperm whale	CHT		
White-sided dolphin	CHT		
Common dolphin	FEA	0.9	14
Fin whale	FEA	0.92	10
Lesser black-backed gull	FEA	0.263	89
Northern gannet	FEA	0.0214	41
Orca	FEA	0.634	48
Sperm whale	FEA		
White-sided dolphin	FEA		
Orca	BAT	0.312	100
Risso's dolphin	BAT	0.998	
Sperm whale	BAT		

Razorbill, TPM, proposal distribution = 0.15 (smallest absolute m value of all variables), the coefficient values range from around -0.3 to 0.69, and the majority of coefficients have values between -0.05 and 0.35. The density of coefficient values are roughly normally distributed where the peak density is around 0.15. There is a high density of coefficients with values around 0, providing support for the *p* values probability score that the null hypothesis cannot be rejected. There is also a high density of coefficients with values around 0.25. the density of coefficients with positive values was still much greater than those with negative values (proposal is positive).

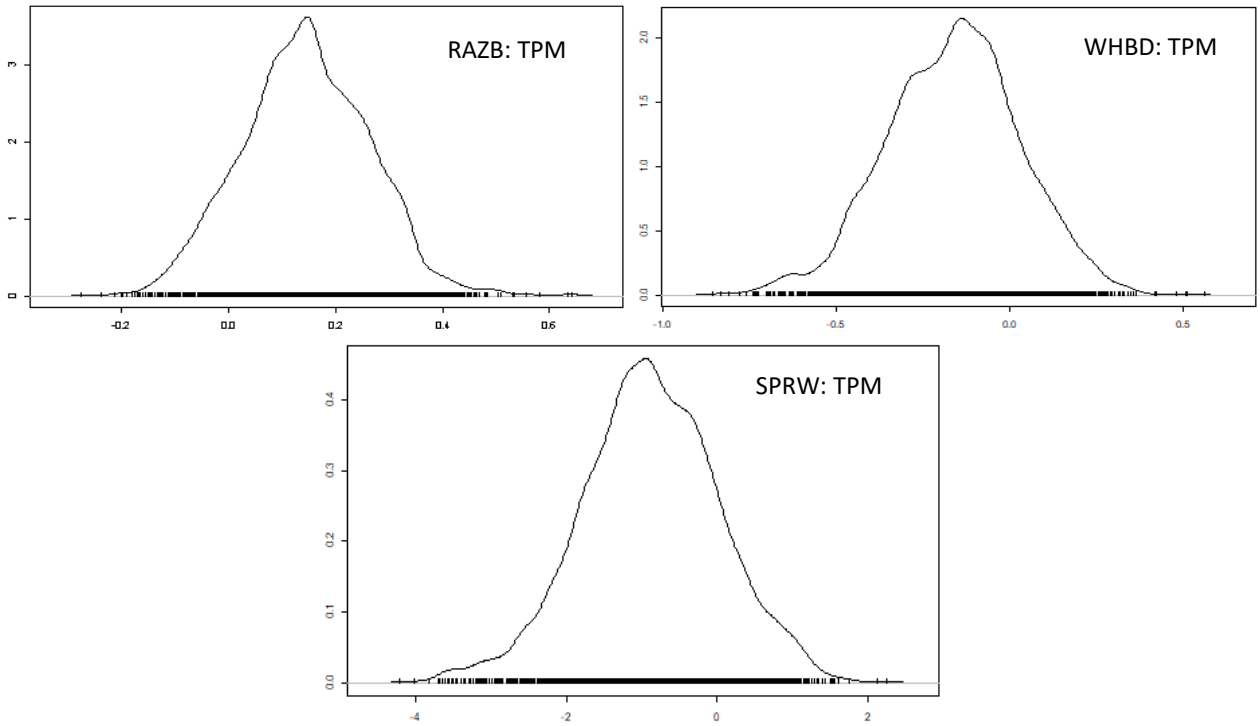

Figure 6.2.3. *density plot (bottom) of random-walk metropolis sampling of the conditional model mean sea temperature coefficients.*

Herring gull, TPF, the proposal distribution was centred at 0.11, there was greater density of predicted coefficients over 0.2, than the density of coefficients below 0, and the greatest density of coefficients had values between 0.025 and 0.21. The density of values not equal to zero was much larger than the density of values equal to zero. European shag, TPF, tail of metropolis sampling overlaps zero, but density is extremely low. Storm petrel, TPF, tail of metropolis sampling overlaps zero, but density is extremely low. Orca, CHT, tail overlaps 0, but greatest density of coefficients had values between around -1.25 and 0, and proposal distribution was -0.67. Pilot whale, CHT, proposal distribution -0.15, similar density of coefficients with positive and negative values, greatest density between around -1 and 0.75, slightly greater density of negative values than positive (proposal is negative). European shag, CHT, normal distribution around 0, base range < all other variables. Northern gannet, FEA, proposal distribution was centred at -0.17. The range of coefficient values was from around -0.4 to around 0.1. The majority of values were between -0.3 and -0.05.

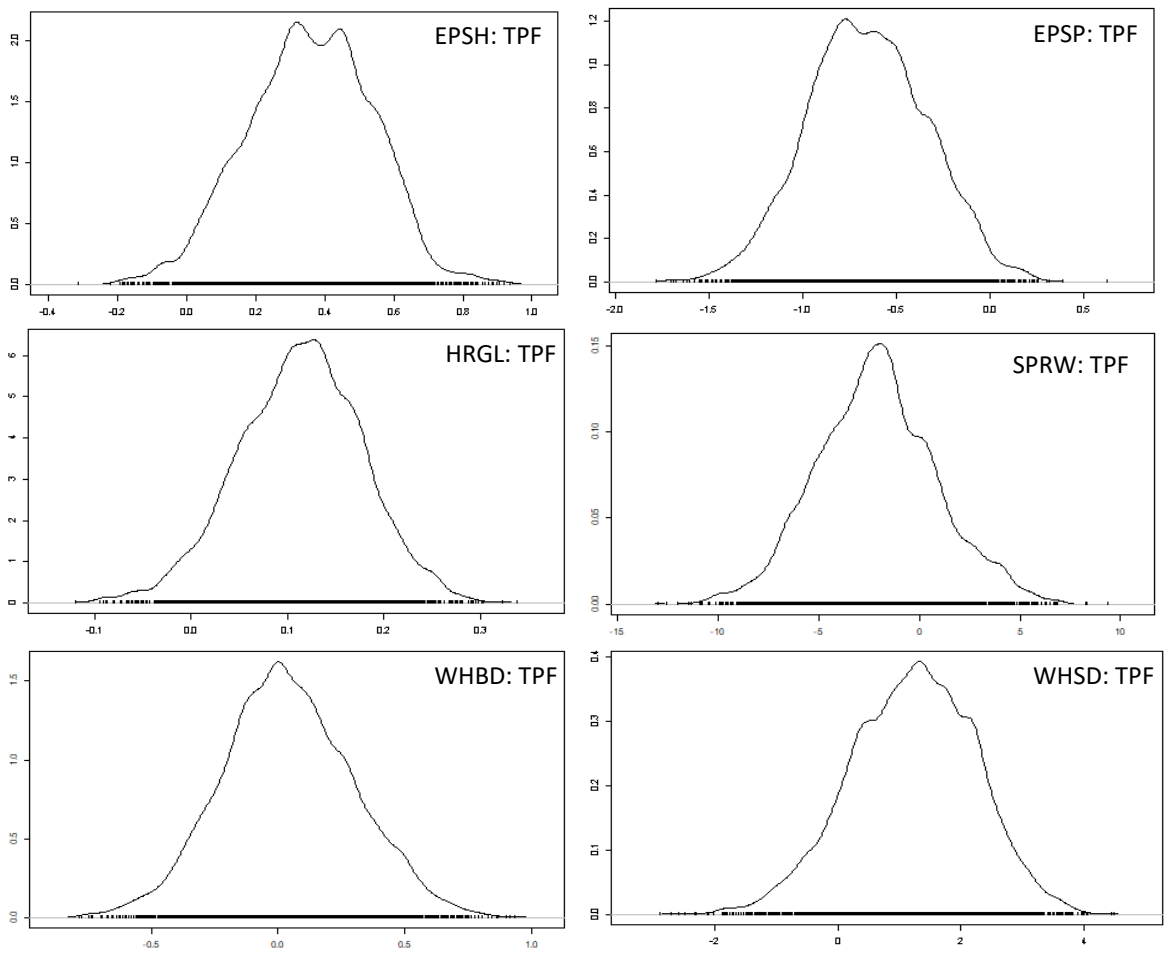

Figure 6.2.4. *density plot (bottom) of random-walk metropolis sampling of the conditional model thermal front potential coefficients.*

There was a high-density coefficients with values around -0.14 and another peak in density of values around -0.225. There was also a high density of coefficients with values around -0.1. The density of coefficients with a value of zero was much less than the density of coefficients with a value not equal to zero. Orca, FEA, proposal distribution was 0.51, and greatest density of coefficients was between around -1 and 1.75, close to a normal distribution centred around 0, with similar density of coefficients being positive and negative, although a slightly greater density of positive values than negative. Lesser black-backed gull, FEA, high density of coefficients overlapping 0, although greatest density of coefficients is between 0 and ~-0.3 (proposal distribution -0.154). Common dolphin, FEA, normal distribution around 0, base range < all other variables. Fin whale, FEA, normal distribution around 0, base range < all other variables.

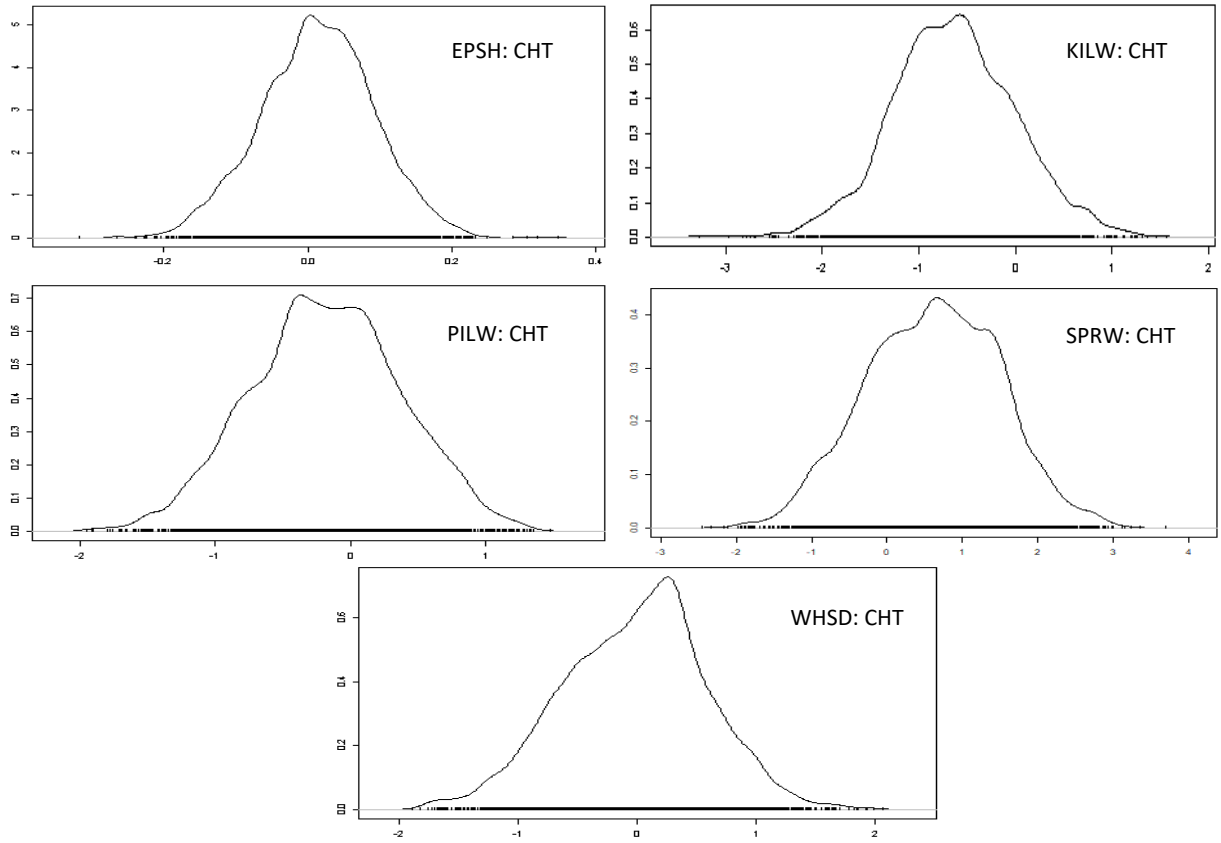

Figure 6.2.5. *density plot (bottom) of random-walk metropolis sampling of the conditional model chlorophyll concentration coefficients.*

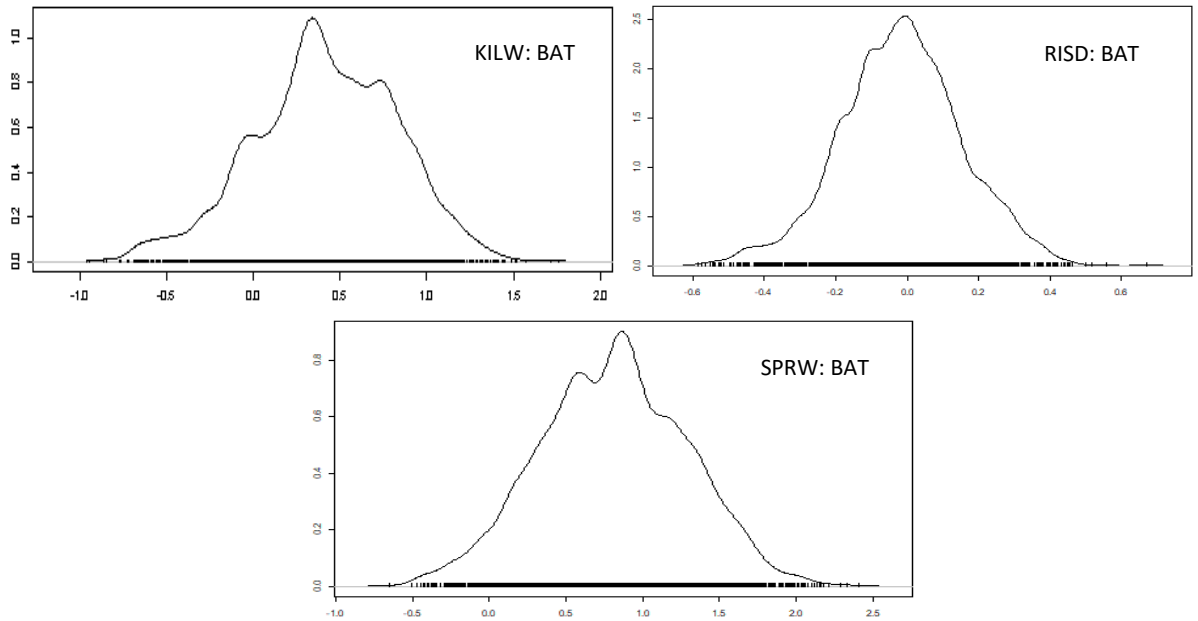

Figure 6.2.6. *density plot (bottom) of random-walk metropolis sampling of the conditional model water depth coefficients.*

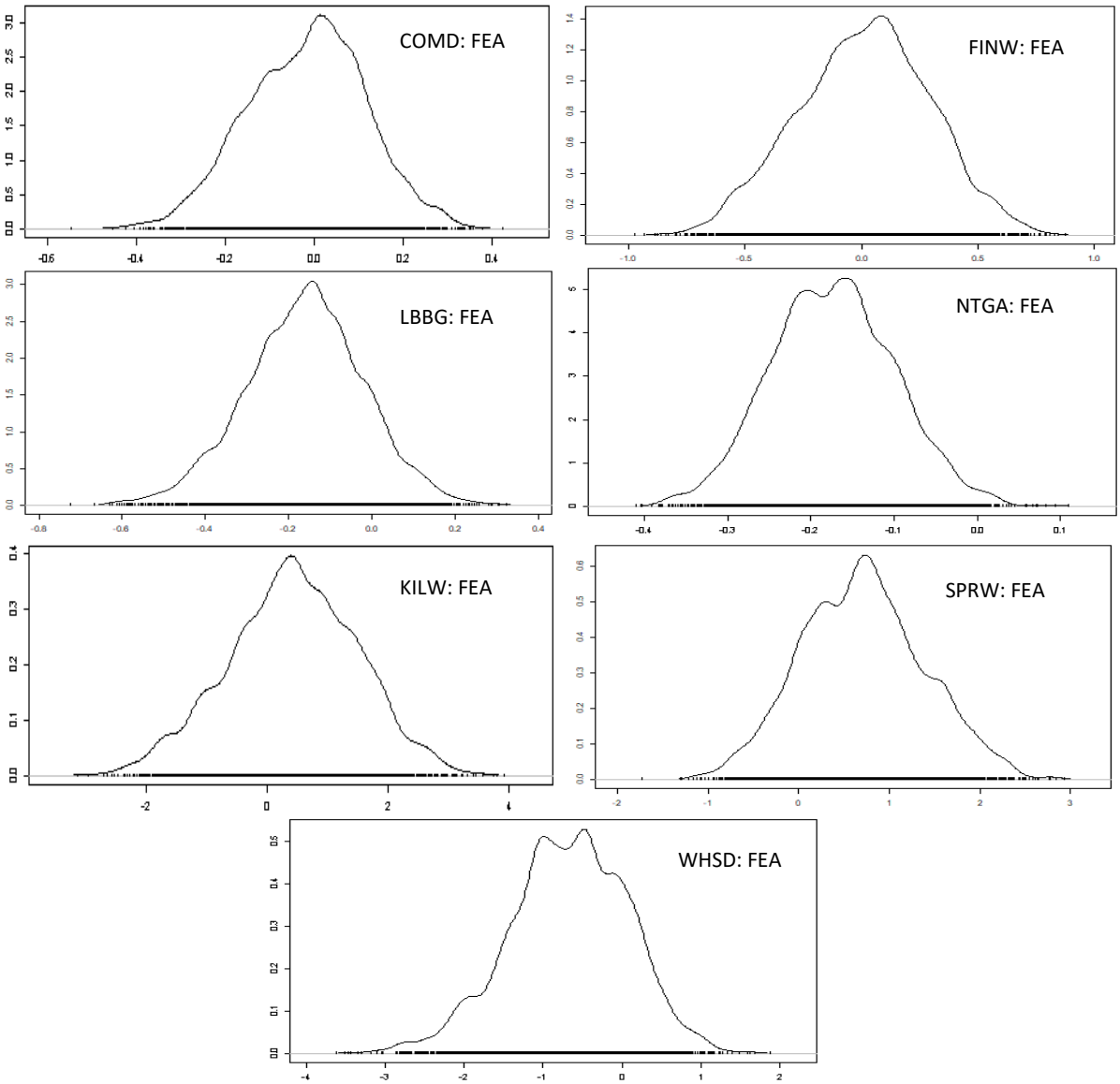

Figure 6.2.7. *density plot (bottom) of random-walk metropolis sampling of the conditional model seabed gradient coefficients.*

Orca, BAT, proposal distribution was 0.4, and the greatest density of coefficients had values between around -0.15 and 0.75, and the majority of coefficients were positive rather than negative (proposal was positive). Risso's dolphin, BAT, similar density of coefficients with positive and negative values, greatest density of coefficients have values between -0.2 and 0.2 (both still smallest absolute slope value of all variables), normal density distribution of predicted coefficients centred around 0.

2.2 Model Outputs

Table 6.2.3.1. Atlantic puffin *ZIGLM model outputs.* Slope estimate, standard error, *z*-value, and *p*-value for each parameter within both nested models (conditional and logistic). Parameter details are the full names of each parameter, corresponding to the parameter code.

Model	Parameter Code	Slope Estimate	Standard Error	*z*-Value	*p*-Value
Conditional	(Intercept)	3.16	0.07	44.14	0
	TPM_s	-6.44	0.13	-51.38	0
	TPF_s	3.96	0.17	22.67	9.37E-114
	CHT_s	1.35	0.08	15.9	6.65E-57
	FEA_s	-2.11	0.24	-8.68	3.79E-18
	BAT_s	-2.56	0.15	-17.37	1.36E-67
Logistic	(Intercept)	3.88	0.17	22.82	2.63E-115
	CHT_s	3.32	0.28	11.93	8.66E-33
	TPS_s	-2.87	0.35	-8.15	3.65E-16
	BAT_s	-149.17	9.07	-16.45	8.86E-61
	TPF_s	-65.28	2.58	-25.34	1.25E-141

Table 6.2.3.2. *Black-legged kittiwake ZIGLM model outputs.* Slope estimate, standard error, *z*-value, and *p*-value for each parameter within both nested models (conditional and logistic). Parameter details are the full names of each parameter, corresponding to the parameter code.

Model	Parameter Code	Slope Estimate	Standard Error	*z*-Value	*p*-Value
Conditional	(Intercept)	2.77	0.03	102.80	0
	TPM_s	-2.81	0.05	-55.30	0
	TPF_s	1.69	0.10	16.30	1.16E-59
	FEA_s	-1.41	0.12	-11.90	8.18E-33
	BAT_s	-1.07	0.06	-17.60	1.83E-69
	CHT_s	-0.97	0.04	-24.40	2.29E-131
Logistic	(Intercept)	4.48	0.26	17.26	9.34E-67
	TPM_s	-21.70	1.03	-20.97	1.14E-97
	TPF_s	-44.89	10.82	-4.15	3.33E-05

Table 6.2.3.3. *Bottlenose dolphin ZIGLM model outputs.* Slope estimate, standard error, *z*-value, and *p*-value for each parameter within both nested models (conditional and logistic). Parameter details are the full names of each parameter, corresponding to the parameter code.

Model	Parameter Code	Slope Estimate	Standard Error	*z*-Value	*p*-Value
conditional	(Intercept)	2.73	0.05	51.91	0
	TPM_s	-1.93	0.08	-22.78	7.90E-115
	TPF_s	2.55	0.17	15.27	1.26E-52
	FEA_s	1.85	0.05	34.13	2.78E-255
	BAT_s	0.34	0.06	5.71	1.14E-08
	CHT_s	-0.71	0.13	-5.29	1.20E-07
logistic	(Intercept)	7.53	0.12	61.15	0
	CHT_s	-3.39	0.30	-11.40	4.35E-30
	BAT_s	-0.18	0.20	-0.89	0.38
	TPS_s	-4.32	0.19	-22.81	3.34E-115
	CHT_s:BAT_s	5.16	2.02	2.56	0.01

Table 6.2.3.4. *Common guillemot ZIGLM model outputs.* Slope estimate, standard error, *z*-value, and *p*-value for each parameter within both nested models (conditional and logistic). Parameter details are the full names of each parameter, corresponding to the parameter code.

Model	Parameter Code	Slope Estimate	Standard Error	*z*-Value	*p*-Value
conditional	(Intercept)	3.52	0.03	138.34	0
	TPM_s	-3.30	0.05	-67.54	0
	TPF_s	4.02	0.12	33.46	2.11E-245
	FEA_s	-1.51	0.19	-7.98	1.49E-15
	BAT_s	-7.41	0.18	-41.09	0
	CHT_s	-1.28	0.04	-28.50	1.08E-178
logistic	(Intercept)	5.32	0.27	20.07	1.32E-89
	TPM_s	-18.78	0.96	-19.64	7.14E-86
	SPM_s	-9.42	0.69	-13.61	3.53E-42
	CHS_s	-2.67	0.73	-3.65	0.0003
	TPF_s	16	0.88	18.23	3.01E-74

Table 6.2.3.5. *Common dolphin ZIGLM model outputs.* Slope estimate, standard error, *z*-value, and *p*-value for each parameter within both nested models (conditional and logistic). Parameter details are the full names of each parameter, corresponding to the parameter code.

Model	Parameter Code	Slope Estimate	Standard Error	*z*-Value	*p*-Value
conditional	(Intercept)	-5.21	0.18	-28.65	1.67E-180
	TPM_s	10.26	0.37	28.02	9.51E-173
	TPF_s	1.68	0.27	6.33	2.48E-10
	FEA_s	-0.02	0.14	-0.12	0.9
	BAT_s	0.71	0.08	8.76	2.03E-18
	CHT_s	-3.05	0.27	-11.09	1.45E-28
logistic	(Intercept)	-20.96	1.11	-18.85	3.17E-79
	TPM_s	32.18	1.57	20.52	1.51E-93
	CON_s	34.85	2.55	13.66	1.65E-42
	CHT_s	-2.66	0.69	-3.86	0.0001
	TPR_s	-0.78	0.20	-3.89	9.92E-05
	TPM_s:CON_s	-42.53	3.59	-11.84	2.52E-32

Table 6.2.3.6. *European shag ZIGLM model outputs.* Slope estimate, standard error, *z*-value, and *p*-value for each parameter within both nested models (conditional and logistic). Parameter details are the full names of each parameter, corresponding to the parameter code.

Model	Parameter Code	Slope Estimate	Standard Error	*z*-Value	*p*-Value
conditional	(Intercept)	2.11	0.04	47.01	0
	TPM_s	-0.99	0.09	-10.85	1.94E-27
	TPF_s	0.35	0.18	1.99	0.047
	FEA_s	3.13	0.34	9.32	1.13E-20
	BAT_s	-26.43	1.90	-13.92	4.66E-44
	CHT_s	0.01	0.08	0.17	0.862
logistic	(Intercept)	3.09	0.06	55.73	0
	SPM_s	2.95	0.19	15.59	8.94E-55
	TPF_s	-7.21	0.37	-19.51	9.18E-85
	CHS_s	-1.54	0.23	-6.75	1.47E-11
	TPR_s	9.41	0.42	22.46	9.13E-112

Table 6.2.3.7. *European storm petrel ZIGLM model outputs.* Slope estimate, standard error, *z*-value, and *p*-value for each parameter within both nested models (conditional and logistic). Parameter details are the full names of each parameter, corresponding to the parameter code.

Model	Parameter Code	Slope Estimate	Standard Error	*z*-Value	*p*-Value
conditional	(Intercept)	0.39	0.19	2.08	0.04
	TPM_s	-1.03	0.30	-3.43	0.001
	TPF_s	-0.65	0.31	-2.08	0.038
	FEA_s	-1.18	0.28	-4.14	3.51E-05
	BAT_s	-3.06	0.18	-17.08	1.97E-65
	CHT_s	-1.06	0.20	-5.30	1.15E-07
logistic	(Intercept)	4.67	0.22	21.70	1.85E-104
	TPM_s	-3.25	0.38	-8.51	1.68E-17
	TPF_s	-12.48	2.27	-5.49	3.93E-08
	TPR_s	-48.63	2.33	-20.92	3.44E-97

Table 6.2.3.8. *Fin whale ZIGLM model outputs.* Slope estimate, standard error, *z*-value, and *p*-value for each parameter within both nested models (conditional and logistic). Parameter details are the full names of each parameter, corresponding to the parameter code.

Model	Parameter Code	Slope Estimate	Standard Error	*z*-Value	*p*-Value
conditional	(Intercept)	-6.25	0.29	-21.73	1.06E-104
	TPM_s	4.45	0.46	9.68	3.55E-22
	TPF_s	5.36	0.88	6.08	1.22E-09
	FEA_s	0.03	0.29	0.10	0.92
	BAT_s	2.08	0.25	8.31	9.71E-17
	CHT_s	-4.40	0.75	-5.90	3.58E-09
logistic	(Intercept)	1.90	0.26	7.30	2.99E-13
	CHT_s	17.00	2.48	6.86	6.80E-12
	BAT_s	4.39	1.37	3.21	0.001
	CHT_s:BAT_s	-690.83	89.05	-7.76	8.66E-15

Table 6.2.3.9. *Harbour porpoise ZIGLM model outputs.* Slope estimate, standard error, *z*-value, and *p*-value for each parameter within both nested models (conditional and logistic). Parameter details are the full names of each parameter, corresponding to the parameter code.

Model	Parameter Code	Slope Estimate	Standard Error	*z*-Value	*p*-Value
conditional	(Intercept)	-1.19	0.04	-31.50	4.23E-218
	TPM_s	-0.50	0.07	-7.00	2.64E-12
	TPF_s	0.95	0.14	6.60	4.01E-11
	FEA_s	6.43	0.30	21.20	6.35E-100
	BAT_s	-55.37	1.36	-40.80	0
	CHT_s	3.16	0.12	26.40	5.29E-154
Logistic	(Intercept)	-10.60	0.62	-17.17	4.56E-66
	TPM_s	7.11	1.45	4.92	8.85E-07
	BAT_s	414.17	87.01	4.76	1.93E-06
	CHT_s	7.42	0.95	7.79	6.60E-15
	SPM_s	13.46	0.68	19.76	6.22E-87
	TPM_s:BAT_s	-1204.43	262.92	-4.58	4.63E-06

Table 6.2.3.10. *Herring gull ZIGLM model outputs.* Slope estimate, standard error, *z*-value, and *p*-value for each parameter within both nested models (conditional and logistic). Parameter details are the full names of each parameter, corresponding to the parameter code.

Model	Parameter Code	Slope Estimate	Standard Error	*z*-Value	*p*-Value
conditional	(Intercept)	2.81	0.01	306.47	0
	TPM_s	-1.02	0.02	-52.38	0
	TPF_s	0.11	0.06	1.74	0.08
	FEA_s	-2.03	0.13	-15.36	3.25E-53
	BAT_s	-10.28	0.23	-44.79	0
	CHT_s	-0.33	0.02	-16.23	3.19E-59
logistic	(Intercept)	0.05	0.04	1.42	0.155
	CHT_s	0.19	0.06	3.03	0.00242
	TPM_s	3.37	0.07	49.31	0
	SPM_s	-0.46	0.06	-7.58	3.56E-14

Table 6.2.3.11. *Lesser black-backed gull ZIGLM model outputs.* Slope estimate, standard error, *z*-value, and *p*-value for each parameter within both nested models (conditional and logistic). Parameter details are the full names of each parameter, corresponding to the parameter code.

Model	Parameter Code	Slope Estimate	Standard Error	*z*-Value	*p*-Value
conditional	(Intercept)	-1.02	0.0377	-27.04	4.97E-161
	TPM_s	1.171	0.0642	18.24	2.33E-74
	TPF_s	-0.891	0.1544	-5.77	8.07E-09
	FEA_s	-0.154	0.1376	-1.12	0.263
	BAT_s	-2.78	0.1248	-22.28	5.84E-110
	CHT_s	3.471	0.0753	46.09	0
logistic	(Intercept)	-3.85	0.386	-9.96	2.23E-23
	CHT_s	10.01	0.53	18.88	1.71E-79
	TPM_s	-3.57	0.558	-6.39	1.68E-10
	SPM_s	-3.46	0.943	-3.67	0.000243

Table 6.2.3.12. *Manx shearwater ZIGLM model outputs.* Slope estimate, standard error, *z*-value, and *p*-value for each parameter within both nested models (conditional and logistic). Parameter details are the full names of each parameter, corresponding to the parameter code.

Model	Parameter Code	Slope Estimate	Standard Error	*z*-Value	*p*-Value
conditional	(Intercept)	0.91	0.02	49.80	0
	TPM_s	3.19	0.03	113.10	0
	TPF_s	2.48	0.02	108.60	0
	FEA_s	1.10	0.07	15.00	1.52E-50
	BAT_s	-5.93	0.07	-85.50	0
	CHT_s	0.88	0.02	40.00	0
logistic	(Intercept)	3.48	0.03	115.46	0
	CHT_s	-3.77	0.08	-49.52	0
	SPM_s	-0.68	0.08	-8.19	2.65E-16

Table 6.2.3.13. *Minke whale ZIGLM model outputs.* Slope estimate, standard error, *z*-value, and *p*-value for each parameter within both nested models (conditional and logistic). Parameter details are the full names of each parameter, corresponding to the parameter code.

Model	Parameter Code	Slope Estimate	Standard Error	*z*-Value	*p*-Value
conditional	(Intercept)	-2.70	0.13	-21.14	3.58E-99
	TPM_s	-1.45	0.21	-6.88	5.86E-12
	TPF_s	1.19	0.42	2.85	0.004
	FEA_s	3.26	0.35	9.38	6.70E-21
	BAT_s	-6.45	0.60	-10.71	9.35E-27
	CHT_s	-0.80	0.30	-2.66	0.008
logistic	(Intercept)	0.76	0.17	4.57	4.84E-06
	TPF_s	-95.03	8.18	-11.62	3.32E-31
	SPM_s	6.76	0.62	10.89	1.24E-27

Table 6.2.3.14. *Northern gannet ZIGLM model outputs.* Slope estimate, standard error, *z*-value, and *p*-value for each parameter within both nested models (conditional and logistic). Parameter details are the full names of each parameter, corresponding to the parameter code.

Model	Parameter Code	Slope Estimate	Standard Error	*z*-Value	*p*-Value
conditional	(Intercept)	4.17	0.005	880.6	0
	TPM_s	-2.43	0.010	-240.4	0
	TPF_s	1.81	0.020	91.5	0
	FEA_s	1.69	0.021	79.6	0
	BAT_s	-0.64	0.014	-46.4	0
	CHT_s	-0.53	0.008	-69	0
logistic	(Intercept)	0.25	0.010	25.61	1.21E-144
	CHT_s	0.27	0.043	6.33	2.53E-10
	FEA_s	3.47	0.109	31.9	2.86E-223

Table 6.2.3.15. *Northern gannet ZIGLM model outputs.* Slope estimate, standard error, *z*-value, and *p*-value for each parameter within both nested models (conditional and logistic). Parameter details are the full names of each parameter, corresponding to the parameter code.

Model	Parameter Code	Slope Estimate	Standard Error	*z*-Value	*p*-Value
conditional	(Intercept)	1.40	0.03	46.12	0
	TPM_s	-0.46	0.05	-8.96	3.30E-19
	TPF_s	1.90	0.08	24.33	9.41E-131
	FEA_s	-0.17	0.07	-2.30	0.0214
	BAT_s	-1.59	0.05	-30.90	1.06E-209
	CHT_s	0.47	0.03	13.92	4.81E-44
logistic	(Intercept)	5.57	0.14	40.18	0
	TPM_s	-18.09	0.43	-41.77	0
	TPF_s	-7.42	2.02	-3.67	0.0002

Table 6.2.3.16. *Orca ZIGLM model outputs.* Slope estimate, standard error, *z*-value, and *p*-value for each parameter within both nested models (conditional and logistic). Parameter details are the full names of each parameter, corresponding to the parameter code.

Model	Parameter Code	Slope Estimate	Standard Error	*z*-Value	*p*-Value
conditional	(Intercept)	2.47	0.28	8.91	5.19E-19
	TPM_s	-2.73	0.60	-4.57	4.83E-06
	TPF_s	3.02	0.78	3.86	0.0001
	FEA_s	0.51	1.07	0.48	0.634
	BAT_s	0.40	0.40	1.01	0.312
	CHT_s	-0.67	0.61	-1.09	0.278
logistic	(Intercept)	5.33	0.53	10.13	4.04E-24
	TPR_s	-4.69	1.90	-2.48	0.01
	TPS_s	1.92	1.06	1.80	0.07
	CON_s	5.43	0.78	6.93	4.09E-12
	BAT_s	0.84	0.88	0.96	0.34
	TPR_s:TPS_s	5.70	3.25	1.75	0.08
	CON_s:BAT_s	-5.04	7.82	-0.64	0.519

Table 6.2.3.17. *Pilot whale ZIGLM model outputs.* Slope estimate, standard error, *z*-value, and *p*-value for each parameter within both nested models (conditional and logistic). Parameter details are the full names of each parameter, corresponding to the parameter code.

Model	Parameter code	Slope Estimate	Standard Error	*z*-Value	*p*-Value
Conditional	(Intercept)	3.13	0.38	8.35	6.84E-17
	TPM	-3.27	0.76	-4.29	1.78E-05
	TPF	-9.31	1.76	-5.29	1.20E-07
	CHL	-0.15	0.56	-0.28	0.78
	FEA	1.33	0.36	3.75	0.0002
	BAT	1.52	0.26	5.91	3.53E-09
Logistic	(Intercept)	4.36	0.33	13.33	1.56E-40
	CON	22.55	3.51	6.43	1.32E-10
	TPM	-1.85	0.66	-2.79	0.005
	FEA	-1.53	0.31	-4.98	6.24E-07
	CON: TPM	-16.77	6.27	-2.67	0.0075

Table 6.2.3.18. *Razorbill ZIGLM model outputs.* Slope estimate, standard error, *z*-value, and *p*-value for each parameter within both nested models (conditional and logistic). Parameter details are the full names of each parameter, corresponding to the parameter code.

Model	Parameter Code	Slope Estimate	Standard Error	*z*-Value	*p*-Value
conditional	(Intercept)	0.61	0.05	12.32	6.76E-35
	TPM_s	0.15	0.11	1.31	0.19
	TPF_s	5.01	0.25	20.20	1.05E-90
	FEA_s	4.33	0.35	12.19	3.66E-34
	BAT_s	-30.36	0.96	-31.58	6.77E-219
	CHT_s	-1.28	0.07	-18.85	2.93E-79
logistic	(Intercept)	-10.78	0.34	-32.11	3.46E-226
	LND_s	16.28	0.57	28.49	1.53E-178
	TPF_s	3.47	0.47	7.37	1.67E-13
	TPM_s	15.19	0.47	32.46	3.51E-231
	TPR_s	3.07	0.20	15.05	3.56E-51

Table 6.2.3.19. *Risso's dolphin ZIGLM model outputs.* Slope estimate, standard error, *z*-value, and *p*-value for each parameter within both nested models (conditional and logistic). Parameter details are the full names of each parameter, corresponding to the parameter code.

Model	Parameter Code	Slope Estimate	Standard Error	*z*-Value	*p*-Value
conditional	(Intercept)	1.94	0.18	10.90	1.21E-27
	TPM_s	-0.86	0.34	-2.57	0.0101
	TPF_s	2.22	0.41	5.41	6.37E-08
	FEA_s	0.90	0.23	3.93	8.47E-05
	BAT_s	0.00	0.17	0.00	0.998
	CHT_s	-2.33	0.46	-5.08	3.76E-07
logistic	(Intercept)	6.36	0.30	21.53	7.4E-103
	BAT_s	7.95	2.35	3.38	0.000715
	TPM_s	-2.34	0.51	-4.56	5.11E-06
	CON_s	3.92	0.33	11.93	8.13E-33
	BAT_s:TPM_s	-10.05	3.51	-2.87	0.00414

Table 6.2.3.20. *Sperm whale ZIGLM model outputs.* Slope estimate, standard error, *z*-value, and *p*-value for each parameter within both nested models (conditional and logistic). Parameter details are the full names of each parameter, corresponding to the parameter code.

Model	Parameter Code	Slope Estimate	Standard Error	*z*-Value	*p*-Value
Conditional	(Intercept)	-3.93	0.43	-9.23	2.65E-20
	TPM_s	-0.91	0.94	-0.97	0.33
	TPF_s	-2.26	2.99	-0.76	0.45
	FEA_s	0.89	0.66	1.37	0.17
	BAT_s	0.75	0.48	1.55	0.12
	CHT_s	0.64	0.89	0.72	0.47
logistic	(Intercept)	4.28	0.96	4.46	8.06E-06
	BAT_s	-50.72	9.41	-5.39	7.06E-08
	FEA_s	-6.45	3.54	-1.82	0.07
	CON_s	28.05	14.53	1.93	0.05
	BAT_s:FEA_s	80.08	18.75	4.27	1.94E-05

Table 6.2.3.21. *Striped dolphin ZIGLM model outputs.* Slope estimate, standard error, *z*-value, and *p*-value for each parameter within both nested models (conditional and logistic). Parameter details are the full names of each parameter, corresponding to the parameter code.

Model	Parameter Code	Slope Estimate	Standard Error	*z*-Value	*p*-Value
conditional	(Intercept)	2.28	0.132	17.25	1.10E-66
	TPM_s	0.43	0.193	2.21	0.0272
	TPF_s	-2.01	0.609	-3.3	0.000966
	FEA_s	0.39	0.070	5.55	2.81E-08
	BAT_s	0.40	0.062	6.38	1.82E-10
	CHT_s	0.75	0.176	4.27	1.99E-05
logistic	(Intercept)	13.07	0.540	24.2	2.15E-129
	BAT_s	-11.23	1.064	-10.56	4.71E-26
	TPM_s	-9.77	0.806	-12.13	7.52E-34
	BAT_s:TPM_s	10.02	1.581	6.34	2.34E-10

Table 6.2.3.22. *White-beaked dolphin ZIGLM model outputs.* Slope estimate, standard error, *z*-value, and *p*-value for each parameter within both nested models (conditional and logistic). Parameter details are the full names of each parameter, corresponding to the parameter code.

Model	Parameter Code	Slope Estimate	Standard Error	*z*-Value	*p*-Value
conditional	(Intercept)	1.55	0.09	16.90	4.26E-64
	TPM_s	-0.16	0.19	-0.82	0.41
	TPF_s	0.03	0.27	0.11	0.91
	FEA_s	-1.91	0.91	-2.09	0.04
	BAT_s	2.49	0.49	5.08	3.83E-07
	CHT_s	1.03	0.22	4.68	2.81E-06
logistic	(Intercept)	3.93	0.10	38.22	0
	BAT_s	8.18	3.79	2.16	0.0307
	TPM_s	1.48	0.21	7.15	8.45E-13
	BAT_s:TPM_s	-0.47	7.52	-0.06	0.95

Table 6.2.3.23. *White-sided dolphin ZIGLM model outputs.* Slope estimate, standard error, *z*-value, and *p*-value for each parameter within both nested models (conditional and logistic). Parameter details are the full names of each parameter, corresponding to the parameter code.

Model	Parameters	Slope Estimate	Standard Error	*z*-Value	*p*-Value
conditional	(Intercept)	7.52	0.85	8.85	8.51E-19
	TPM_s	-18.77	1.48	-12.73	3.99E-37
	TPF_s	1.36	1.01	1.34	0.18
	CHT_s	-0.05	0.61	-0.09	0.93
	FEA_s	-0.59	0.75	-0.78	0.43
	BAT_s	1.18	0.32	3.69	2.26E-04
logistic	(Intercept)	12.19	1.00	12.19	3.76E-34
	SPM_s	9.54	6.08	1.57	0.12
	TPM_s	-28.10	2.39	-11.74	8.47E-32
	SPM_s: TPM_s	8.58	13.89	0.62	0.54

Atlantic Puffin

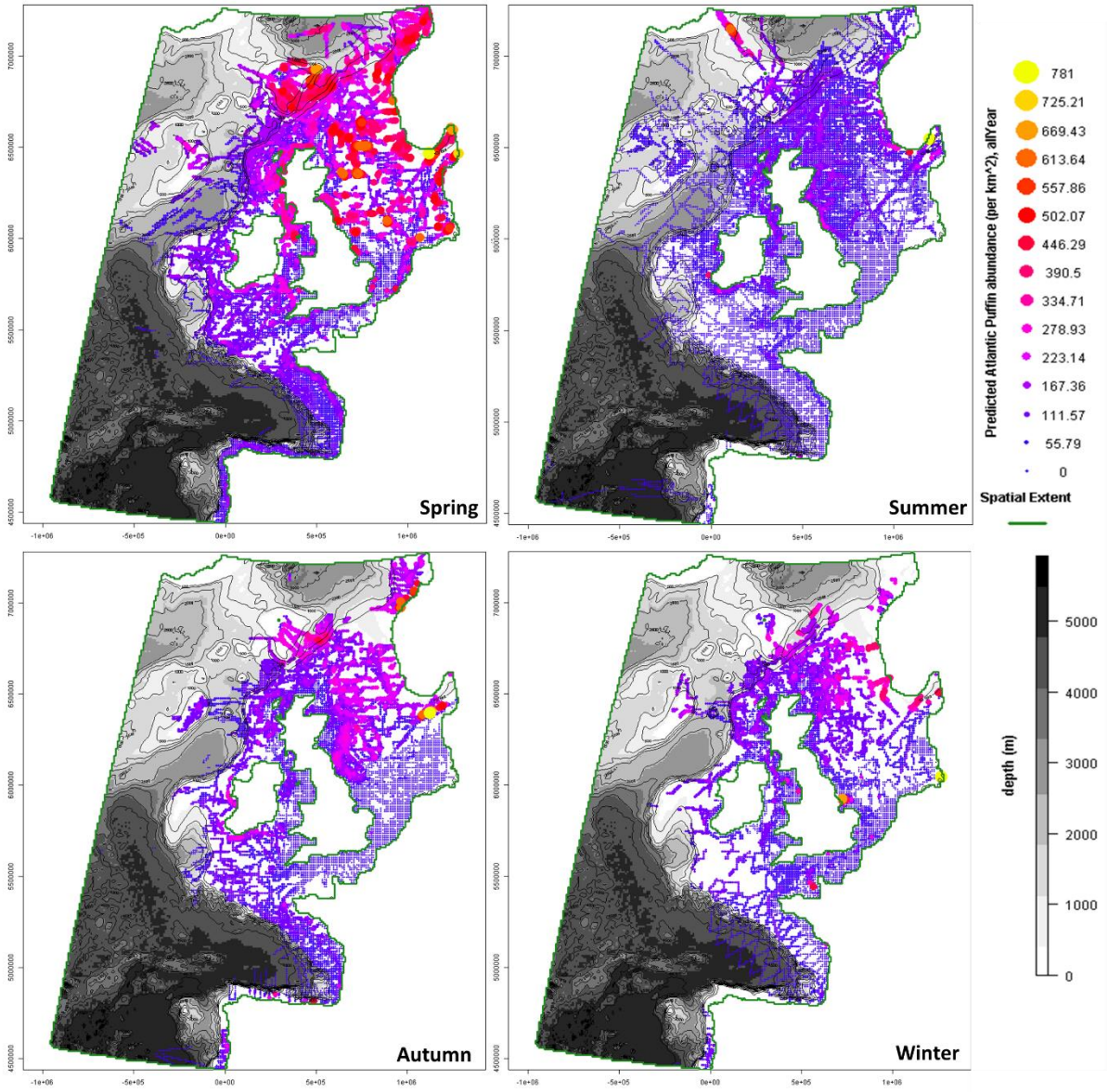

Figure 6.2.8.1. *Maps of predicted abundance of Atlantic puffin, overlaying bathymetry.* Maximum predicted abundance (per 10 km^2) subset by season, from the same model, expressed as the expected value (mean of the conditional distribution multiplied by 1 minus the zero-inflation probability) scaled to the maximum observed abundance value in the Atlantic puffin dataset; represented by colour and size (blue-red-yellow scalebar). Each season covers 3 months, with spring starting in March. Water depth (m) represented by greyscale contours. Green line represents coastline or spatial extent.

Black-legged Kittiwake

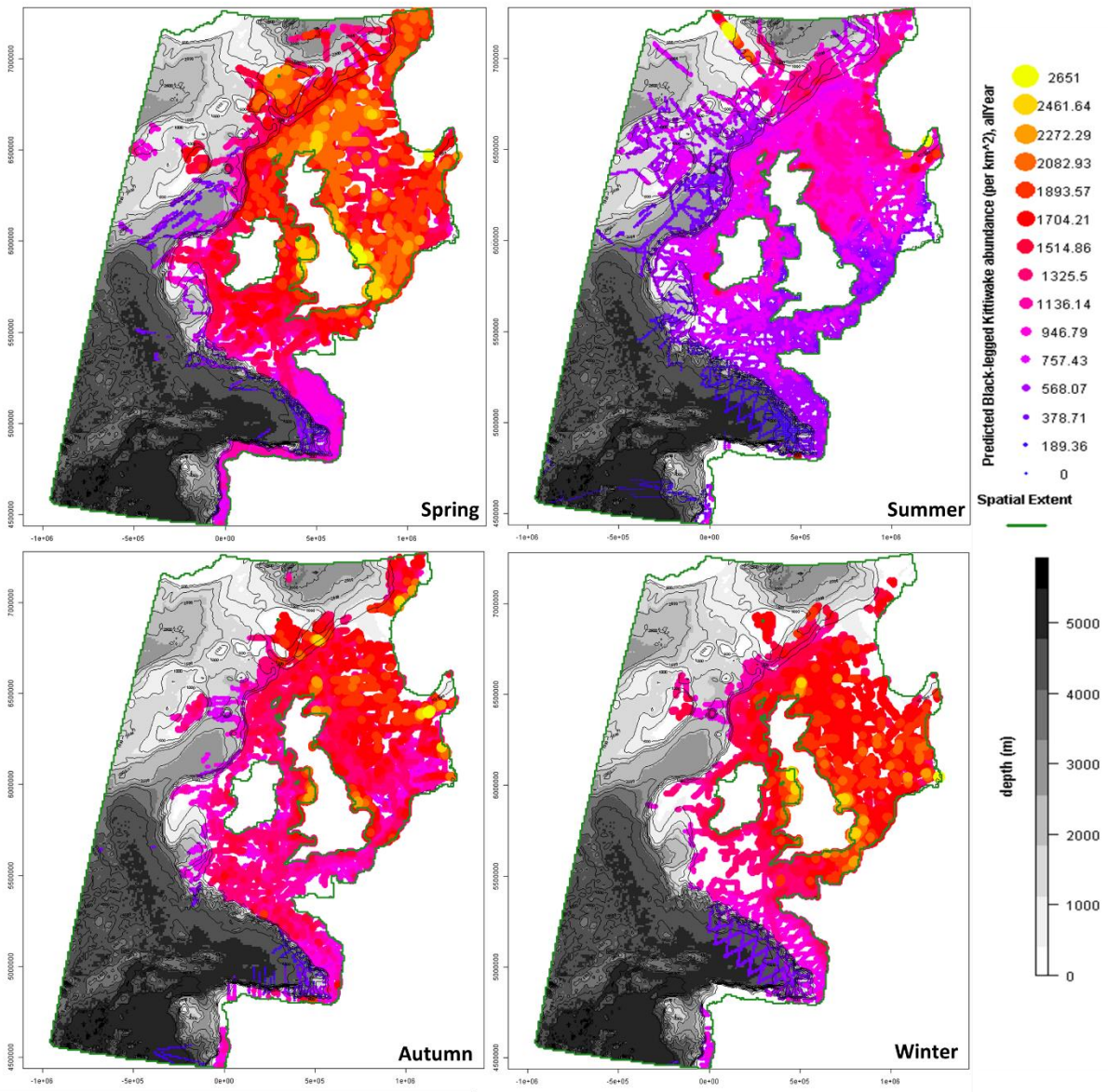

Figure 6.2.8.2. *Maps of predicted abundance of black-legged kittiwakes, overlaying bathymetry.* Maximum predicted abundance (per 10 km^2) subset by season, from the same model, expressed as the expected value (mean of the conditional distribution multiplied by 1 minus the zero-inflation probability) scaled to the maximum observed abundance value in the black-legged kittiwake dataset; represented by colour and size (blue-red-yellow scalebar). Each season covers 3 months, with spring starting in March. Water depth (m) represented by greyscale contours. Green line represents coastline or spatial extent.

Bottlenose Dolphin

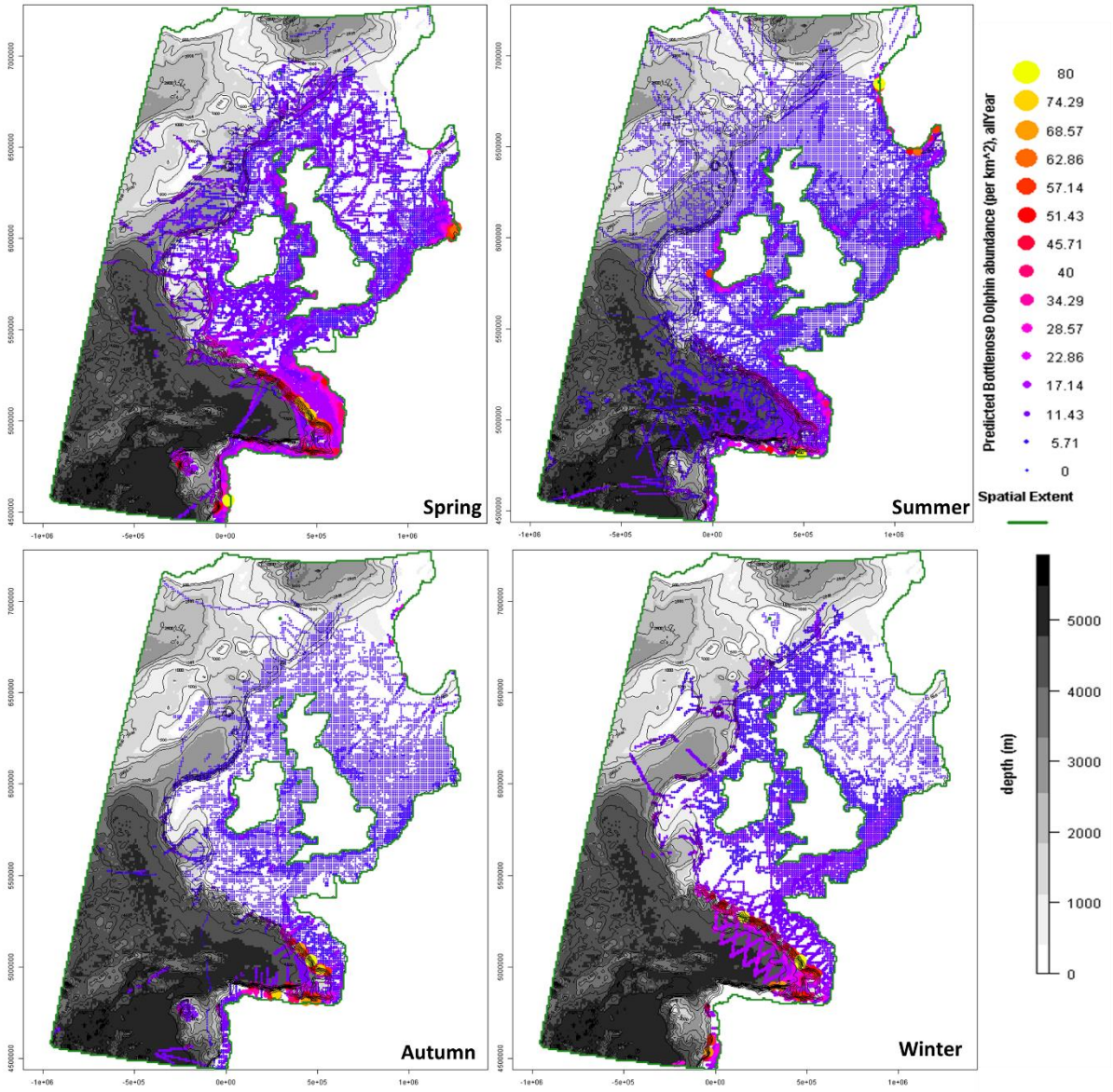

Figure 6.2.8.3. *Maps of predicted abundance of bottlenose dolphins, overlaying bathymetry.* Maximum predicted abundance (per 10 km^2) subset by season, from the same model, expressed as the expected value (mean of the conditional distribution multiplied by 1 minus the zero-inflation probability) scaled to the maximum observed abundance value in the bottlenose dolphin dataset; represented by colour and size (blue-red-yellow scalebar). Each season covers 3 months, with spring starting in March. Water depth (m) represented by greyscale contours. Green line represents coastline or spatial extent.

Common Guillemot

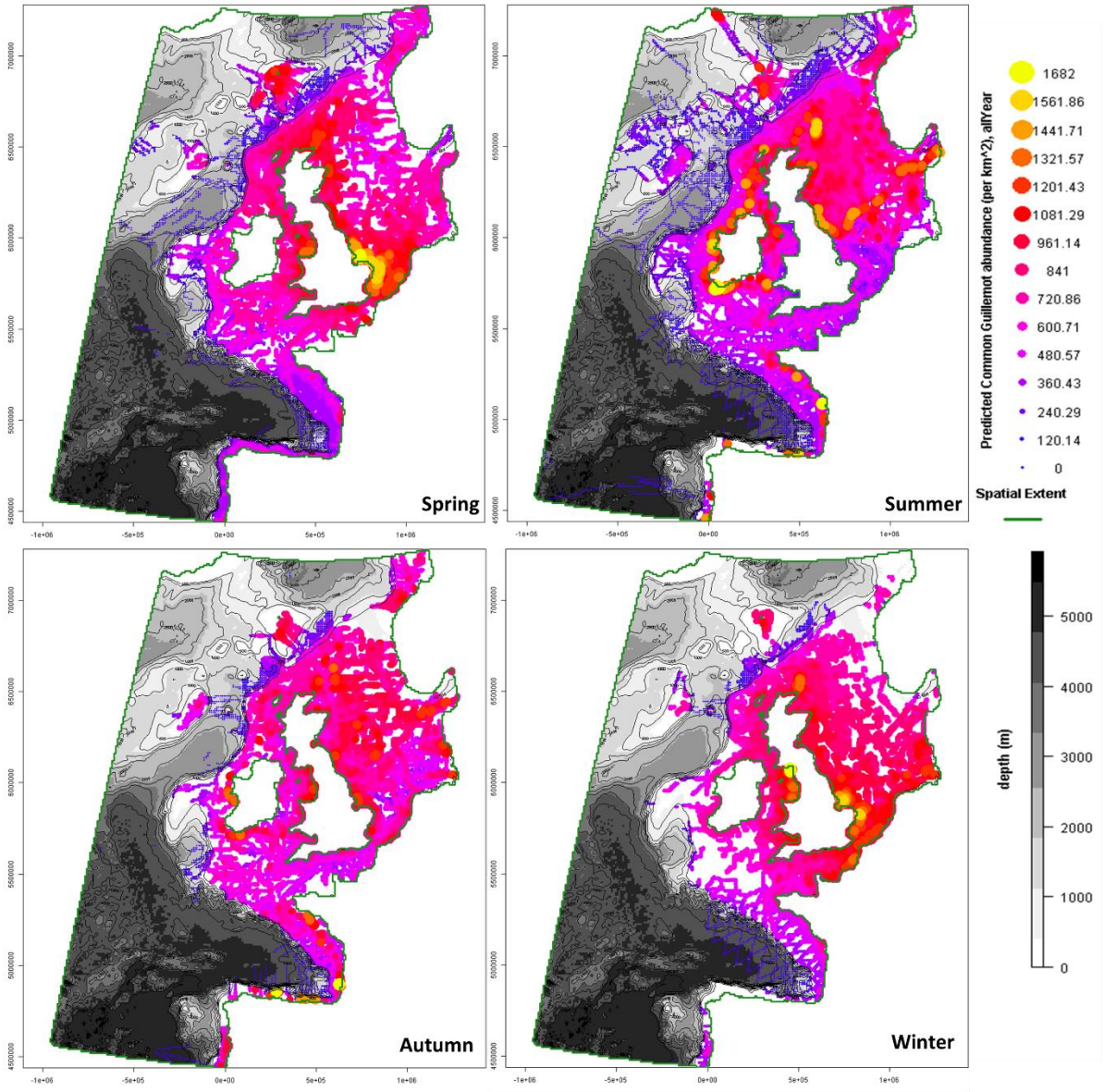

Figure 6.2.8.4. *Maps of predicted abundance of common guillemots, overlaying bathymetry.* Maximum predicted abundance (per 10 km^2) subset by season, from the same model, expressed as the expected value (mean of the conditional distribution multiplied by 1 minus the zero-inflation probability) scaled to the maximum observed abundance value in the common guillemot dataset; represented by colour and size (blue-red-yellow scalebar). Each season covers 3 months, with spring starting in March. Water depth (m) represented by greyscale contours. Green line represents coastline or spatial extent.

Common Dolphin

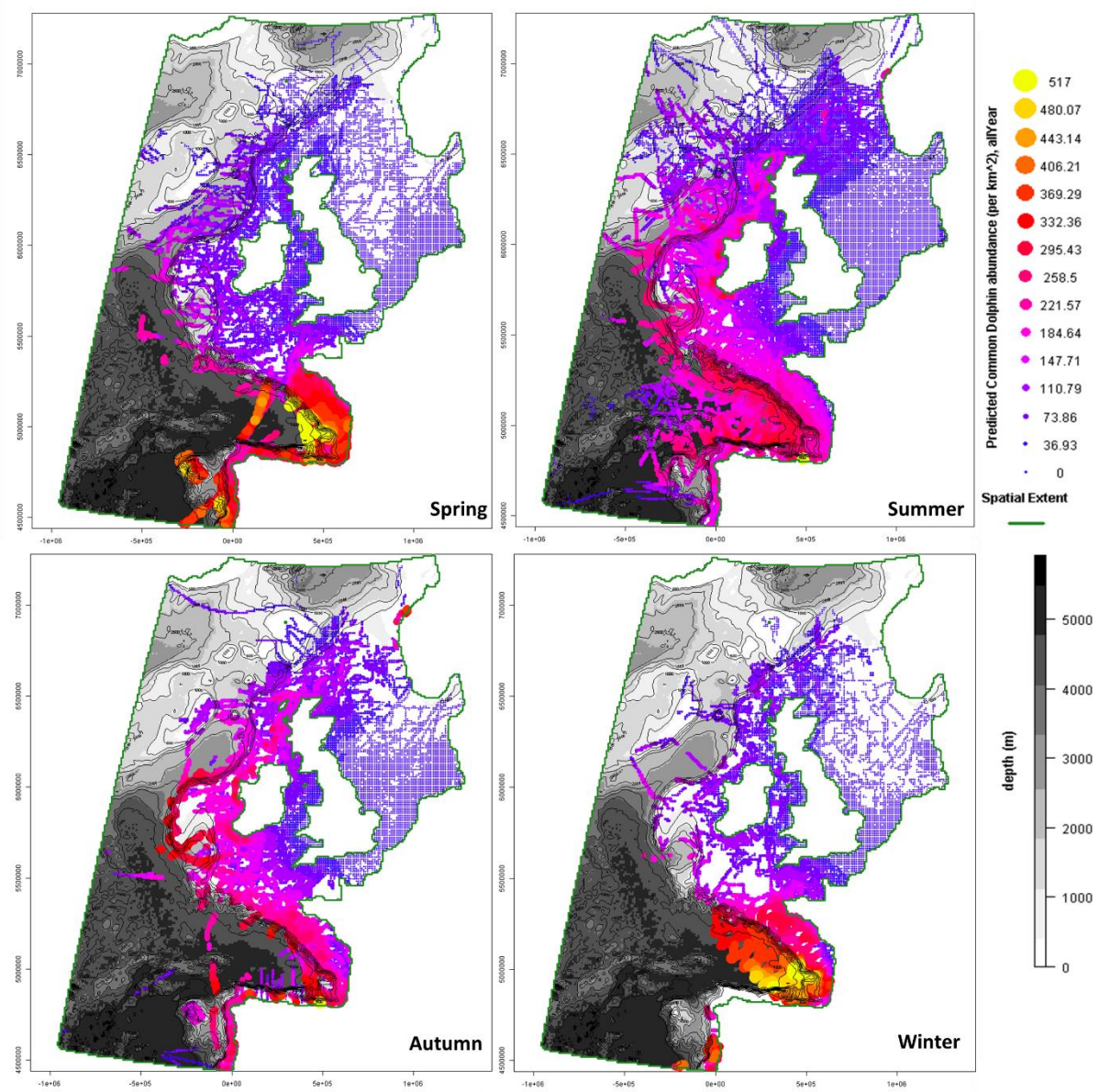

Figure 6.2.8.5. *Maps of predicted abundance of common dolphins, overlaying bathymetry.* Maximum predicted abundance (per 10 km^2) subset by season, from the same model, expressed as the expected value (mean of the conditional distribution multiplied by 1 minus the zero-inflation probability) scaled to the maximum observed abundance value in the common dolphin dataset; represented by colour and size (blue-red-yellow scalebar). Each season covers 3 months, with spring starting in March. Water depth (m) represented by greyscale contours. Green line represents coastline or spatial extent.

European Shag

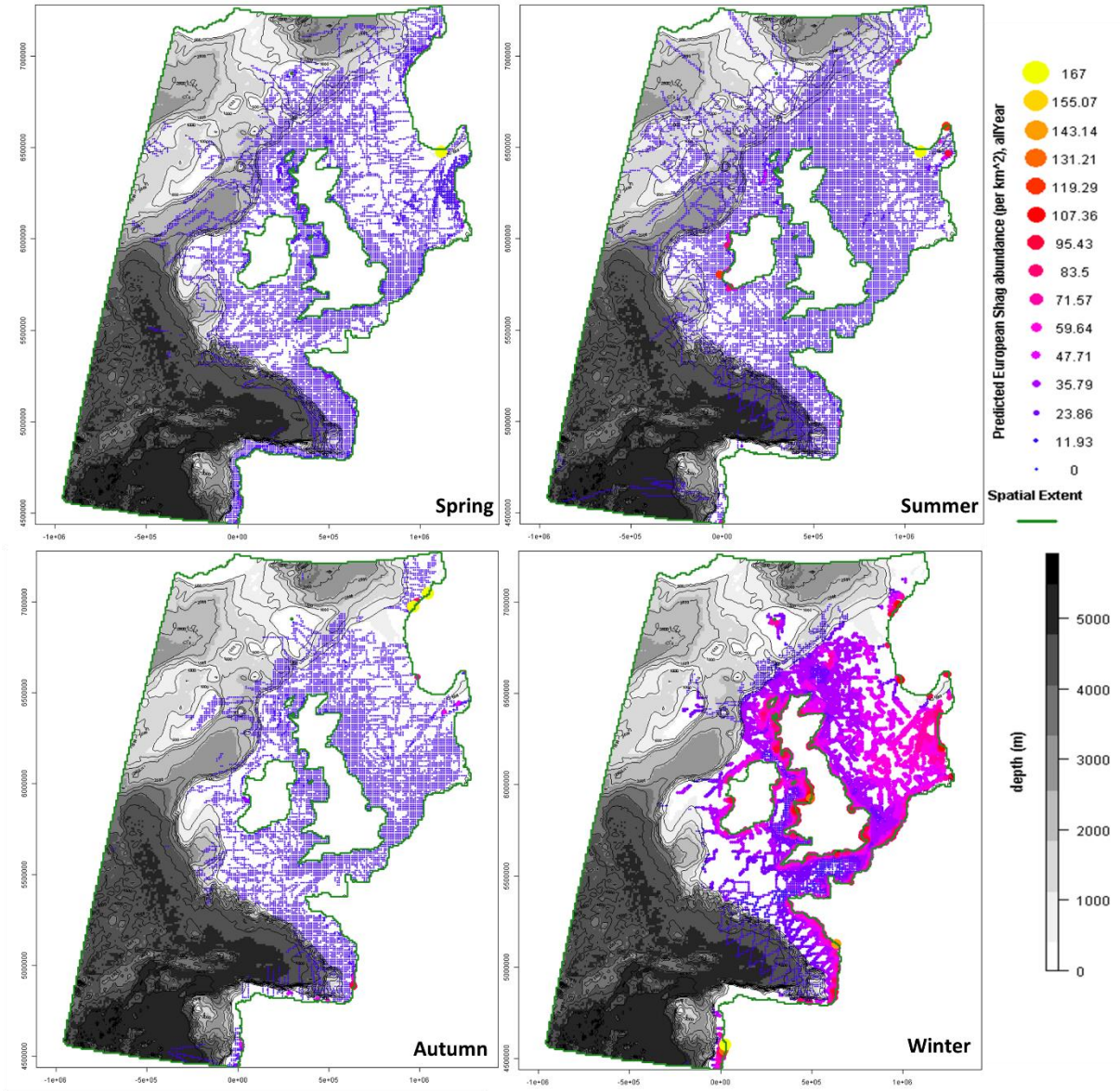

Figure 6.2.8.6. *Maps of predicted abundance of European shags, overlaying bathymetry.* Maximum predicted abundance (per 10 km^2) subset by season, from the same model, expressed as the expected value (mean of the conditional distribution multiplied by 1 minus the zero-inflation probability) scaled to the maximum observed abundance value in the European shag dataset; represented by colour and size (blue-red-yellow scalebar). Each season covers 3 months, with spring starting in March. Water depth (m) represented by greyscale contours. Green line represents coastline or spatial extent.

European Storm Petrel

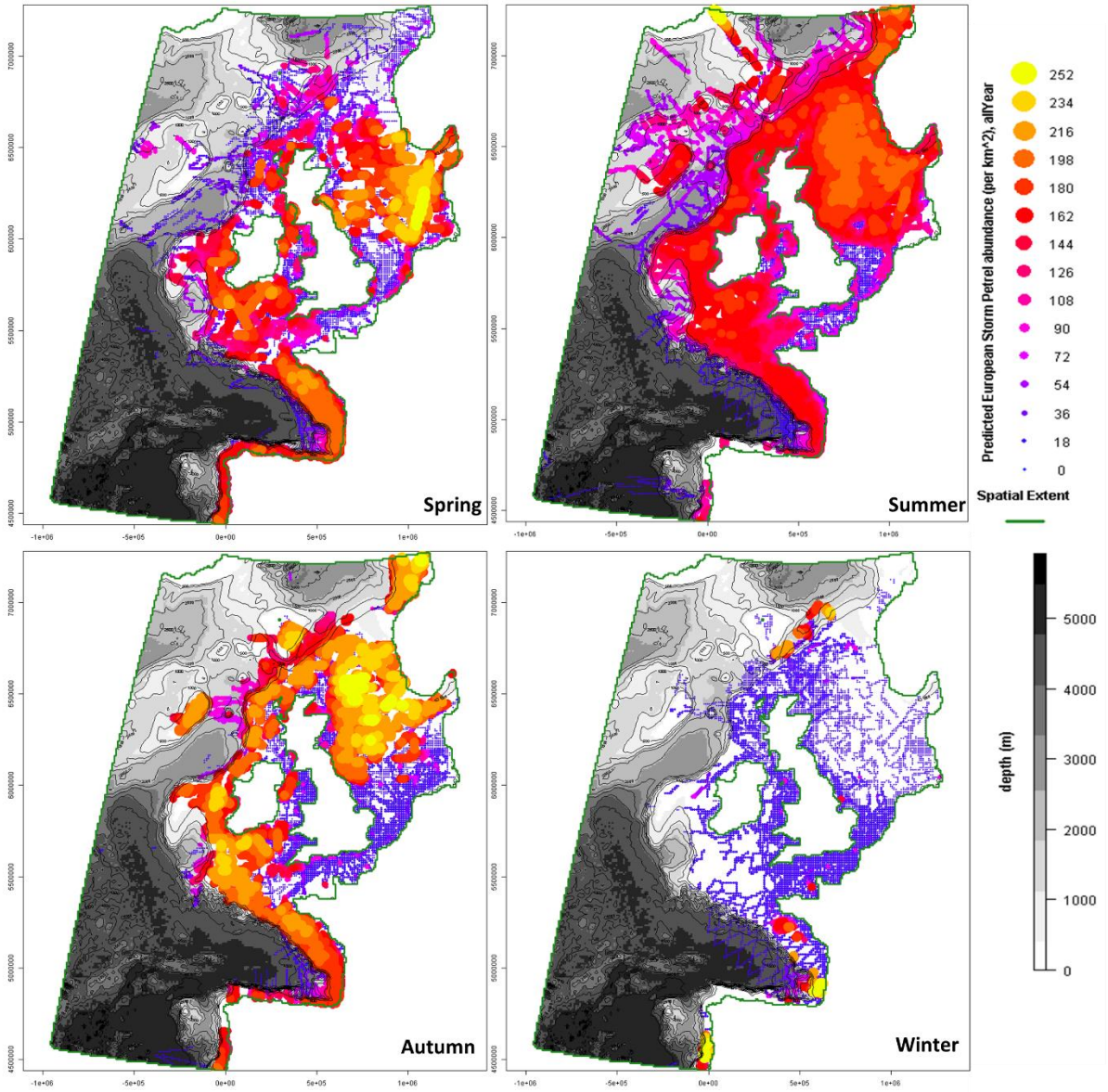

Figure 6.2.8.7. *Maps of predicted abundance of European storm petrel, overlaying bathymetry.* Maximum predicted abundance (per 10 km^2) subset by season, from the same model, expressed as the expected value (mean of the conditional distribution multiplied by 1 minus the zero-inflation probability) scaled to the maximum observed abundance value in the European storm petrel dataset; represented by colour and size (blue-red-yellow scalebar). Each season covers 3 months, with spring starting in March. Water depth (m) represented by greyscale contours. Green line represents coastline or spatial extent.

Fin Whale

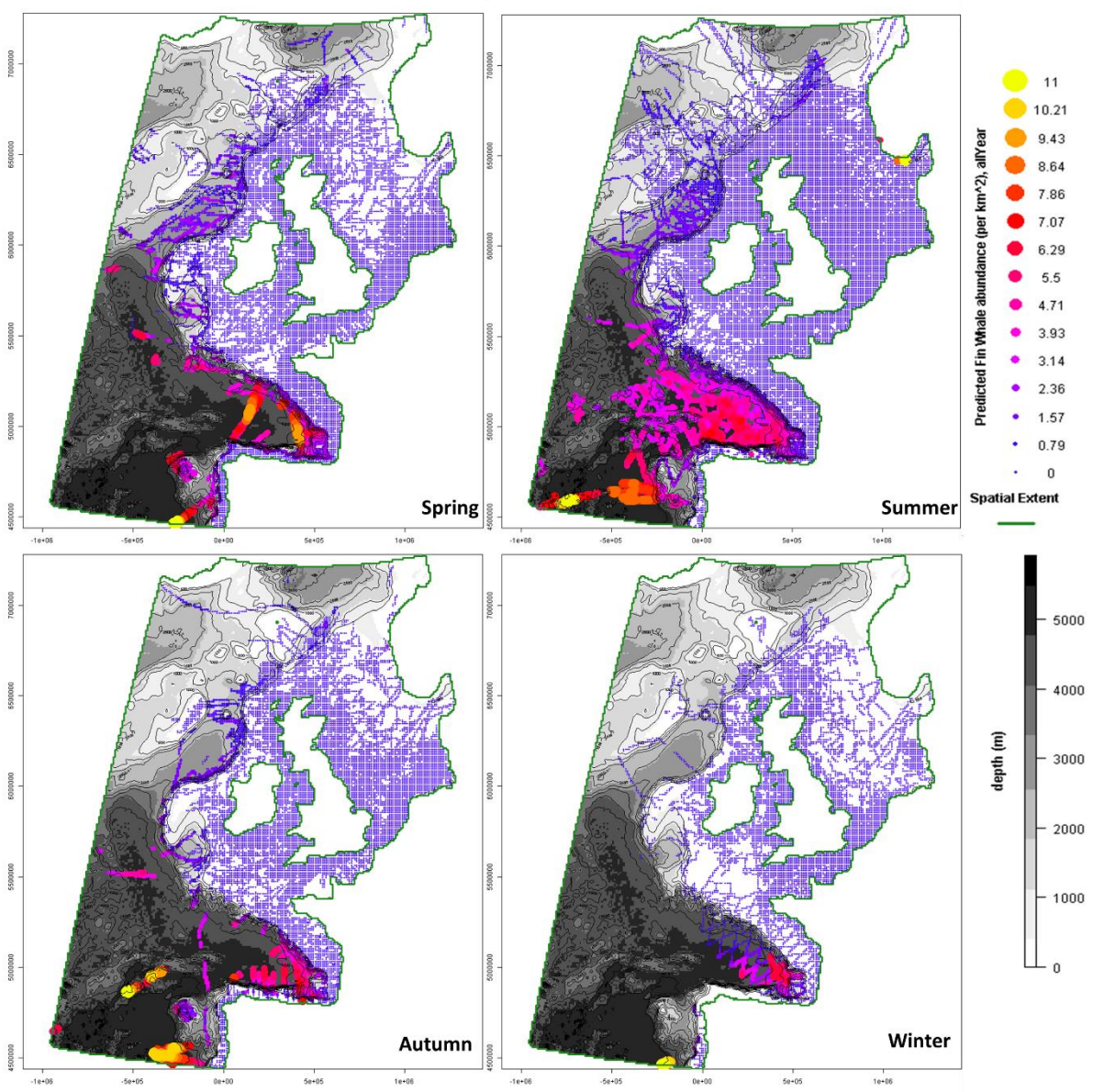

Figure 6.2.8.8. *Maps of predicted abundance of fin whales, overlaying bathymetry.* Maximum predicted abundance (per 10 km^2) subset by season, from the same model, expressed as the expected value (mean of the conditional distribution multiplied by 1 minus the zero-inflation probability) scaled to the maximum observed abundance value in the fin whale dataset; represented by colour and size (blue-red-yellow scalebar). Each season covers 3 months, with spring starting in March. Water depth (m) represented by greyscale contours. Green line represents coastline or spatial extent.

Harbour Porpoise

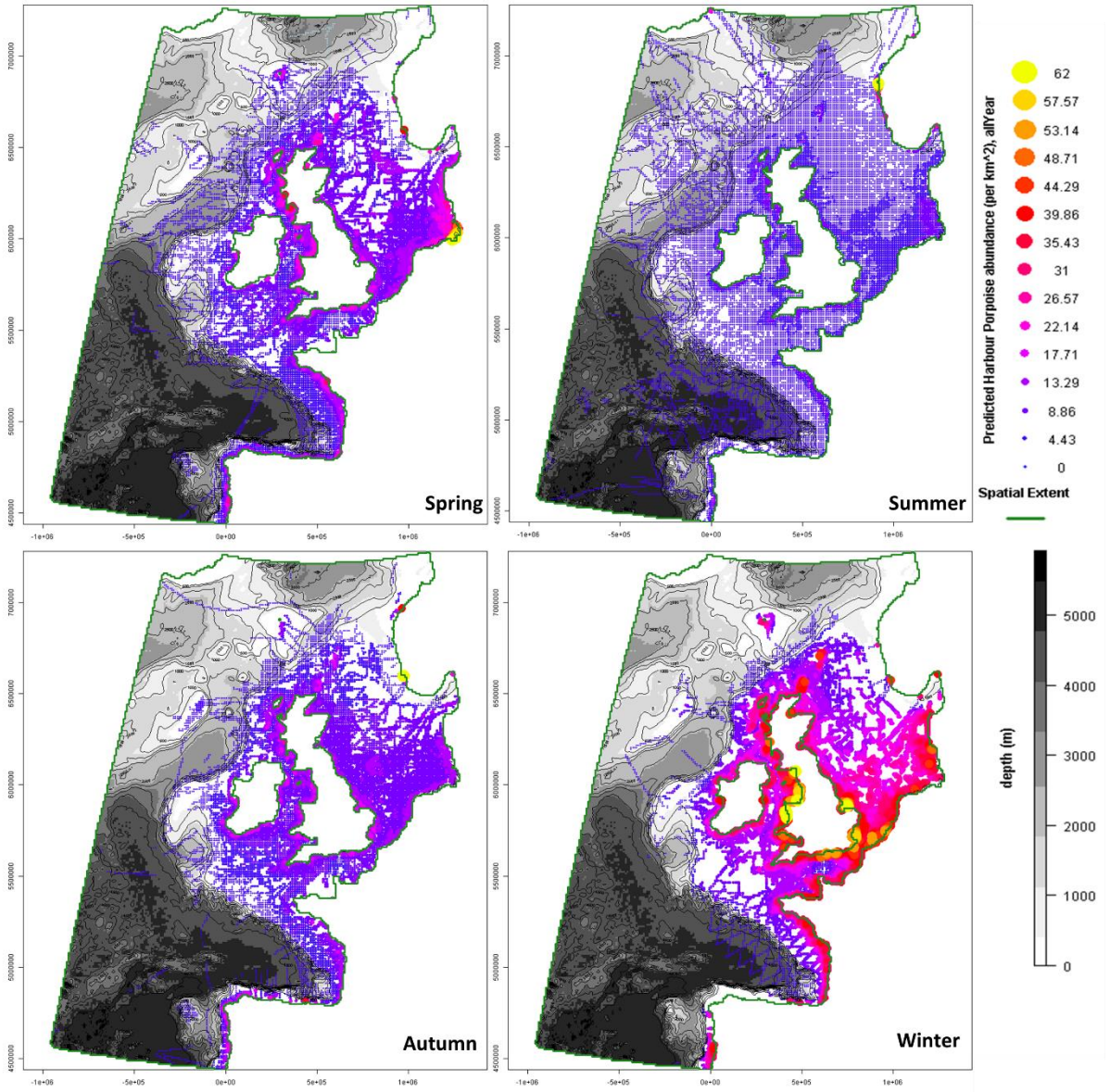

Figure 6.2.8.9. *Maps of predicted abundance of harbour porpoise, overlaying bathymetry.* Maximum predicted abundance (per 10 km^2) subset by season, from the same model, expressed as the expected value (mean of the conditional distribution multiplied by 1 minus the zero-inflation probability) scaled to the maximum observed abundance value in the harbour porpoise dataset; represented by colour and size (blue-red-yellow scalebar). Each season covers 3 months, with spring starting in March. Water depth (m) represented by greyscale contours. Green line represents coastline or spatial extent.

Herring Gull

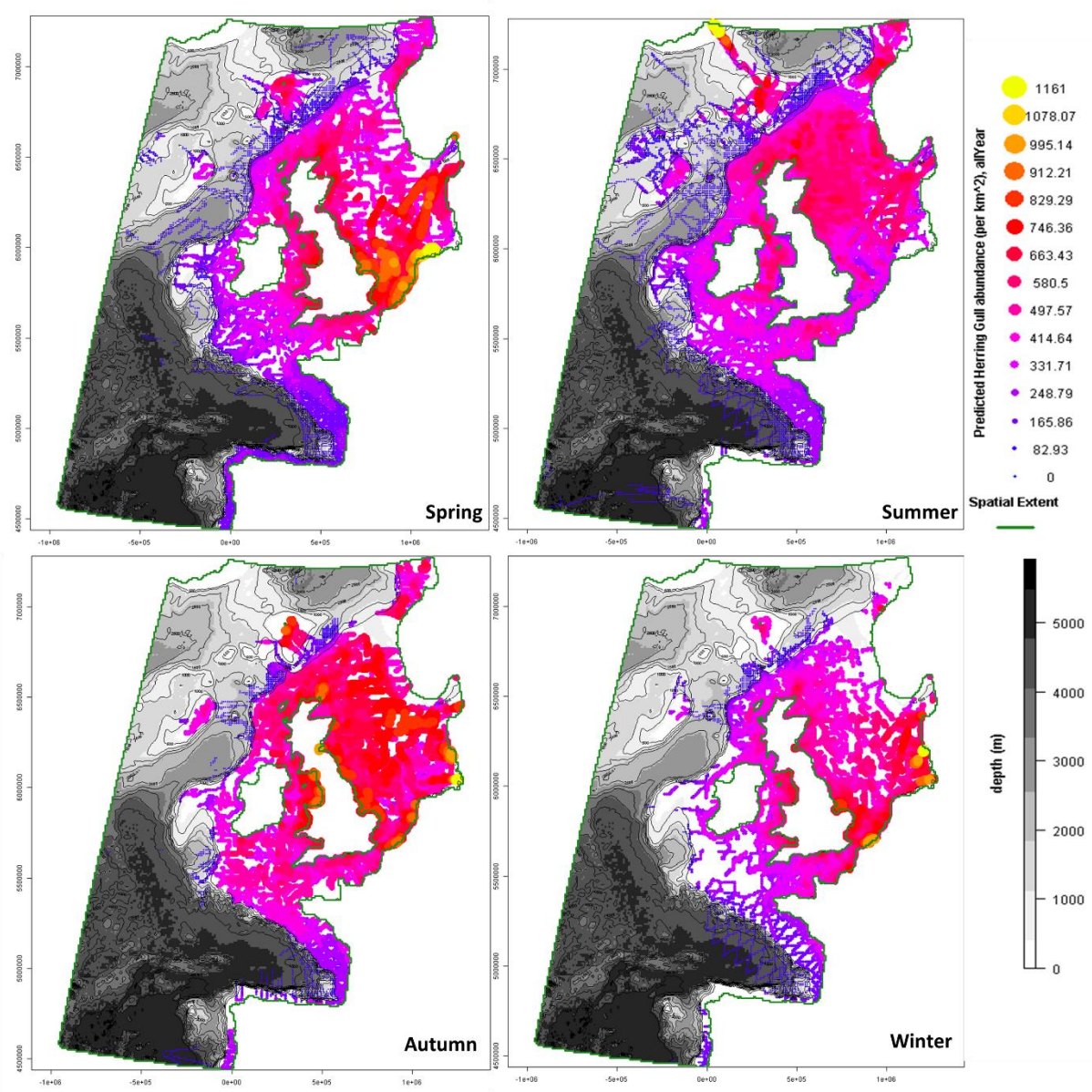

Figure 6.2.8.10. *Maps of predicted abundance of herring gulls, overlaying bathymetry.* Maximum predicted abundance (per 10 km^2) subset by season, from the same model, expressed as the expected value (mean of the conditional distribution multiplied by 1 minus the zero-inflation probability) scaled to the maximum observed abundance value in the herring gull dataset; represented by colour and size (blue-red-yellow scalebar). Each season covers 3 months, with spring starting in March. Water depth (m) represented by greyscale contours. Green line represents coastline or spatial extent.

Lesser Black Backed Gull

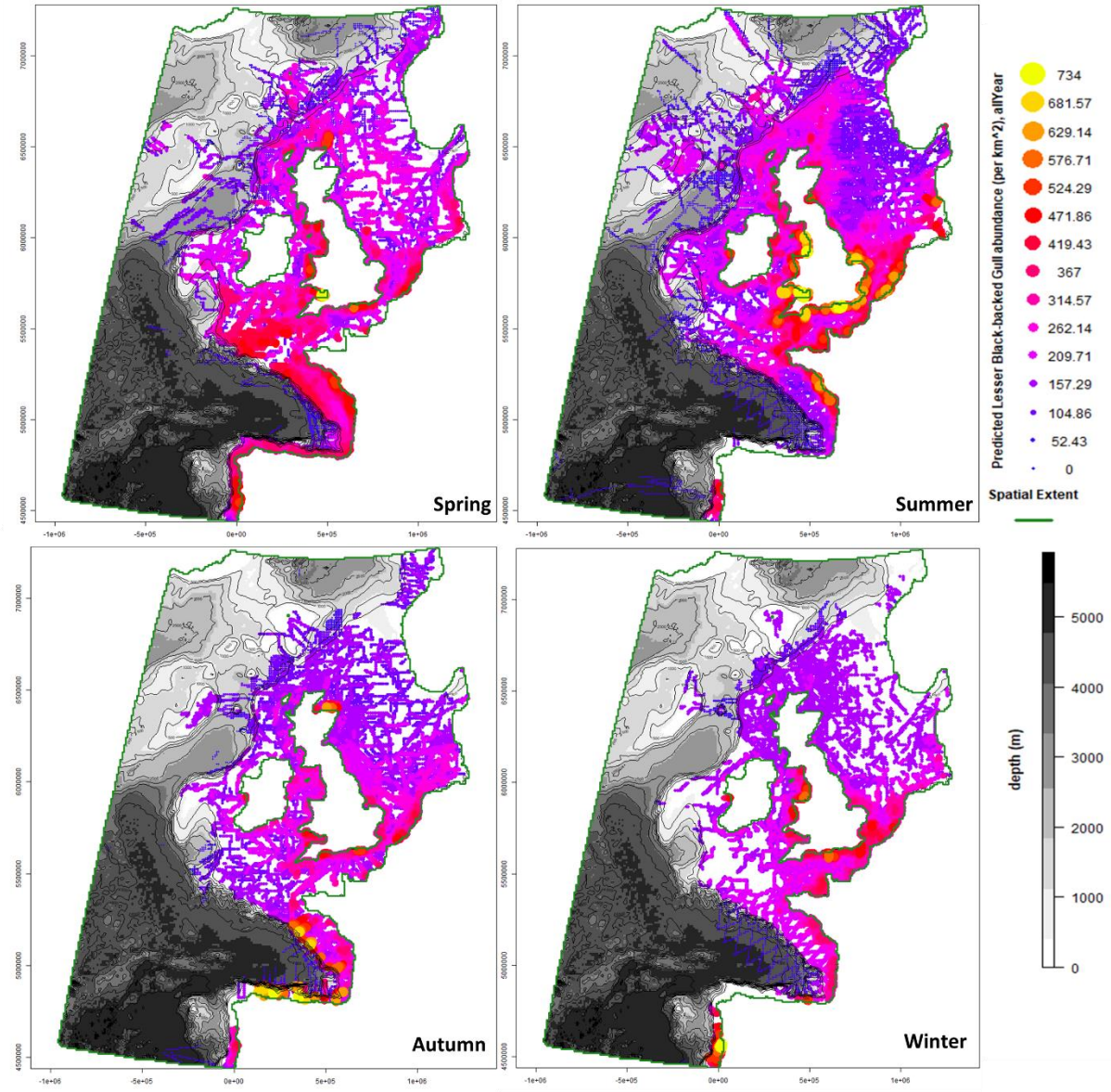

Figure 6.2.8.11. *Maps of predicted abundance of lesser black-backed gulls, overlaying bathymetry.* Maximum predicted abundance (per 10 km^2) subset by season, from the same model, expressed as the expected value (mean of the conditional distribution multiplied by 1 minus the zero-inflation probability) scaled to the maximum observed abundance value in the lesser black-backed gull dataset; represented by colour and size (blue-red-yellow scalebar). Each season covers 3 months, with spring starting in March. Water depth (m) represented by greyscale contours. Green line represents coastline or spatial extent.

Manx Shearwater

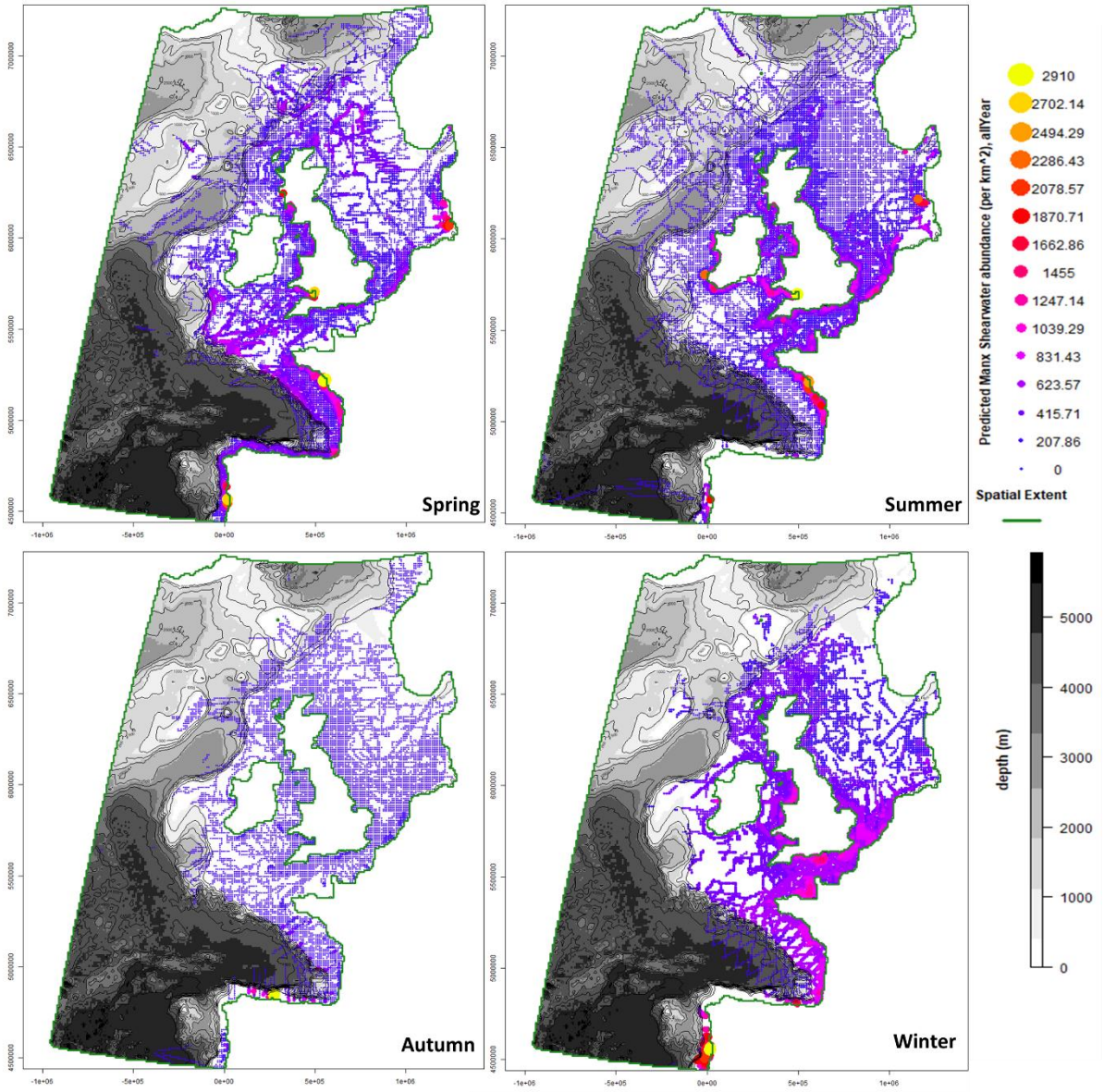

Figure 6.2.8.12. *Maps of predicted abundance of Manx shearwaters, overlaying bathymetry.* Maximum predicted abundance (per 10 km^2) subset by season, from the same model, expressed as the expected value (mean of the conditional distribution multiplied by 1 minus the zero-inflation probability) scaled to the maximum observed abundance value in the Manx shearwater dataset; represented by colour and size (blue-red-yellow scalebar). Each season covers 3 months, with spring starting in March. Water depth (m) represented by greyscale contours. Green line represents coastline or spatial extent.

Minke Whale

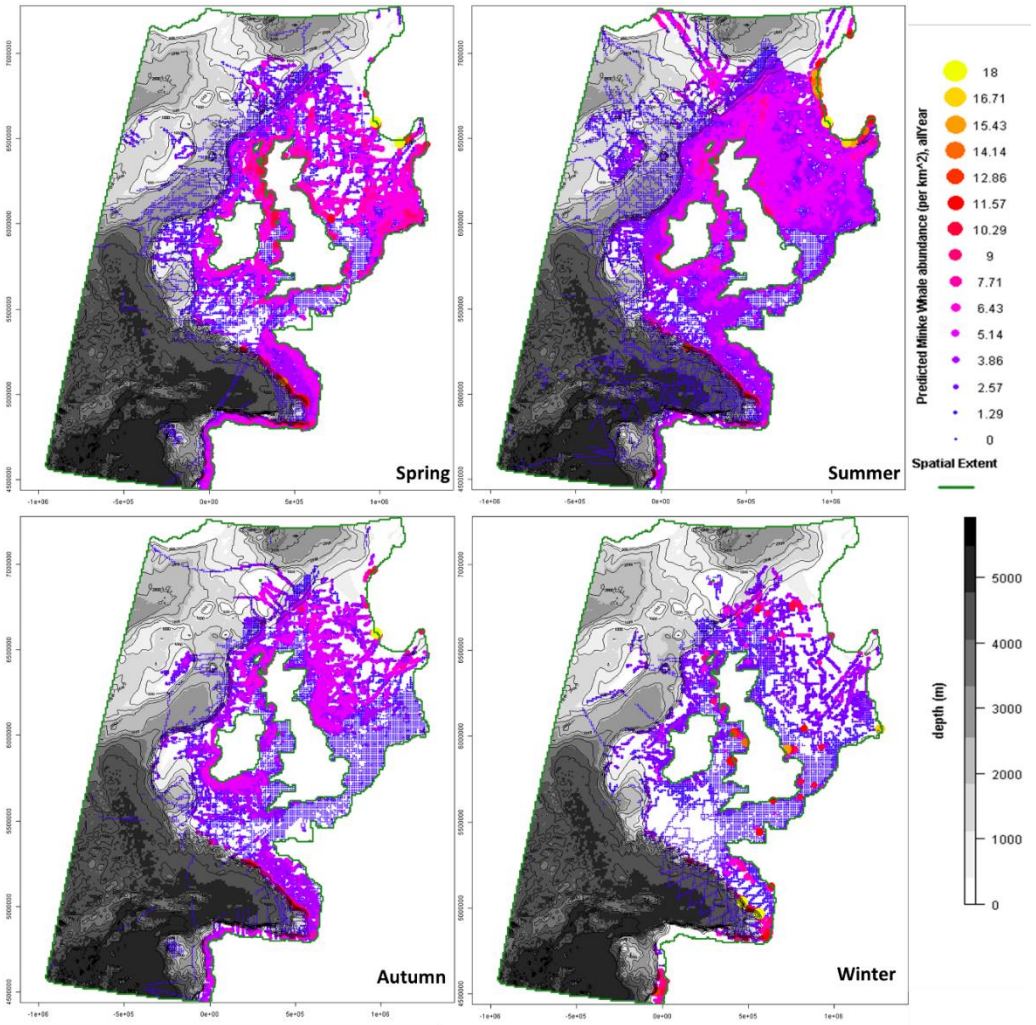

Figure 6.2.8.13. *Maps of predicted abundance of minke whales, overlaying bathymetry.* Maximum predicted abundance (per 10 km^2) subset by season, from the same model, expressed as the expected value (mean of the conditional distribution multiplied by 1 minus the zero-inflation probability) scaled to the maximum observed abundance value in the minke whale dataset; represented by colour and size (blue-red-yellow scalebar). Each season covers 3 months, with spring starting in March. Water depth (m) represented by greyscale contours. Green line represents coastline or spatial extent.

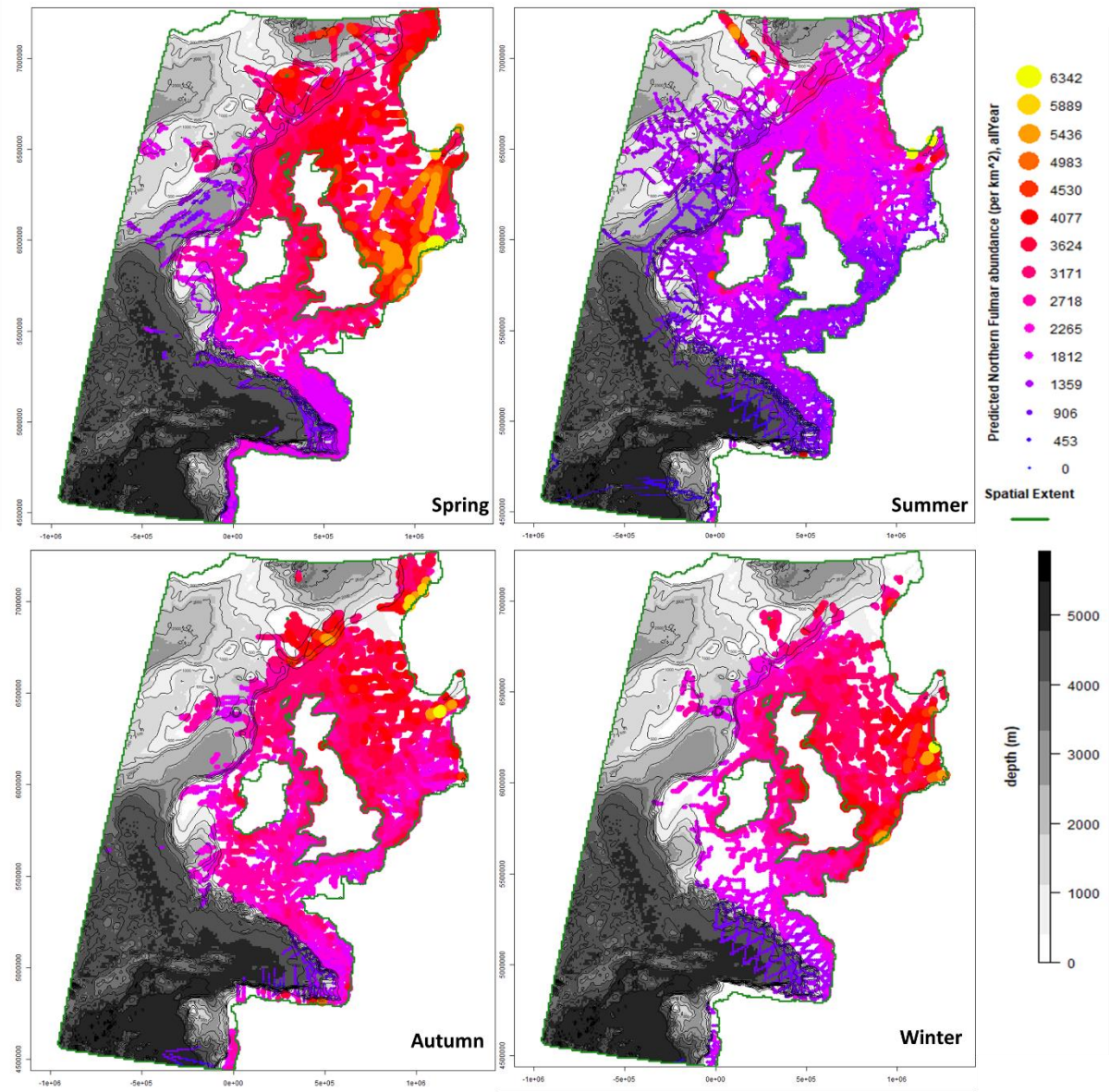

Figure 6.2.8.14. *Maps of predicted abundance of northern fulmars, overlaying bathymetry.* Maximum predicted abundance (per 10 km^2) subset by season, from the same model, expressed as the expected value (mean of the conditional distribution multiplied by 1 minus the zero-inflation probability) scaled to the maximum observed abundance value in the northern fulmar dataset; represented by colour and size (blue-red-yellow scalebar). Each season covers 3 months, with spring starting in March. Water depth (m) represented by greyscale contours. Green line represents coastline or spatial extent.

Northern Gannet

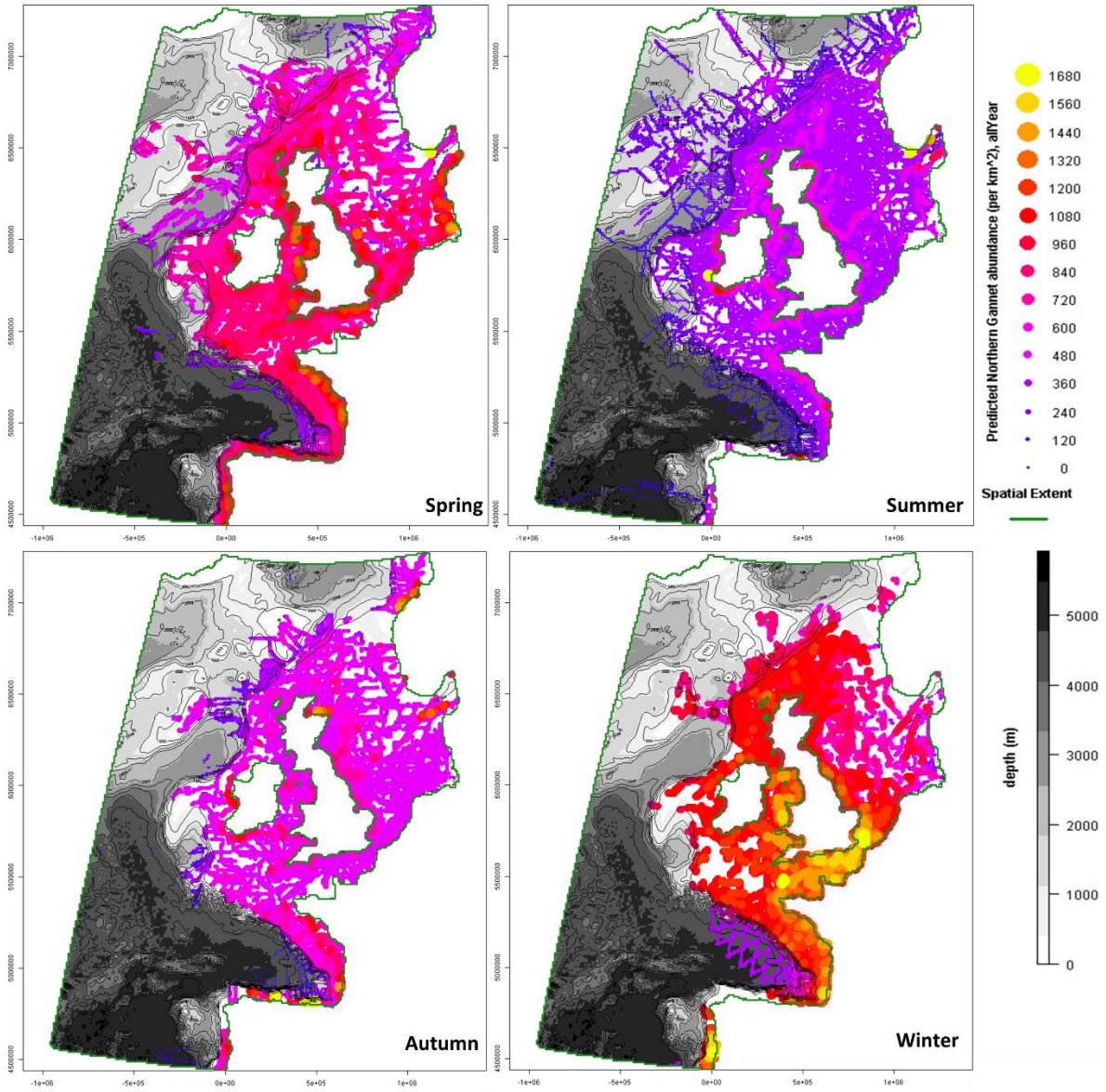

Figure 6.2.8.15. *Maps of predicted abundance of northern gannets, overlaying bathymetry.* Maximum predicted abundance (per 10 km^2) subset by season, from the same model, expressed as the expected value (mean of the conditional distribution multiplied by 1 minus the zero-inflation probability) scaled to the maximum observed abundance value in the northern gannet dataset; represented by colour and size (blue-red-yellow scalebar). Each season covers 3 months, with spring starting in March. Water depth (m) represented by greyscale contours. Green line represents coastline or spatial extent.

Orca

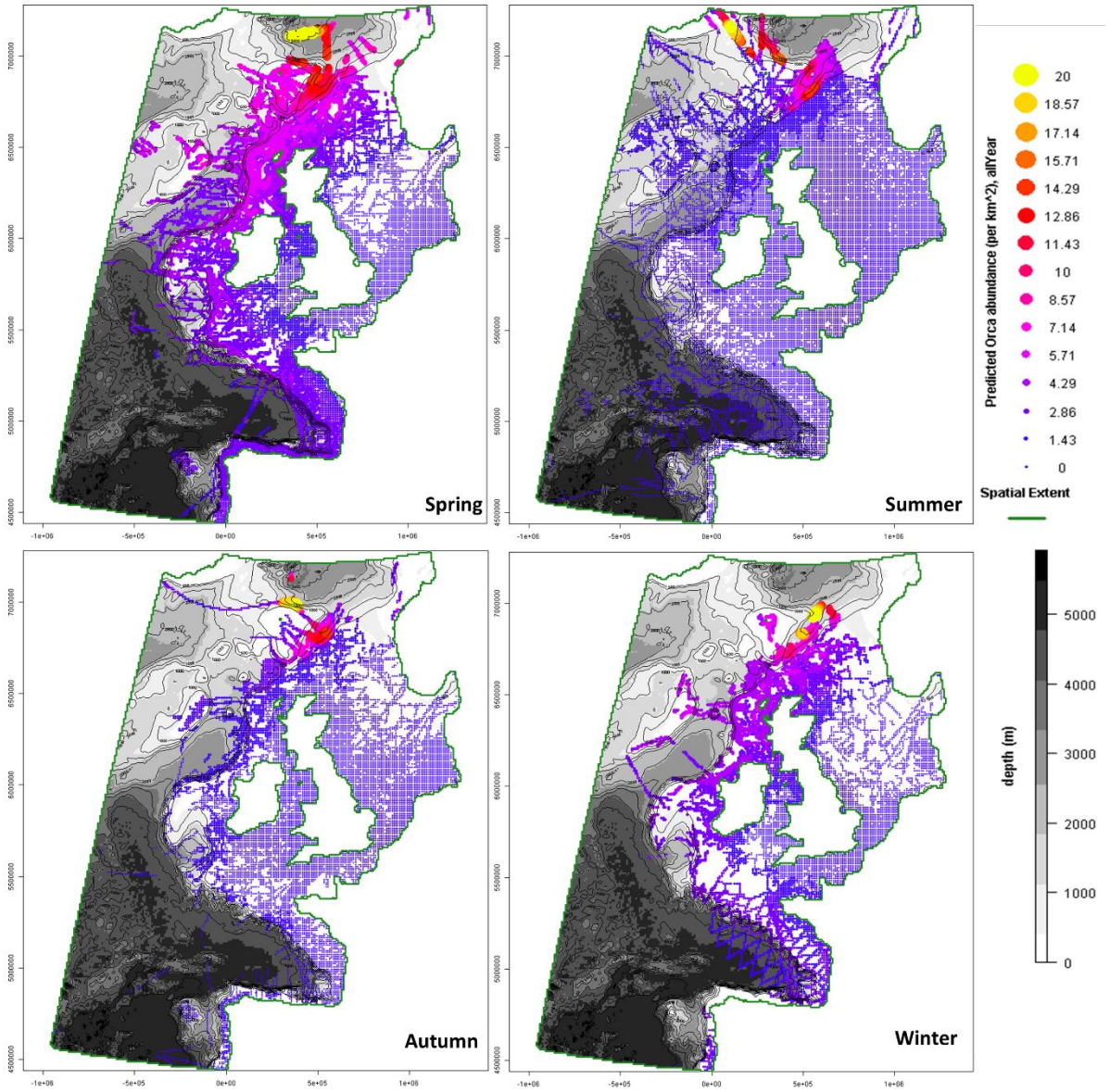

Figure 6.2.8.16. *Maps of predicted abundance of orcas, overlaying bathymetry.* Maximum predicted abundance (per 10 km^2) subset by season, from the same model, expressed as the expected value (mean of the conditional distribution multiplied by 1 minus the zero-inflation probability) scaled to the maximum observed abundance value in the orca dataset; represented by colour and size (blue-red-yellow scalebar). Each season covers 3 months, with spring starting in March. Water depth (m) represented by greyscale contours. Green line represents coastline or spatial extent.

Pilot Whale

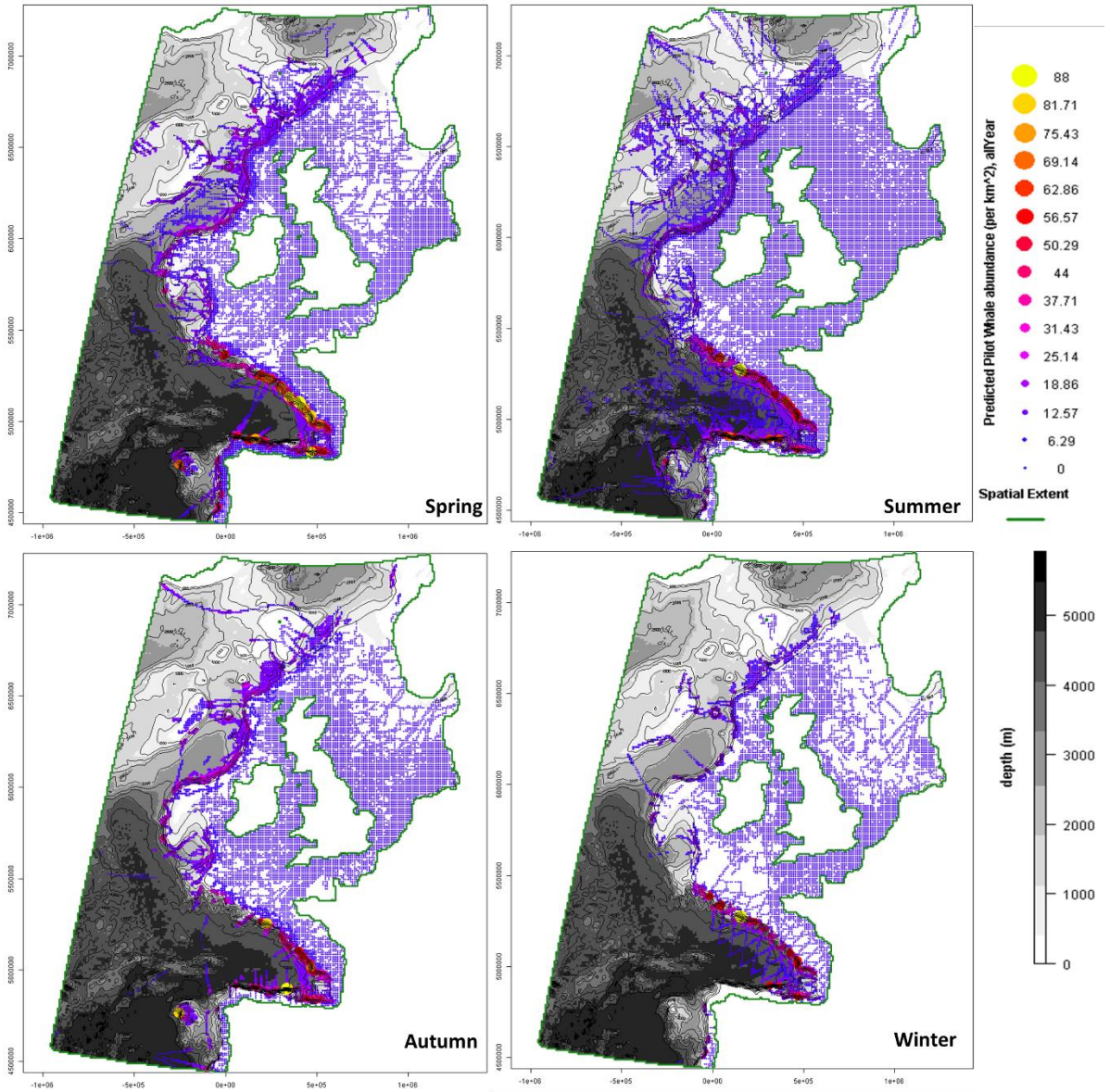

Figure 6.2.8.17. *Maps of predicted abundance of pilot whales, overlaying bathymetry.* Maximum predicted abundance (per 10 km^2) subset by season, from the same model, expressed as the expected value (mean of the conditional distribution multiplied by 1 minus the zero-inflation probability) scaled to the maximum observed abundance value in the pilot whale dataset; represented by colour and size (blue-red-yellow scalebar). Each season covers 3 months, with spring starting in March. Water depth (m) represented by greyscale contours. Green line represents coastline or spatial extent.

Razorbill

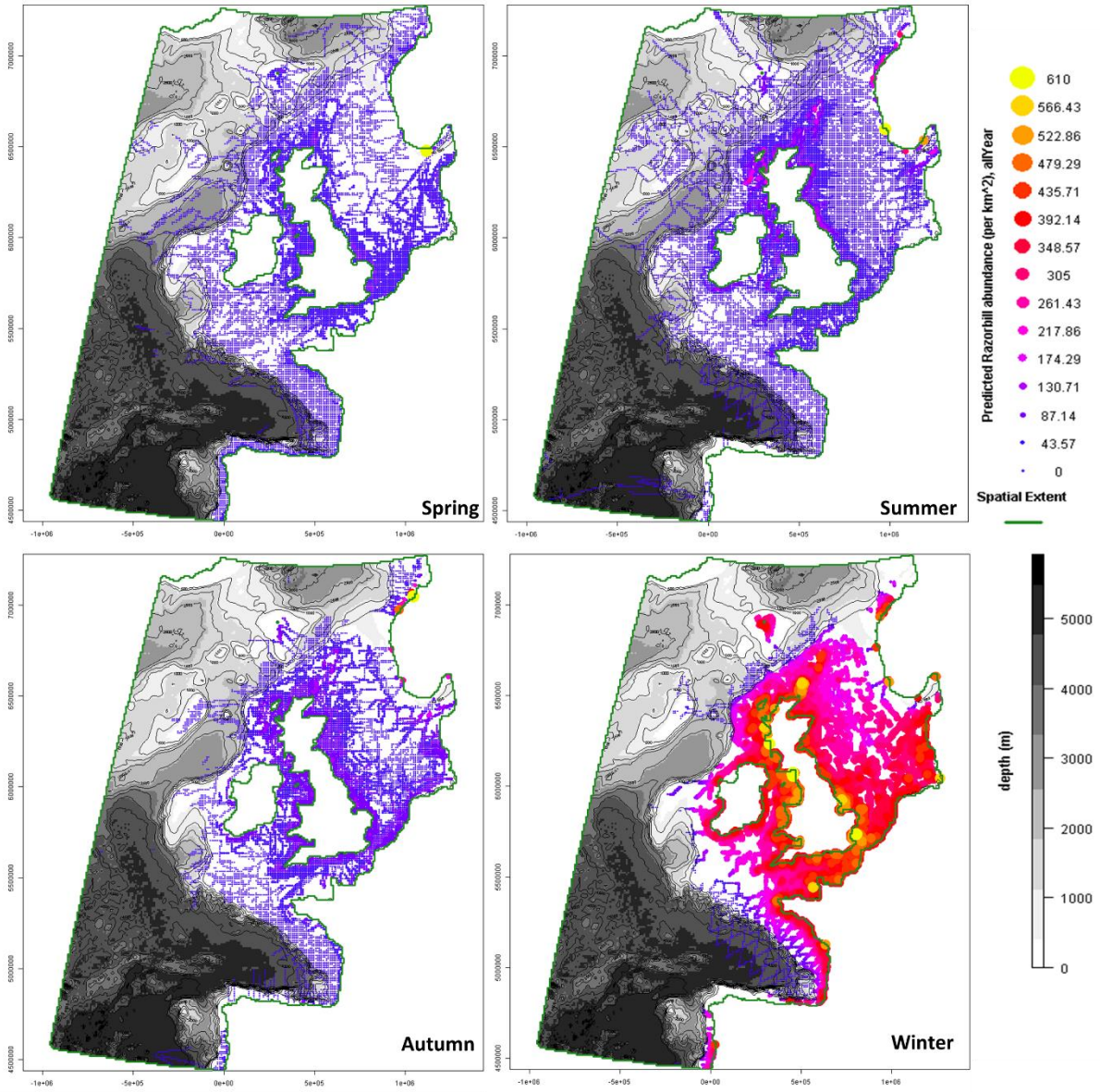

Figure 6.2.8.18. *Maps of predicted abundance of razorbills, overlaying bathymetry.* Maximum predicted abundance (per 10 km^2) subset by season, from the same model, expressed as the expected value (mean of the conditional distribution multiplied by 1 minus the zero-inflation probability) scaled to the maximum observed abundance value in the razorbill dataset; represented by colour and size (blue-red-yellow scalebar). Each season covers 3 months, with spring starting in March. Water depth (m) represented by greyscale contours. Green line represents coastline or spatial extent.

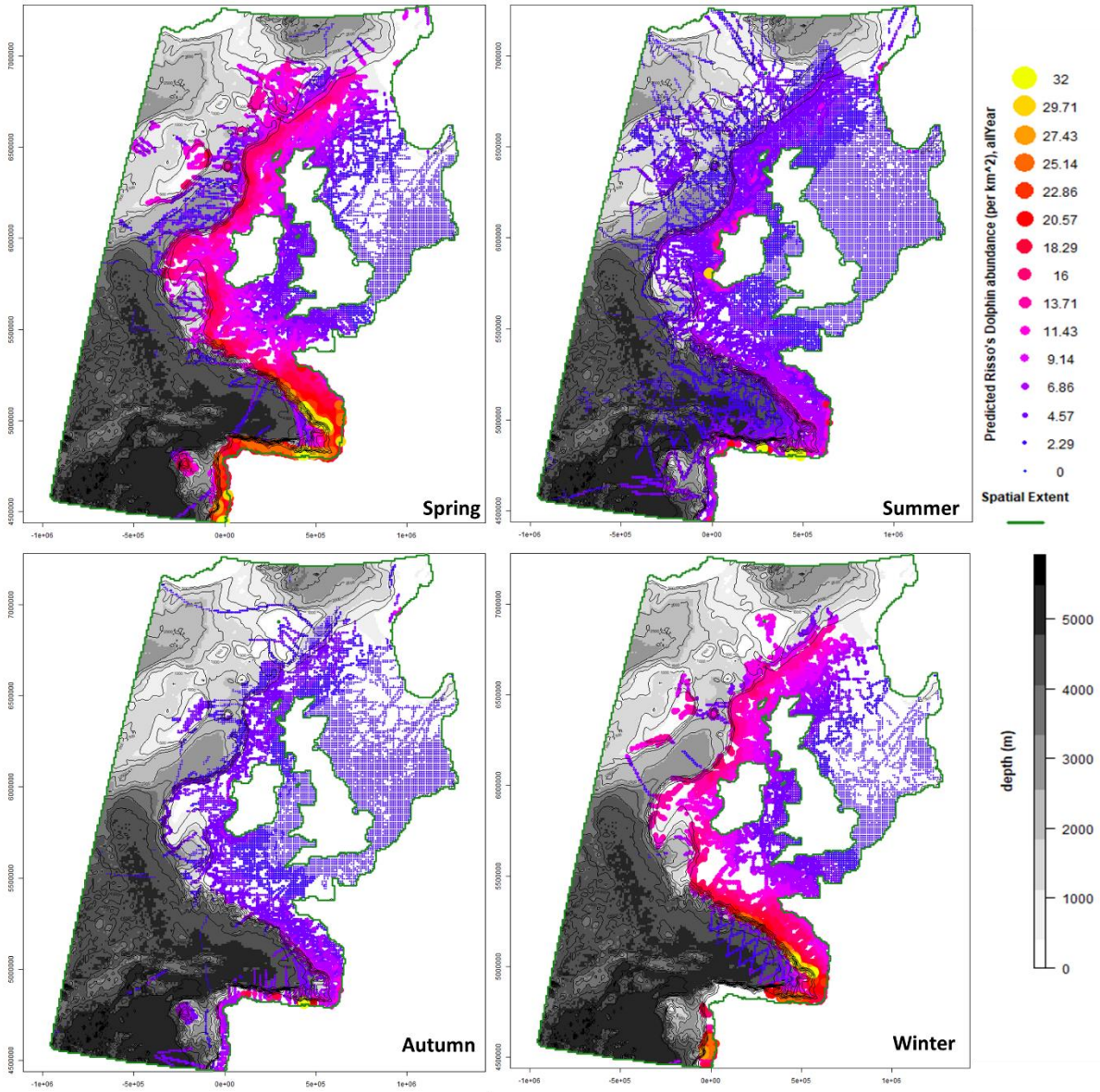

Figure 6.2.8.19. *Maps of predicted abundance of Risso's dolphins, overlaying bathymetry.* Maximum predicted abundance (per 10 km^2) subset by season, from the same model, expressed as the expected value (mean of the conditional distribution multiplied by 1 minus the zero-inflation probability) scaled to the maximum observed abundance value in the Risso's dolphin dataset; represented by colour and size (blue-red-yellow scalebar). Each season covers 3 months, with spring starting in March. Water depth (m) represented by greyscale contours. Green line represents coastline or spatial extent.

Sperm Whale

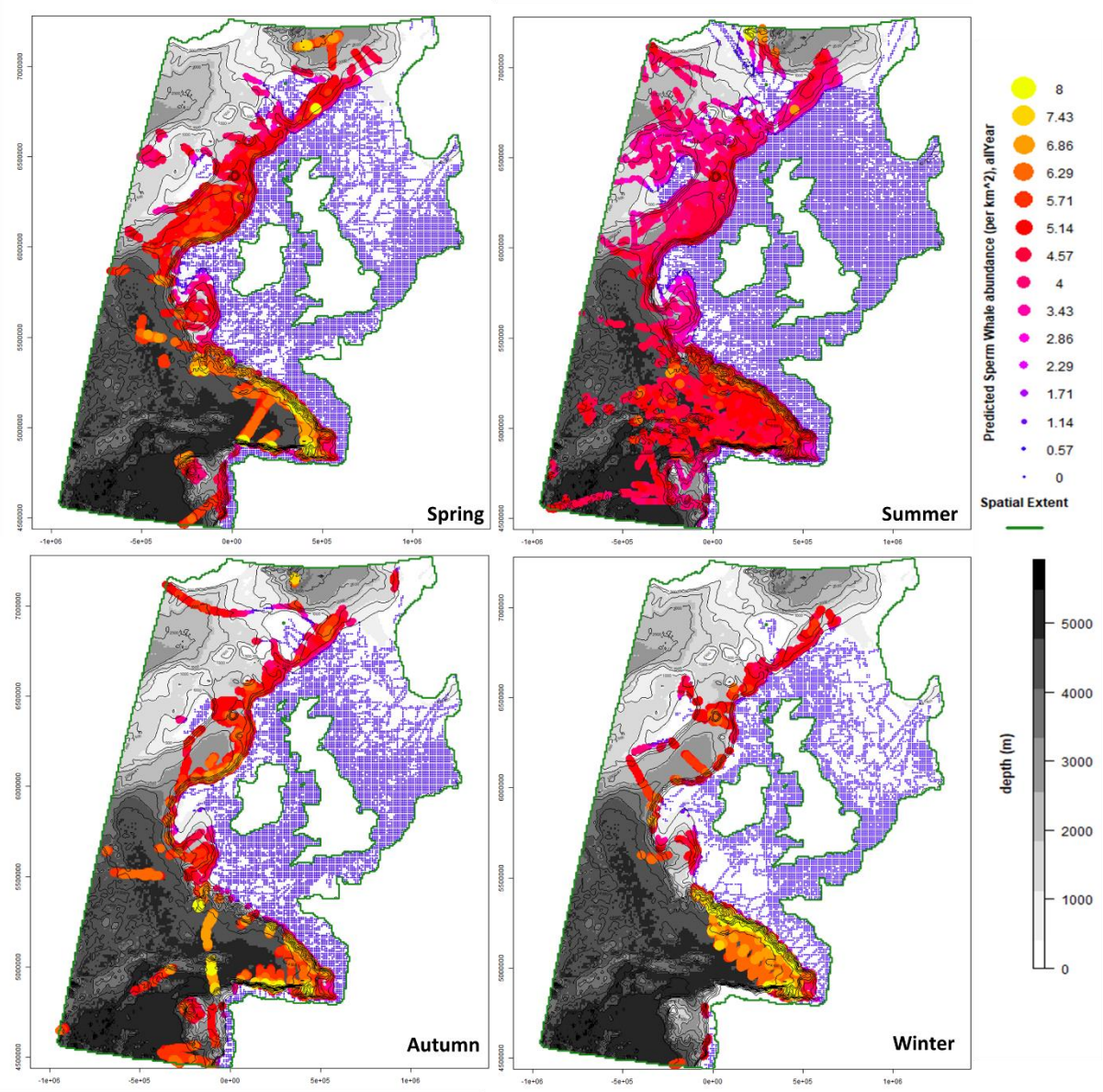

Figure 6.2.8.20. *Maps of predicted abundance of sperm whales, overlaying bathymetry.* Maximum predicted abundance (per 10 km^2) subset by season, from the same model, expressed as the expected value (mean of the conditional distribution multiplied by 1 minus the zero-inflation probability) scaled to the maximum observed abundance value in the sperm whale dataset; represented by colour and size (blue-red-yellow scalebar). Each season covers 3 months, with spring starting in March. Water depth (m) represented by greyscale contours. Green line represents coastline or spatial extent.

Striped Dolphin

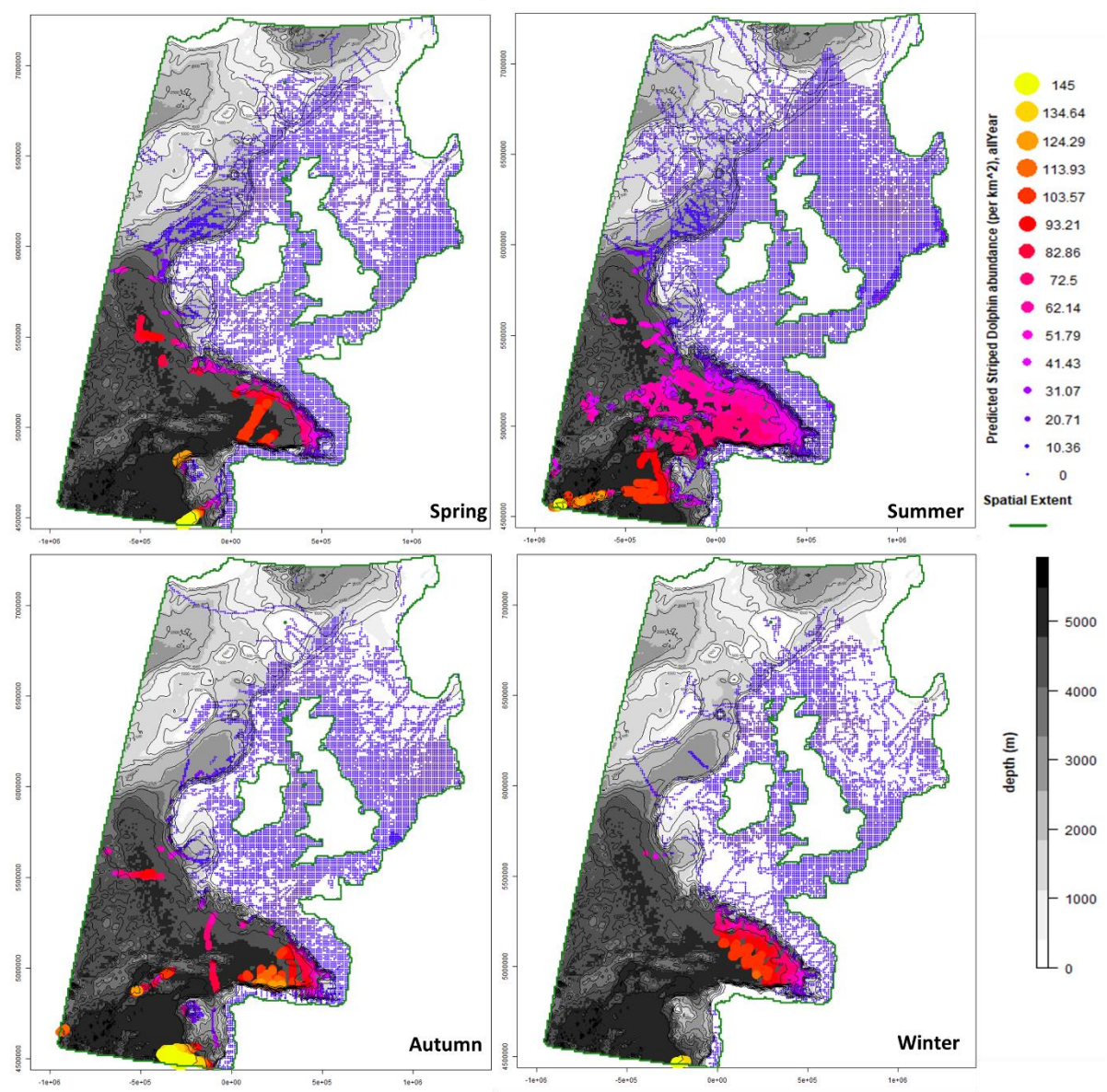

Figure 6.2.8.21. *Maps of predicted abundance of striped dolphins, overlaying bathymetry.* Maximum predicted abundance (per 10 km^2) subset by season, from the same model, expressed as the expected value (mean of the conditional distribution multiplied by 1 minus the zero-inflation probability) scaled to the maximum observed abundance value in the striped dolphin dataset; represented by colour and size (blue-red-yellow scalebar). Each season covers 3 months, with spring starting in March. Water depth (m) represented by greyscale contours. Green line represents coastline or spatial extent.

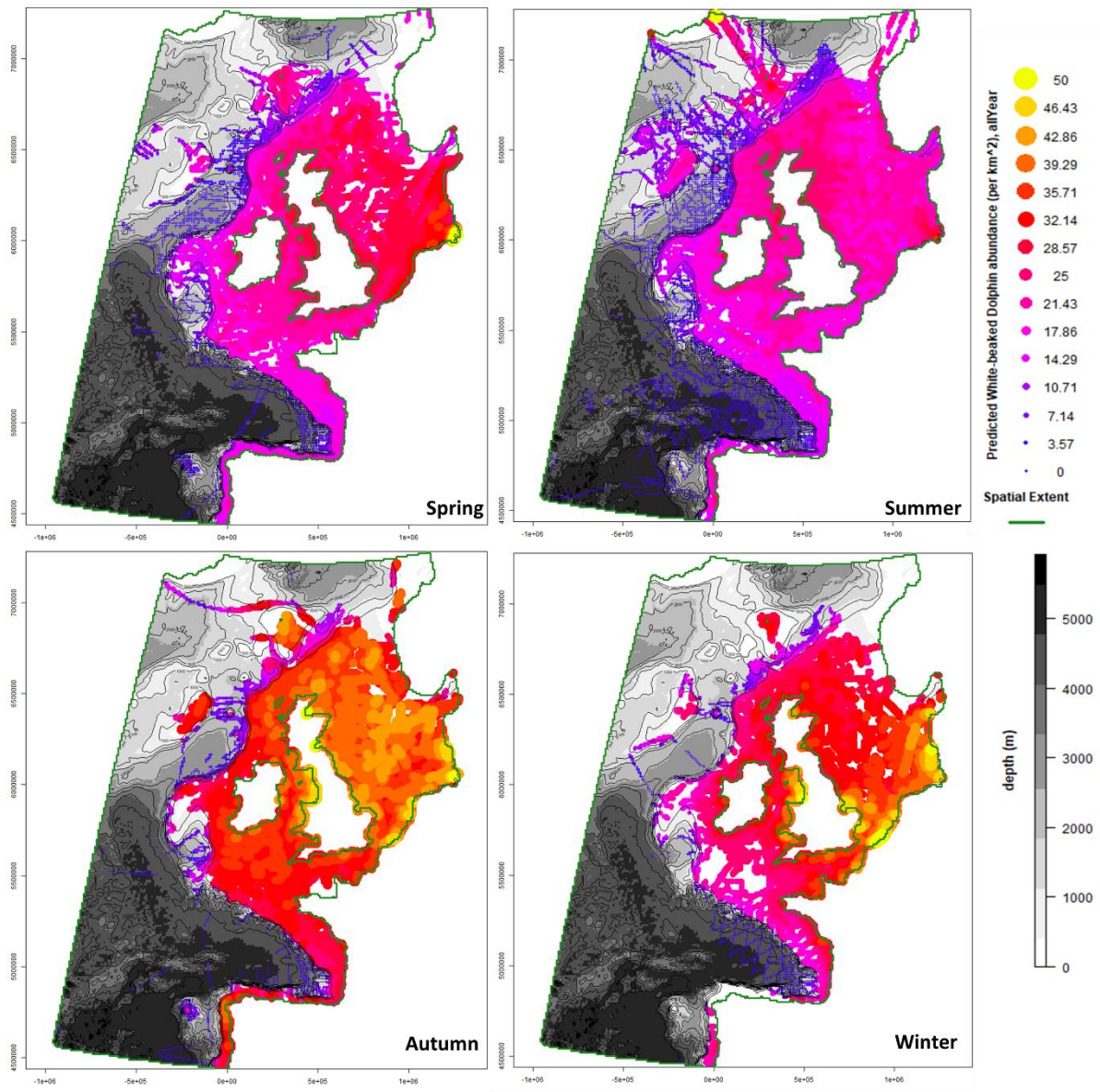

Figure 6.2.8.22. *Maps of predicted abundance of white-beaked dolphins, overlaying bathymetry.* Maximum predicted abundance (per 10 km^2) subset by season, from the same model, expressed as the expected value (mean of the conditional distribution multiplied by 1 minus the zero-inflation probability) scaled to the maximum observed abundance value in the white-beaked dolphin dataset; represented by colour and size (blue-red-yellow scalebar). Each season covers 3 months, with spring starting in March. Water depth (m) represented by greyscale contours. Green line represents coastline or spatial extent.

White-sided Dolphin

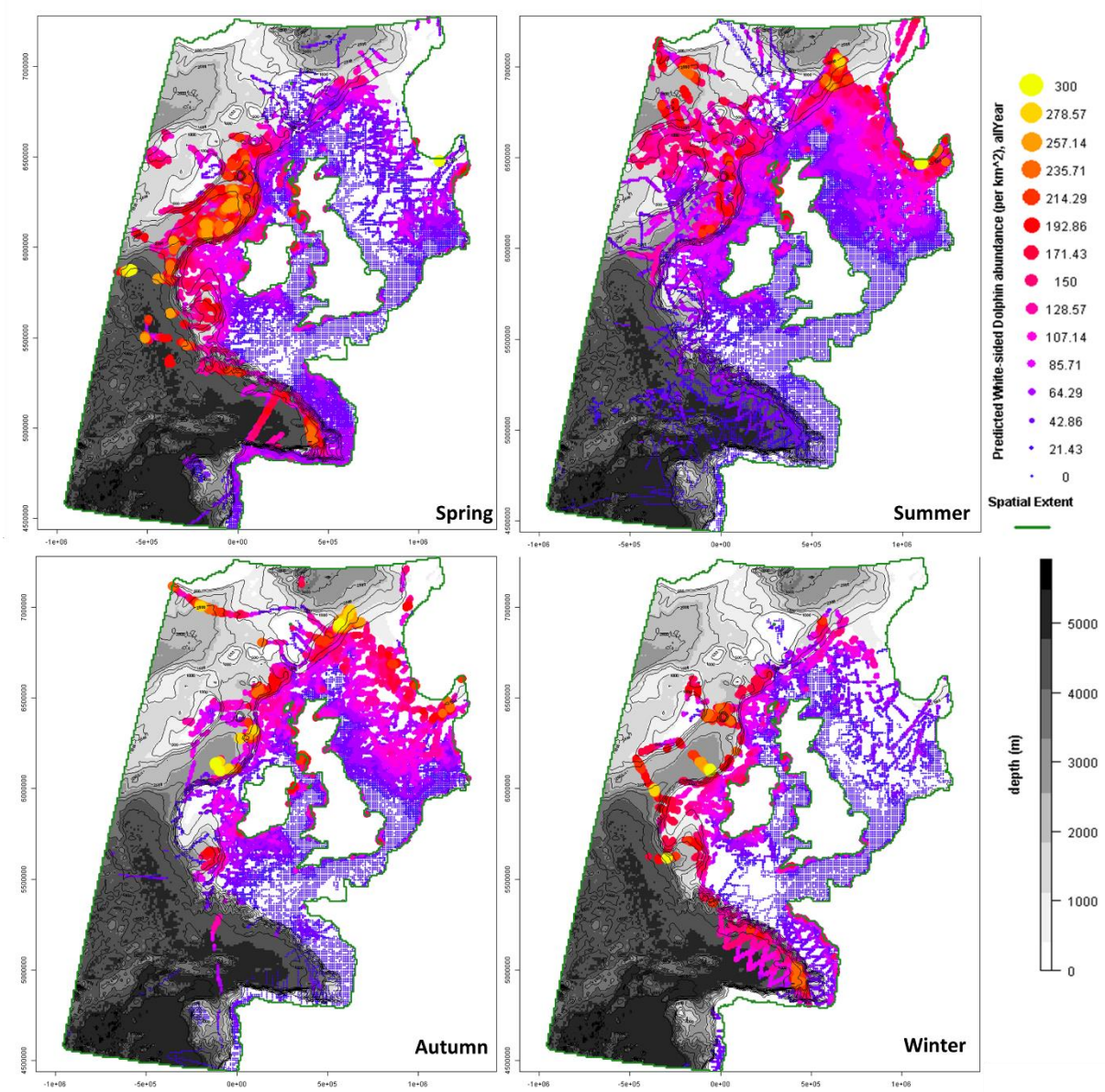

Figure 6.2.8.23. *Maps of predicted abundance of white-sided dolphins, overlaying bathymetry.* Maximum predicted abundance (per 10 km^2) subset by season, from the same model, expressed as the expected value (mean of the conditional distribution multiplied by 1 minus the zero-inflation probability) scaled to the maximum observed abundance value in the white-sided dolphin dataset; represented by colour and size (blue-red-yellow scalebar). Each season covers 3 months, with spring starting in March. Water depth (m) represented by greyscale contours. Green line represents coastline or spatial extent.

2.3 Additional results

Table 6.2.4*. Table of 75th and 25th percentile of absolute values of percentage change in species abundance with a 20% increase in the value of each predictor.*

Parameter	75th percentile (%/20%)	25th percentile (%/20%)
Sea temperature	0.306	0.014
Fronts	0.297	0.011
Chlorophyll	0.27	0.0033
Seabed gradient	0.24	0.007
Depth	0.76	0.017

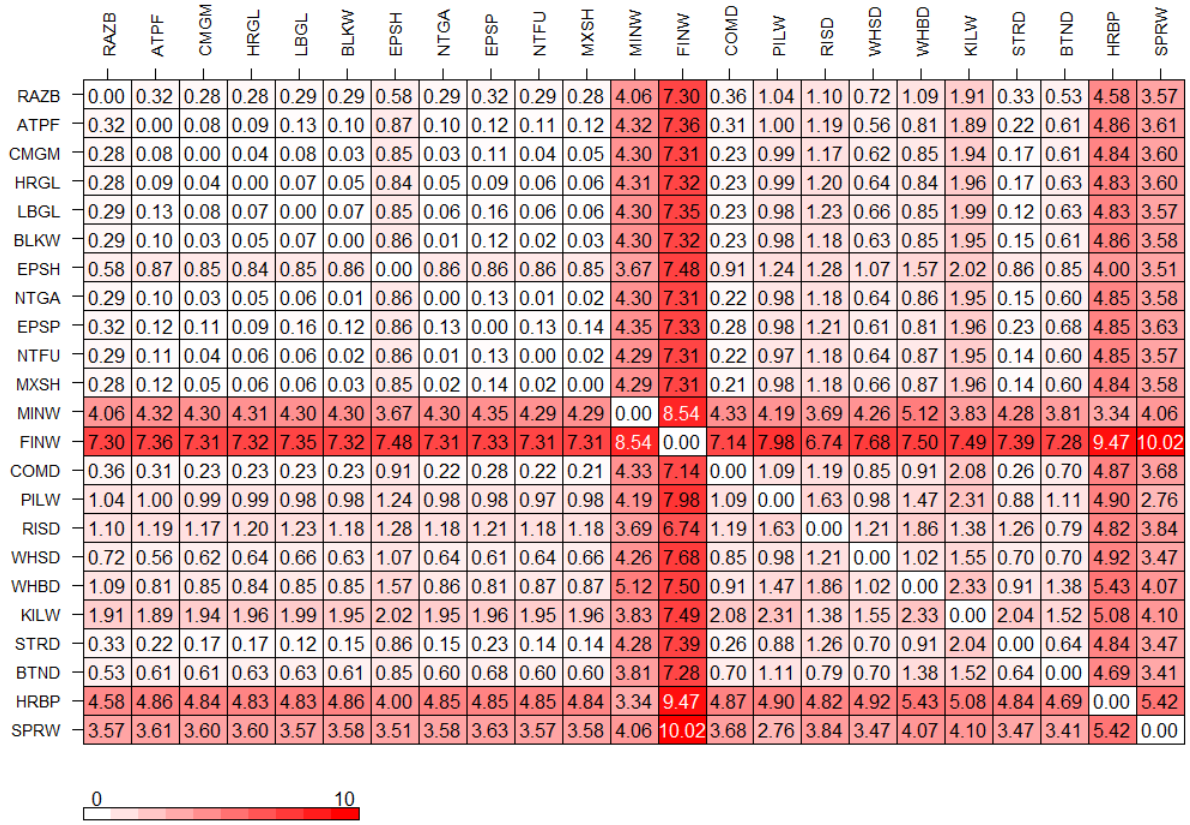

Figure 6.2.9. *Matrix of dissimilarity between species ZIGLM conditional coefficients.* Dissimilarity matrix calculated using Euclidean distances between species ZIGLM conditional coefficients, detailed in dissimilarity section of methodology.

Table 6.2.5. *Eigen values of each principle component, representing percentage of variance explained by components 1 to 5, and the standard deviations of each component.*

Component	Variance explained (%)	Standard Deviation
1	57.2	1.7
2	28.5	1.2
3	9.5	0.7
4	4.6	0.5
5	0.3	0.1

Table 6.2.6. *Variable loadings in components 1 to 5.*

Variable	Component 1	Component 2	Component 3	Component 4	Component 5
Sea Temp	0.54	0.12	0.20	0.74	0.32
Front Potential	0.52	0.27	0.11	-0.66	0.45
Seabed Gradient	-0.24	0.66	-0.65	0.14	0.24
Depth	0.25	-0.65	-0.67	-0.01	0.26
Chlorophyll conc.	-0.56	-0.21	0.28	0.04	0.75

Table 6.2.7. *Scores of each species for principle components 1 to 5.*

Species	Component 1	Component 2	Component 3	Component 4	Component 5
ATPF	-0.039	-0.557	0.214	-0.023	0.041
BLKW	-0.011	-0.531	0.178	0.062	0.045
BTND	-0.070	-0.150	-0.214	-0.215	0.135
CMGM	-0.009	-0.520	0.195	0.045	0.038
EPSH	-0.329	0.246	0.422	0.083	-0.061
EPSP	-0.010	-0.554	0.252	0.042	-0.046
FINW	7.160	1.444	-0.495	0.474	-0.016
HRBP	-1.958	3.717	1.833	0.311	-0.061
HRGL	-0.017	-0.522	0.223	0.063	0.028
LBGL	-0.042	-0.529	0.205	0.096	0.089
MXSH	-0.009	-0.512	0.178	0.081	0.062
NTFU	-0.014	-0.522	0.168	0.071	0.053
NTGA	-0.011	-0.523	0.178	0.067	0.057
PILW	-0.715	-0.642	-0.275	0.388	-0.377
RAZB	-0.060	-0.242	0.239	0.057	0.040
RISD	0.456	0.168	-0.448	-0.448	-0.274
SPRW	-2.831	-0.203	-1.919	1.047	0.022
STRD	-0.098	-0.536	0.137	0.181	0.075
WHBD	0.096	-1.278	0.599	-0.060	0.090
WHSD	-0.332	-0.633	0.059	-0.442	-0.150
COMD	0.155	-0.485	0.194	0.210	0.083
KILW	-0.039	0.016	-0.505	-1.727	0.009
MINW	-1.275	3.346	-1.416	-0.362	0.119

Table 6.2.8. *Table of k means cluster centroids for each explanatory variable (ZIGLM conditional coefficients) in each cluster, and within-cluster sum of squares.*

Cluster Nº	explanatory variables					Within-cluster sum of squares by cluster
	TPM	TPF	FEA	BAT	CHT	
	Cluster centroids					
1	-0.205	-0.509	0.201	0.168	0.144	0
2	-0.145	0.119	0.326	-0.645	-0.080	0
3	-0.013	-0.007	0.002	-0.017	0.001	0.162
4	0.728	0.878	0.004	0.340	-0.719	0
5	-0.014	0.028	0.187	-1.607	0.092	0
6	-0.147	0.199	0.048	0.018	-0.095	0.034

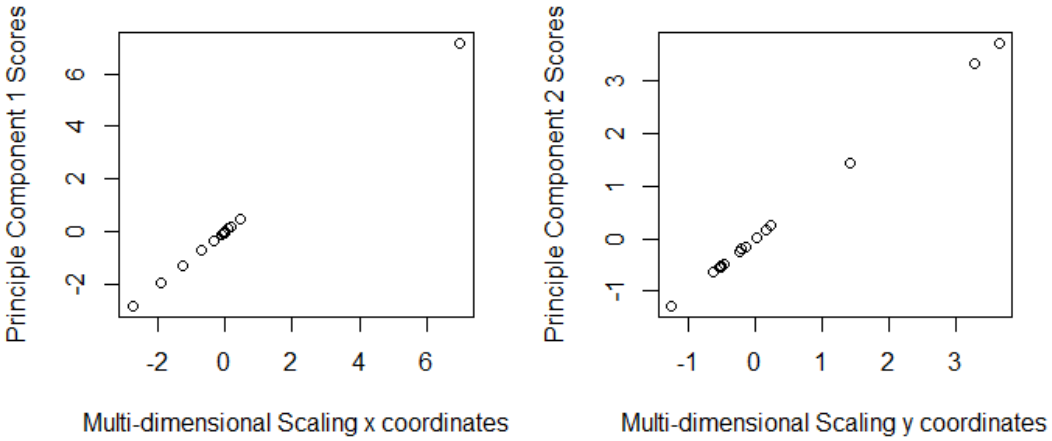

Figure 6.2.10*. Principle components scores as a function of multi-dimensional scaling coordinates.*

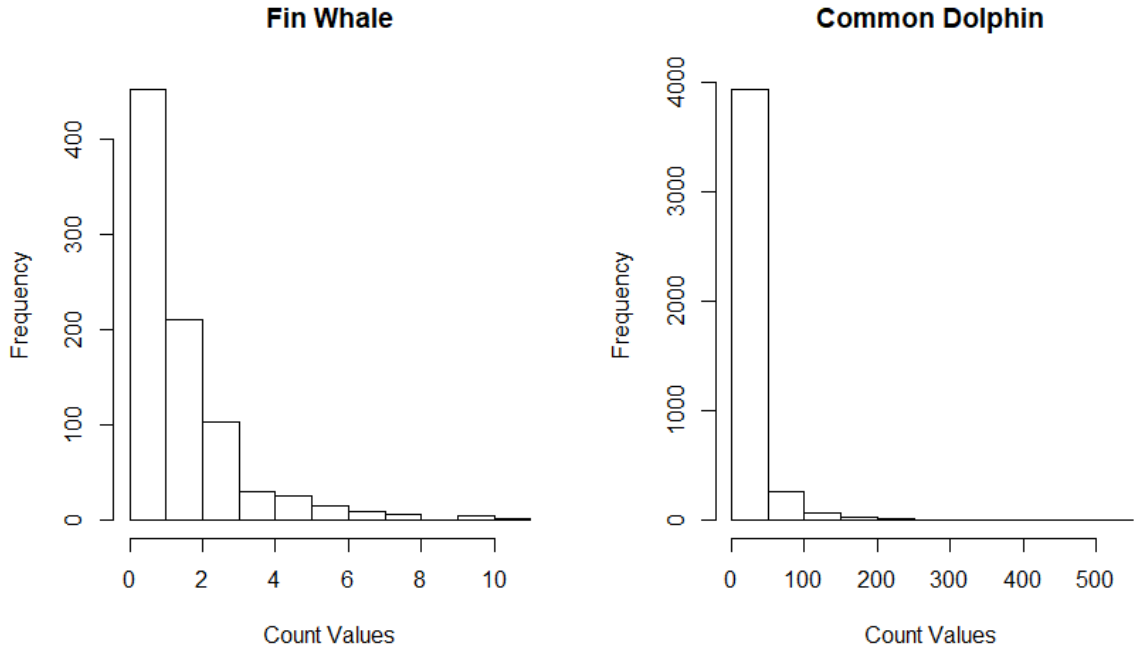

***Figure 6.3.1**. Frequency of observation count values for fin whale and common dolphin.*

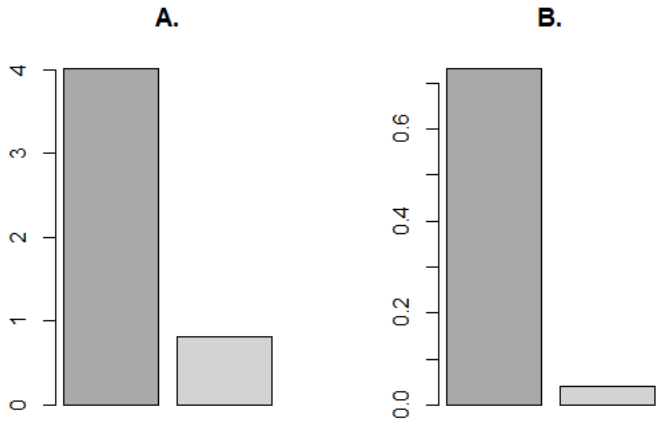

Figure 6.3.2. Fin whale slope estimate is dark grey (left bar) common dolphin slope estimates are light grey (right bar). A = slope scaled with 75th percentile of y, B = slope scaled with maximum y.